

5-1-2000

Atomic oxygen resistant Zr pendent polyimide based on 1,3-aminophenoxybenzene

Derek Chow

Follow this and additional works at: <http://scholarworks.rit.edu/theses>

Recommended Citation

Chow, Derek, "Atomic oxygen resistant Zr pendent polyimide based on 1,3-aminophenoxybenzene" (2000). Thesis. Rochester Institute of Technology. Accessed from

This Thesis is brought to you for free and open access by the Thesis/Dissertation Collections at RIT Scholar Works. It has been accepted for inclusion in Theses by an authorized administrator of RIT Scholar Works. For more information, please contact ritscholarworks@rit.edu.

**ATOMIC OXYGEN RESISTANT Zr PENDENT
POLYIMIDE BASED ON
1,3-AMINOPHENOXYBENZENE**

DEREK CHOW

THESIS

**SUBMITTED IN PARTIAL FULFILLMENT OF THE REQUIREMENTS FOR
THE DEGREE OF MASTER OF SCIENCE**

**DEPARTMENT OF CHEMISTRY
ROCHESTER INSTITUTE OF TECHNOLOGY
ROCHESTER, NEW YORK**

MAY, 2000

**ATOMIC OXYGEN RESISTANT Zr PENDENT
POLYIMIDE BASED ON
1,3-AMINOPHENOXYBENZENE**

Approved:

M. Illingsworth

Thesis Advisor

G. A. Takacs

Department Head

COPYRIGHT STATEMENT

Title of thesis Atomic Oxygen Resistant Zr Pendent Polyimide Based on 1,3-Aminophenoxybenzene.

I, Derek Chow, hereby grant permission to the Wallace Memorial Library, of Rochester Institute of Technology, to reproduce my thesis in whole or in part. Any reproduction will not be for commercial use or profit.

This thesis is dedicated to my mom with love.

ACKNOWLEDGEMENTS

I wish to gratefully acknowledge Dr. Illingsworth for his assistance, care and kindness, in making this project as success. With his knowledge, his strength of character and professionalism were very important contributions to his project. Also, he helps me to select and work toward appropriate goals, provide critical feedback on individual work and on progress in general. On top of that he is able to see the good in everyone, and inspire us to be our better selves.

I would like to thank my committee members, and chemistry department for their great support.

I would like to thank National Starch and Chemical Corporation for generous donation of the APB used in this project.

I would like to thank NASA Langley Center for the GPC measurements and Dr. Fuller of Microelectronic Engineering Department for use of the SEM instrument.

Drew, thank you for your support and patience.

I would also like to thank Wei Wang, Zhiming Wang, Huy Doan, Brain Landi, Scott D Luzzi, Jennifer Jankauskas, Julie Leiston (the ethanol queen), Russ Stapleton, Joe Starling, for your help and support. Thanks GUYS!

*being deeply loved by someone
gives you strength;
while loving someone deeply
gives you courage.*

-Lao-Tzu

Table of Contents

1. Introduction.....	1
2. Experimental.....	7
2.1 Chemicals.....	7
2.2 Instrument and Experimental Methods.....	8
2.2.1 Proton Nuclear Magnetic Resonance (^1H NMR).....	8
2.2.1.1 Molecules.....	8
2.2.1.2 Polymers.....	8
2.2.2 Thermogravimetric Analysis (TGA).....	8
2.2.3 Differential Scanning Calorimetry (DSC).....	9
2.2.4 Molecular Weight (MW), Molecular Weight Distribution (MWD), and Intrinsic Viscosity (IV) Determination.....	9
2.2.5 Fourier Transform Infrared Spectroscopy (FTIR).....	10
2.2.6 Preparation of Multilayer Films.....	10
2.2.7 Oxygen Plasma Asher.....	11
2.2.8 Scanning Electron Microscopy (SEM).....	11
2.2.9 Solvent Resistance.....	12
2.3 Preparation of Starting Materials.....	12
2.4 Mellitic Dianhydride (MADA).....	15
2.5 Poly(amic acid) Co-polymers, co-PAA(ODPA/APB/MADA).....	15
2.6 Zirconium Pendent Poly(amic acid) Co-polymers.....	17
2.7 Films.....	18
3. Results.....	19
3.1 Preparation of Starting Materials and Mellitic Dianhydride (MADA).....	19
3.2 Polymer Synthesis.....	23
3.2.1 co-PAA(ODPA/APB/MADA)	
3.2.2 co-PAA(ODPA/APB/MADA/Zr)	
3.3 Thermal Imidization of Poly(amic acid)s.....	25
3.4 Proton Nuclear Magnetic Resonance (^1H NMR) Study	43
3.5 Gel Permeation Chromatography (GPC)	50
3.6 Thermal Properties (TGA)	55
3.7 Differential Scanning Calorimetry (DSC).....	60
3.8 Scanning Electron Micrographs (SEM).....	67
3.9 Solvent Resistance Test.....	72
3.10 Preparation of Zr(adsp)(dsp) Pendent Polyimide Films.....	72
4. Discussion.....	74
4.1 Mellitic Dianhydride (MADA)	74
4.2 PAA(ODPA/APB/MADA) Co-Polymer Synthesis.....	75
4.3 Zr(adsp)(dsp)pendentPAA(ODPA/APB/MADA),PAA(ODPA/APB/ MADA/Zr).....	77
4.4 Preparation of Zr(adsp)(dsp) Pendent Polyimide Films.....	78
4.5 Polymer Characterization.....	79
4.5.1 TLC, NMR, and IR.....	79
4.5.2 GPC and Viscosity.....	80
4.5.3 TGA and DSC.....	81
4.5.4 Atomic Oxygen Resistance.....	85

4.5.5 Solvent Resistance.....	85
5. Suggestion for Future Work.....	87
6. References.....	88
7. Conclusion.....	91
Appendix: NMR Spectra Used to Facilitate Peak Assignments, and Pictures.....	92

Figure and Table Captions

- Figure 3.1. Synthesis of H_2ndsp (page 19)
- Figure 3.2 Synthesis of H_2dsp (page 19)
- Figure 3.3. The structure of $Zr(ndsp)(dsp)$ (page 20)
- Figure 3.4. The structure of $Zr(adsp)(dsp)$ (page 20)
- Figure 3.5. Shows the TGA curve of mellitic dianhydride (page 22)
- Figure 3.6. The Synthesis Reactions for Mellitic Acid and 5.8% wt loss to Mellitic Acid Trianhydride (page 21)
- Figure 3.7. Synthesis of co-PAA(ODPA/APB/MADA) (page 23)
- Figure 3.8. The Synthesis of Zr pendent poly(amic acid) (page 24)
- Figure 3.9. FT-IR spectra of PI(ODPA/APB) and $Zr(adsp)(dsp)$ (page 26)
- Figure 3.10. FT-IR Spectrum of Polyamic Acids Films. (page 27)
- Figure 3.11. FT-IR Spectrum of Pendent Polyamic Acids Films. (page 28)
- Figure 3.12. FT-IR Spectrum of Polyimides Films. (page 31)
- Figure 3.13. FT-IR Spectrum of Pendent Polyimides Films. (page 32)
- Figure 3.14. FT-IR spectrum of PAA(ODPA/APB/10 mol% MADA) and PAA(ODPA/APB/50 mol% MADA) (page 33)
- Figure 3.15. FT-IR spectrum of PAA(ODPA/APB/10 mol% MADA/10 mol% Zr) and PAA(ODPA/APB/50 mol% MADA/50 mol% Zr) (page 34)
- Figure 3.16. FT-IR spectrum of PI(ODPA/APB/10 mol% MADA) and PI(ODPA/APB/50 mol% MADA) (page 36)
- Figure 3.17. FT-IR spectrum PI(ODPA/APB/10 mol% MADA/10 mol% Zr) and PI(ODPA/APB/50 mol% MADA/50 mol% Zr) (page 37)
- Figure 3.18. FT-IR spectrum PAA(ODPA/APB/10 mol% MADA) and PAA(ODPA/APB/10 mol% MADA/10 mol% Zr) (page 38)
- Figure 3.19. FT-IR spectrum PI(ODPA/APB/10 mol% MADA) and PI(ODPA/APB/10 mol% MADA/10 mol% Zr) (page 39)
- Figure 3.20. FT-IR spectrum PAA(ODPA/APB/10 mol% MADA) and PI(ODPA/APB/10 mol% MADA) (page 40)
- Figure 3.21. FT-IR spectrum PAA(ODPA/APB/10 mol% MADA/10 mol% Zr) and PI(ODPA/APB/10 mol% MADA/10 mol% Zr) (page 41)
- Figure 3.22. Synthesis of Zr Pendent Polyimide. (page 42)

Figure 3.23. 300 MHz ^1H NMR Spectrum and Assignments of Zr(adsp)(dsp) (page 44)

Figure 3.24. 300 MHz ^1H NMR Spectrum and Assignments of
PAA(ODPA/APB/10 mol% MADA) (page 46)

Figure 3.25. 300 MHz ^1H NMR Spectrum and Assignments of
PAA(ODPA/APB/20 mol% MADA) (page 47)

Figure 3.26. 300 MHz ^1H NMR Spectrum and Assignments of
PAA(ODPA/APB/30 mol% MADA) (page 50)

Figure 3.27. 300 MHz ^1H NMR Spectrum and Assignments of
PAA(ODPA/APB/50 mol% MADA) (page 49)

Figure 3.28. 300 MHz ^1H NMR Spectrum and Assignments of
PAA(ODPA/APB/10 mol% MADA-10 mol% Zr) (page 51)

Figure 3.29. 300 MHz ^1H NMR Spectrum and Assignments of
PAA(ODPA/APB/20 mol% MADA/20 mol Zr) (page 52)

Figure 3.30. 300 MHz ^1H NMR Spectrum and Assignments of
PAA(ODPA/APB/30 mol% MADA/30 mol% Zr) (page 53)

Figure 3.31. 300 MHz ^1H NMR Spectrum and Assignments of
PAA(ODPA/APB/50 mol% MADA/50 mol% Zr) (page 54)

Figure 3.32. GPC Result for Polyamic Acids. (page 56)

Figure 3.33. TGA Curves of Poly(amic acid)s at a Heating Rate of $10^\circ\text{C}/\text{min}$ in air.
(page 58)

Figure 3.34. TGA Curves of Zr Pendant PAAs at a Heating Rate of $10^\circ\text{C}/\text{min}$ in air.
(page 59)

Figure 3.35. DSC Curves of PAA(ODPA/APB/10 mol% MADA),
PAA(ODPA/APB/30 mol% MADA),
PAA(ODPA/APB/50 mol% MADA) (page 63)

Figure 3.36. DSC Curves of PAA(ODPA/APB/10 mol% MADA/10 mol%Zr),
PAA(ODPA/APB/20 mol% MADA/20 mol% Zr),
PAA(ODPA/APB/50 mol% MADA/50 mol% Zr) (page 64)

Figure 3.37. DSC Curves of PI(ODPA/APB/10 mol% MADA),
PI(ODPA/APB/20 mol% MADA),
PI(ODPA/APB/30 mol% MADA),
PI(ODPA/APB/50 mol% MADA) (page 65)

Figure 3.38. DSC Curves of PI(ODPA/APB/10 mol% MADA/10 mol%Zr), PI(ODPA/APB/20 mol% MADA/20 mol% Zr), PI(ODPA/APB/30 mol% MADA/30 mol% Zr), PI(ODPA/APB/50 mol% MADA/50 mol% Zr)	(page 66)
Figure 3.39. PI(ODPA/APB/10% MADA) film before etching.	(page 68)
Figure 3.40. PI(ODPA/APB/10% MADA) film after etching.	(page 68)
Figure 3.41. PI(ODPA/APB/20% MADA) film before etching.	(page 68)
Figure 3.42. PI(ODPA/APB/20% MADA) film after etching.	(page 68)
Figure 3.43. PI(ODPA/APB/30% MADA) film before etching.	(page 69)
Figure 3.44. PI(ODPA/APB/30% MADA) film after etching.	(page 69)
Figure 3.45. PI(ODPA/APB/50% MADA) film before etching.	(page 69)
Figure 3.46. PI(ODPA/APB/50% MADA) film after etching.	(page 69)
Figure 3.47. PI(ODPA/APB/10% MADA-10% Zr) film before etching.	(page 70)
Figure 3.48. PI(ODPA/APB/10% MADA-10% Zr) film after etching.	(page 70)
Figure 3.49. PI(ODPA/APB/20% MADA-20% Zr) film before etching.	(page 70)
Figure 3.50. PI(ODPA/APB/20% MADA-20% Zr) film after etching.	(page 70)
Figure 3.51. PI(ODPA/APB/30% MADA-30% Zr) film before etching.	(page 71)
Figure 3.52. PI(ODPA/APB/30% MADA-30% Zr) film after etching.	(page 71)
Figure 3.53. PI(ODPA/APB/50% MADA-50% Zr) film before etching.	(page 71)
Figure 3.54. PI(ODPA/APB/50% MADA-50% Zr) film after etching.	(page 71)
Figure 4.1 Chemical Structure of the Anhydrides Formed in the Heating of Mellitic Acid	(page 75)
Figure 4.2. Formation of Polyamic Acid After Heat Treatment at 40°C for 5 minutes.	(page 78)
Figure 4.3. Proposed Structure of Zr Pendent Polyimide, PI(ODPA-APB-MADA-Zr).	(page 79)
Table 2.1 Synthesis Condition of ODPA-APB-MADA Polyamic acid	(page 16)
Table 3.1. GPC Analysis Results of PAA(ODPA-APB-MADA)	(page 56)
Table 3.2. Thermal Properties of PAA(ODPA-APB-MADA)	(page 58)

Table 3.3. Thermal Properties of PAA(ODPA-APB-MADA-Zr)	(page 61)
Table 3.4. DSC Result for PAA(ODPA-APB-MADA)	(page 62)
Table 3.5. DSC Result for PAA(ODPA-APB-MADA-Zr)	(page 63)
Table 3.6. DSC Result for PI(ODPA-APB-MADA)	(page 63)
Table 3.7. DSC Result for PI(ODPA-APB-MADA-Zr)	(page 63)
Table 3.8. Chemical Resistance in Organic Solvents	(page 73)
Table 3.9. Preparation of Zr(adsp)(dsp) Pendent Polyimide Films	(page 74)
Table 4.1. Comparing T_g of 3,4'-ODA and APB	(page 85)
Table 4.2. Comparing the Molecular Weight of PAA(ODPA/3,4-ODA/10 mol% MADA/10mol % Zr) and PI(ODPA-APB-10mol% MADA-10mol % Zr)	(page 85)

List of Abbreviations

AO	atomic oxygen
APB	1,3-aminophenoxybenzene
DCC	dicyclohexylcarbodiimide
H ₂ dsp	N,N'-disalicylidene-1,2-phenylenediamine
H ₂ ndsp	4-nitro-N,N'-disalicylidene-1,2-phenylenediamine
LEO	Low Earth Orbit
MA	mellitic acid
MADA	mellitic acid dianhydride
NMP	N-methylpyrrolidone
ODPA	4,4'-oxydiphthalic anhydride
3,4'-ODA	3,4'-oxydianiline
PAA	polyamic acid
PI	polyimide
XPS	X-ray photoelectron spectroscopy
Zr(adsp)(dsp)	(4-amino-N,N'-disalicylidene-1,2-phenylenediaminato)(N,N'-disalicylidene-1,2-phenylenediaminato)zirconium(IV)
Zr(ndsp)(dsp)	(4-nitro-N,N'-disalicylidene-1,2-phenylenediaminato)(N,N'-disalicylidene-1,2-phenylenediaminato)zirconium(IV)

ABSTRACT

We wish to evaluate Zr pendent aromatic polyimides based on oxydipthalic anhydride (ODPA), 1,3-aminophenoxybenzene (APB) and mellitic dianhydride (MADA) as atomic oxygen resistant materials. Eight poly(amic acid) solutions in N-methylpyrrolidone (NMP) with different anhydrides ratios were synthesized, and four of the eight poly(amic) acids allowed to react with the complex (4-amino-N,N'-disalicylidene-1,2-phenylenediaminato)(N,N'-disalicylidene-1,2-phenylenediaminato)zirconium(IV), Zr(adsp)(dsp), in the presence of dicyclohexylcarbodiimide (DCC). The resulting non-pendent polyamic acids and Zr pendent polyamic acids were cast onto glass substrate followed by thermal imidization.

Characterization of polyamic acids and polyimides were accomplished by Thin Layer Chromatography (TLC), Fourier Transform Infrared (FT-IR), Proton Nuclear Magnetic Resonance (^1H NMR) and Gel Permeation Chromatography (GPC). Their thermal properties were investigated by Thermogravimetric Analysis (TGA) and Differential Scanning Calorimetry (DSC). TLC results indicate that no free Zr complex remains following the DCC reaction. Spectroscopic results of Zr(adsp)(dsp), polyamic acids and polyimides were consistent with their proposed structures. GPC results indicate that a moderate degree of polymerization occurred. The incorporation of the ether groups and meta amino position along the polymer backbone decreased the glass transition temperatures vs. analogous polymers without APB. Their T_g 's fell in the ranges 64.1 to 74.6 °C, 57.6 to 83.1 °C, 188.3 to 242.9 °C and 198.5 to 245.3 °C for polyamic acids, pendent polyamic acids, polyimides, pendent polyimides, respectively. The zirconium pendent polyimides were less thermally stable than the parent polyimides,

being stable up to 455.53– 518.15°C and 525.61- 555.43°C, respectively, and affording char yields of 0.993-12.52 % for pendent polymers and 0% for non-pendent polymers at 700°C in air.

Multilayer films of the Zr complex pendent polyimides were made. The maximum number of layers that were made were 10, 10, 8 and 8 for PI(ODPA/APB/10 mol % MADA), PI(ODPA/APB/20 mol % MADA), PI(ODPA/APB/30 mol % MADA) and PI(ODPA/APB/50 mol % MADA), respectively. All fully imidized films passed the solvent resistance test which involved immersion in acetone, methyl ethyl ketone, toluene, 1-methyl-pyrrolidinone (NMP), dimethylsulfoxide (DMSO) and chloroform for one hour followed by a fingernail crease. Their atomic oxygen resistance was studied by Scanning Electronic Microscopy (SEM) before and after atomic oxygen erosion in a plasma asher. The SEM of Zr pendent polyimide film shows substantial erosion occurred in select regions, giving a “pitted” appearance.

INTRODUCTION

Aromatic polyimides are a class of polymers that have commercial importance and academic interest. Some unique properties, such as high thermal and thermo-oxidative stability at elevated temperature, superior chemical resistance and excellent mechanical properties are well known for this class of materials.¹ Therefore, they are being used in such applications as aircraft parts, spacecraft, packaging in printed electronic circuitry and various industrial applications.¹ However, they are difficult materials to process because of their high glass transition and softening temperatures as well as their insolubility in most organic solvents.¹ To enhance the ease of processing of these materials, flexible bonding in the polymer backbone has been introduced to lower the glass transition temperature, T_g , and still provide relatively good thermal stability.^{2,3}

Work has been directed at uncovering relationships between the chemical structure of polyimide and their glass transition temperature (T_g) value by using 1,3-aminophenoxybenzene (APB).^{3, 4, 5} These studies are aimed at acquiring insights that would identify approaches to lowering the T_g , thus making polyimides more easily manageable and processable without surrendering very much of their other outstanding characteristics.³

T_g is a characteristic temperature at which glassy amorphous polymers become flexible or rubberlike because of the onset of segmental motion.⁶ The introduction of flexible linkages into a macromolecule increases the segmental motion available and tends to lower the T_g of a polymer.³ Therefore, efforts at reducing the T_g of polyimides have focused on reducing their rigidity by the introduction of flexible linkages, such as oxygen in either or both the diamine and the dianhydride moieties.^{3,5} Studies have shown

that increasing the chain lengths in the polymers through ether linkages decrease the T_g value.^{3,5}

While the rigidity of the chain is certainly an important factor for lowering the T_g value, the position of the amino-substitution in the APB portion of a polyimide is a more dominant factor in lowering T_g than the presence of a flexible segment within the polymer. Since the difference in T_g cannot be due to difference in chain rigidity, it must reflect differences in chain interaction.

The use of meta-substituted diamines does not give the polymer the flexibility nor the additional degrees of freedom. However, the linearity of the polyimide chain will be distorted, and chain packing will be interfered. The resulting increase in volume of the polymer solution due to the interchain distance lowers the energy necessary for rotation and therefore the T_g . Recent literature has described the effect of the amino-substituted position of the ether diamine on the T_g of obtained polyimides.³ From the studies, it has shown the use of a meta-amino-substituted ether diamine in the polyimides decrease the T_g value.³

In Low Earth Orbit (LEO), altitudes of 180-650 km, satellites encounter a very low density residual atmosphere.⁷ This atmosphere is composed primarily of oxygen in an atomic state.⁸ A satellite moves through the atomic oxygen (AO) at a velocity of about 8 km/s. Although the density of AO is relatively low, the flux is high. The large flux of atomic oxygen, which is in a highly reactive state, can produce serious erosion on the polymer surface through oxidation.⁹ Thermal cycling of surfaces, which occurs when spacecraft go in and out of the earth's shadow, can remove the oxidized layer from the surface.¹⁰ The oxidation of polymers produces gaseous carbon oxides, water vapor, and

nitrogen oxides and results in material lost which can hinder system performance of the spacecraft.¹¹

The polyimide made from 4,4'-oxydianiline, ODA, and pyromellitic dianhydride, PMDA (KaptonTM, DuPont) is commonly used on exterior spacecraft and satellites surfaces for thermal control in the Low Earth Orbit environment.¹² KaptonTM is the material of choice for the outer layers of the thermal control blanket due to its light weight, flexibility, strength and IR transparency.^{12,13} However, it is prone to attack by atomic oxygen at a relative kinetic energy of 5 eV (500 kJ/mol) in the Low Earth Orbital environment.¹⁴ The erosion rate is great enough to cause significant material loss and structure failure in less than the desired 15 years operating life, if left unprotected.¹⁵

Films coated with metal oxides, such as SiO₂, are employed in the Space Station Freedom (now called the International Space Station, ISS) power system. It acts as a barrier to protect Kapton from oxidation by atomic oxygen. In both the Long Duration Exposure Facility (LDEF) and ground based laboratory tests have demonstrated that the metal oxide is an effective way to protect Kapton. However, defects on the surface of the metal oxides as a result of contaminant particle, nonuniform surface, abrasion during processing and debris impacts while in orbit allows atomic oxygen to attack and ultimately leads to complete oxidation of the underlying polyimide Kapton.^{16,17}

A modified Kapton designated as Atomic Oxygen Resistance (AOR) Kapton (manufactured by DuPont) has been proposed as a back up material for the ISS solar arrays. AOR KaptonTM is a blend of polysiloxane-polyimide which is cast from the homogeneous solution in an experimental batch process. Since the polysiloxane is distributed throughout the polyimide, metal oxide forms whenever AO exposure occurs.

In both ground-based plasma and space testing, AOR the silicon dioxide formed by AO has been demonstrated to be effective in protecting the film beneath from further oxidation. Although AOR KaptonTM possesses this attractive “self healing” property, evolution of a of volatile substance which is deposited on adjacent surfaces is a major factor limiting their use. These volatile substances form dark contaminant film, and, therefore the solar cell suffers from reduce illumination, which will greatly reduce the operation life of spacecraft.^{8, 17, 18}

In 1993, Dr. Illingsworth found that a zirconium complex showed comparable AO resistance to the silicon containing materials, but without production of volatile intermediates upon ground based plasma AO exposure. Glassy films of the zirconium material bis(N,N'-disalicylidene-1,2-phenylenediaminato)zirconium(IV), Zr(dsp)₂ were exposed to atomic oxygen in an oxygen beam facility. Upon exposure to a Kapton effective fluence of 8.8×10^{20} atoms/cm², the AO erosion was very nonuniform, occurring substantially in select regions, while the adjacent regions apparently remained unchanged. In an eroded area, the population of carbon atoms decreased, oxygen atoms increased, and zirconium atoms remain unchanged, as expected for the AO oxidation process. The films become more opaque with increased AO exposure, but only to a very small extent in the glassy areas. After extended exposure, the nonvolatile oxide, zirconium dioxide was the predominate product. X-ray photoelectron spectroscopy (XPS) examination of a pristine surface adjacent to the Zr(dsp)₂ film during AO exposure showed that no volatile Zr-containing intermediates were produced during the oxidation process¹⁹.

In addition, zirconium complexes were thought to exhibit thermodynamic and chemical stability criteria necessary for use in AOR materials: a) ZrO_2 has a standard free energy of formation of $\Delta G_f^\circ = -1042.8 \text{ KJ/mol}^{20}$ and therefore is one of the most stable metal oxides; b) organically wrapped Zr should blend better than ZrO_2 in the polyamic acid of Kapton; c) a ZrO_2 protective layer should form a similar “self-healing” property to that of Si AOR films; d) Zr(dsp)_2 has been shown to be stable at 450°C in air by thermogravimetric analysis (TGA); e) Zr is one of the more abundant elements, and is not expensive: Zr ranks 18th in terms of abundance in the earth’s crust.²¹ 99.9% purity Zr is about \$222.2/kg.²²

The Zr(dsp)_2 was first introduced into polyamic acid solution of Kapton as a polymer additive. The white, protective oxide was observed to form upon AO exposure. However, very brittle film was obtained when the concentration of Zr(dsp)_2 was increased to 4 mol%, which cracked upon imidization.²³ It was readily recognized that the phase separation and film quality were the main obstacles to achieving good AO resistance for the zirconium containing polyimide materials. Efforts were made to synthesize poly[bis(4-amino-N,N'-disalicylidene-1,2-phenylenediaminato)zirconium(IV)-co-(pyromellitic dianhydride)] copolymer, p[Zr(adsp)₂-PMDA] and poly[bis(4-amino-N,N'-disalicylidene-1,2-phenylenediamino)zirconium(IV)-co-(pyromellitic dianhydride)-co-(4,4'-oxydianiline)] terpolymer, p[Zr(adsp)₂-PMDA-ODA]. However, upon using a mixture of 10 mol% of the copolymer or terpolymer with poly(amic acid) of Kapton, only one layer of film remained uncracked upon imidization.²⁴

So, a novel mixed ligand zirconium complex, (4-amino-N,N'-disalicylidene-1,2-phenylenediaminato)(N,N'-disalicylidene-1,2-phenylenediaminato)zirconium(IV),

Zr(adsp)(dsp) ,²⁵⁻²⁷ was prepared for appending onto a premade functionalized modified polyimide for the purpose of improving the mole ratio of zirconium incorporation.²⁶⁻²⁸ Gelation during the DCC appending reaction limited the concentration of pendent complex during these preliminary trials.

Therefore, the goals of this project are to synthesis and characterize a novel class of atomic oxygen durable polymer, poly(4,4'-oxydiphthalic anhydride/1,3-aminophenoxybenzene/mellitic dianhydride), where the additional degree of freedom provided by the APB component of the polymer will, hopefully, suppress the tendency to form gel. We also hope to optimized the AO resistance of these materials, while avoiding gel formation, by binding various concentrations of Zr(adsp)(dsp) to the MADA- modified polymer chain.

2. EXPERIMENTAL

2.1 Chemicals

1,2-Phenylenediamine, 4-nitro-1,2-phenylenediamine, salicylaldehyde, zirconium(IV) n-butoxide ($[\text{Zr}-(\text{O}-n\text{-Bu})]_4$ 80% wt% solution in 1-butanol), *N,N'*-dicyclohexylcarbodiimide (DCC), and palladium on activated carbon (Pd 10%) were purchased from Aldrich. 1,3-Aminophenoxybenzene (APB) and 4,4'-oxydiphthalic anhydride (ODPA) were supplied by National Starch and Chemical Corp., and ChrisKev Company, Inc., respectively. APB and ODPA were purified by sublimation in triplicate under vacuum, and stored in a desiccator with P_2O_5 to prevent the absorption of water. The sublimation of APB was performed at 117 to 125°C, and air was blown into the cold finger of the sublimator. The sublimation of ODPA was performed at 180 to 200°C. Benzenhexacarboxylic acid (mellitic acid) was purchased from TCI, Tokyo KASEI and used as received. 1-Methyl-2-pyrrolidinone (NMP) was purchased from Aldrich. NMP was purified by heating at reflux over calcium hydride, and vacuum distilling just prior to use. Plastic supported silica plates with indicator for thin layer chromatography were obtained from Kodak.

2.2 Instruments and Experimental Methods

2.2.1 Proton Nuclear Magnetic Resonance (^1H NMR)

2.2.1.1 Molecules

The structure/ identity of Zr(adsp)(dsp) was confrimed in CD_2Cl_2 using TMS as internal standard.

2.2.1.2 Polymers

The anhydrous ethyl ether precipitated polyamic acids and Zr pendent polyamic acids powders were dissolved, very slowly, in deuterated dimethylsulfoxide ($\text{DMSO-}d_6$) with TMS as internal standard. ^1H NMR spectra of samples above were obtained using a 300 MHz Bruker NMR Spectrometer using Bruker's ICON-NMR 1.1 software at room temperature. The low concentration caused a poor signal-to-noise ratio in the ^1H -NMR spectra of polymers. To optimize the signal-to-noise ratio, different scan rates and delay times were monitored. As a result, the best scan rate and delay time wass determined to be 228 scan with a time delay of 2 seconds.

2.2.2 Thermogravimetric Anaylsis (TGA)

TGA was performed with a either a Seiko TG/DTA 200 system (Seiko Instruments Inc.) or a TA Instruments TGA 2050 (TA Instruments Inc.). Ground polymer samples of about 5-10 mg each were examined. Absolute weight loss or relative weight

loss as a function of temperature was plotted. TGA measurements were made at a heating rate of 10°C/min in atmospheres of nitrogen or air at a flow rate of 250 mL/min.

2.2.3 Differential Scanning Calorimetry (DSC)

DSC was performed with a TA Instruments DSC 2010 (TA Instrument Inc.). For DSC analysis, the samples were contained in aluminum pans under nitrogen. The heating rates of 10°C/min were established by programming the temperature. The starting temperature for polyamic acid was 30°C and the upper limit was 100°C. The starting temperature for polyimide was 30°C and the upper limit was 550°C.

2.2.4 Molecular Weight (MW), Molecular Weight Distribution (MWD), and Intrinsic Viscosity (IV) Determination

MW, MWD, and IV of poly(amic acid) with and without Zr(adsp)(dsp) pendent polymer were conducted at NASA Langley.

The PAA solutions were prepared a few minutes before injections into the chromatograph. The powders were shaken for several hours and either heated for a total of 5 minutes or 15 minutes at about 120°C. Solubilities were determined by separating the insoluble material using a centrifuge, rinsing the insoluble portion with distilled NMP and ethanol several times, centrifuging at every step and weighing the residue after drying overnight at 100°C. Solutions were filtered through a 0.2 µm teflon filter prior to injection.

Chromatography was done in filtered and degassed, freshly distilled NMP/0.02M LiBr, on a three column bank consisting of a linear Water Styragel HT 6E column, which covers a molecular weight range from 10^3 to 10^7 g/mol, in series with a Styragel HT 3 column, which covers the range from 5×10^2 to 3×10^4 g/mol. The Waters 150C Gel Permeation Chromatograph was equipped with a model 150R differential viscosity detector and a differential refractive index detector. The universal calibration curve used was generated with Polymer Laboratories narrow molecular weight distribution polystyrene standards having molecular weights ranging from 472 to 2,890,000 g/mol.

2.2.5 Fourier Transform Infrared Spectroscopy (FTIR)

Fourier Transform Infrared spectra were recorded on a BIO-RAD Excalibur Series FTS 3000. A thin layer film was prepared by spreading the 15 wt% poly(amic acid)/NMP solution onto a glass plate. The polymer film was then heated at 100°C, 200°C and 300°C each for one hour and submitted for spectral measurements. Changes in transmittance were recorded between 4000 and 400 cm^{-1} .

2.2.6 Preparation of Multilayer Films

Commercial scotch tape with thickness of 0.055mm was applied to the long sides of a glass slide. Then, a 15 wt% poly(amic acid)/NMP solution was used to cast a wet film between the strips of tape on the glass slide followed by using repeated smoothing fresh edges of glass slides each times. The solvent was evaporated and imidization

accomplished by heating in a programmable forced-air oven at 100°C, 200°C and 300°C for one hour. Multilayer films were prepared by repeating this process using additional layers of tape. The film was removed from the glass slide by soaking it in cold water.

2.2.7 Oxygen Plasma Asher

A plasma asher (SPI Plasma Prep II) was used to evaluate the atomic oxygen durability of the polymer films. It uses a 13.56 MHz RF discharge to create an air plasma of oxygen ions and atoms in various energy states were discharged in a glass sample chamber. The species in the plasma impact surfaces placed in the plasma at thermal energies which is much lower than the energy in space but still energetic enough for chemical reactions to occur.

2.2.8 Scanning Electron Microscopy (SEM)

Samples with a single layer of film were cut into small pieces to make the stub and coated with approximately 100 angstroms of gold. SEM photographs were taken by using a Philips 501 Scanning Electron Microscope, with a 30 KV value, 500 spot size, magnifications were 10,000K, and photos of each samples were taken at 55° tilt angle.

2.2.9 Solvent Resistance

One layer film samples were immersed in acetone, toluene, chloroform and dimethylsulfoxide (DMSO) at room temperature for a period of 1 hour. The physical condition was noted, and then they were removed and blotted dry. When completely dried, the films were tested by fingernail crease method. The films pass the solvent resistance tests if there is no change in their creasability.

2.3 Preparation of starting materials

4-Nitro-N,N'-disalicylidene-1,2-phenylenediamine, H₂ndsp

4-Nitro-1,2-phenylenediamine [8.0 g (0.075 mol)] and salicylaldehyde [17 mL (0.15 mol)] are dissolved in 80 mL of absolute ethanol, and the solution heated at reflux for 1 hour. The orange solution obtained is cooled, filtered off, washed thoroughly with absolute ethanol, then air dried to afford 24.0 g of reddish orange crystals; 80% yield.²⁵

The purity of the product is confirmed by spotting the product in methylene chloride onto a silica gel TLC plate and eluting with methylene chloride, ethyl-actate solution (7:3) against a known H₂dsp sample previously prepared. Only one spot was obtained in the resultant chromatogram.

N,N'-Disalicylidene-1,2-phenylenediamine, H₂dsp

In a 1000 mL flask, 400 mL of absolute ethanol is added to 1,2-phenylenediamine [8.0g (0.052)] and 12.0 mL (0.122 mol) of salicylaldehyde. The mixture is maintained at reflux for 8 h, and the resulting mixture is cooled, suction filtered and then washed with absolute ethanol. After the product is air dried, 8.5 g of fluffy yellow Schiff base was obtained; 45% yield.²⁵

The purity of the product is confirmed by TLC as described above. Only one spot was observed.

Zr(ndsp)₂, Zr(dsp)₂, and Zr(ndsp)(dsp) Mixture

In a 500 mL flask, 150 mL of tetrahydrofuran is added to H₂ndsp [6.0g (0.016 mol)] and H₂dsp [5.2g (0.016)], and the mixture stirred until the solid dissolved completely. Under dry nitrogen atmosphere, Zr(O-n-Bu)₄ n-BuOH [7.5 mL (0.016 mol)] is then added to the solution of Schiff bases, and stirring maintained overnight. The mixture was spotted onto silica gel TLC plate and eluted with 7:3 methylene chloride/ethyl acetate solution; three spots were observed in the resultant chromatogram. From the highest to lowest R_f spot, they are Zr(dsp)₂, Zr(ndsp)(dsp), Zr(ndsp)₂, respectively, as determined by side by side comparison with known Zr(dsp)₂ and Zr(ndsp)₂ samples.

(4-Amino-N,N'-disalicylidene-1,2-phenylenediaminato)(N,N'-disalicylidene-1,2-phenylenediaminato)zirconium(IV), Zr(adsp)(dsp)^{25,29}

Zr(adsp)(dsp) is prepared as bright yellow crystals by reacting the zirconium mixture with hydrogen gas in the presence of palladium on activated carbon (Pd 10%). The mixture in the Parr bottle is subsequently agitated for more than 24 hours in a hydrogen gas atmosphere of 70 lb/in² gauge pressure using a Parr pressure reaction apparatus. The completion of the hydrogenation reaction is confirmed by TLC of the reaction mixture with 7:3 methylene chloride/ethyl acetate as eluent. The higher R_f yellow spot (0.42) of Zr(ndsp)₂ is no longer present at the end of the reaction. Instead, a very low R_f spot (0.063) of Zr(adsp)₂ appears. The catalyst is removed by filtration through a 4 cm high Celit 545TM gel. The filtrate is rotary evaporated and then dried to yield a mixture of the three complexes Zr(dsp)₂, Zr(adsp)(dsp), Zr(adsp)₂.

The three complexes are then separated on silica gel column using methylene chloride-ethyl acetate (7:3) as eluting solution producing three bands in the column. The second band is collected and concentrated by rotary evaporation. Hexane is added to induce precipitation. The precipitate is filtered and dried to yield the mixed ligand complex, Zr(adsp)(dsp). The purity of the product is confirmed by spotting a dilute methylene chloride solution onto a silica gel TLC plate and eluting with a methylene chloride-ethyl acetate solution (7:3). Only one spot was observed in the resultant chromatogram.

2.4 Mellitic Dianhydride

Mellitic acid dianhydride (MADA) is prepared as a light brown solid from cyclodehydration of four carboxylic acids of the mellitic acid. More specifically, cyclodehydration is accomplished by heating the mellitic acid at 185°C with 100 mL/min flow of dried air (Dririte) for 20.5 hours in one apparatus. In another apparatus, it took 48 hours to prepare the mellitic acid. Ethylene glycol is heated and maintained at reflux to produce the constant heating to the sample.

The purity of the product is confirmed by its thermogravimetric analysis (TGA) curve. A one step weight lost of 5.8% is shown on the TGA curve, which is the result of 1 molecule of water removed per molecular of MADA.

2.5 Poly(amic acid) Co-polymers

***co-Poly(oxydiphthalic anhydride/mellitic dianhydride/1,3-aminophenoxybenzene),
co-PAA[ODPA/MADA/APB]***

Co-poly(amic acid) samples are prepared by allowing four different mole ratios of APB, ODPA, MADA in NMP as shown in Table 2.1. For reaction1), a 1.0: 0.9: 0.1 molar ratio is used, respectively. The three other reactions are carried out using: 2) 1.0: 0.8: 0.2, 3) 1.0: 0.7: 0.3, and 4) 1.0: 0.5: 0.5 mole ratio, respectively, to obtain poly(amic acid) with a higher mole percentage of MADA in the copolymer.

Table 2.1 Synthesis Conditions for ODPA/APB/MADA Polyamic acids

	MADA		ODPA		APB		NMP
	Weight (g)	Moles (mmol)	Weight (g)	Moles (mmol)	Weight (g)	Moles (mmol)	Total Vol (ml)
1) PAA10%	0.124	0.4	1.12	3.6	1.17	4.0	13.2
2) PAA20%	0.245	0.8	0.993	3.2	1.17	4.0	13.2
3) PAA30%	0.367	1.2	0.869	2.8	1.17	4.0	13.2
4) PAA50%	0.612	2.0	0.620	2.0	1.17	4.0	13.2

In a 25 mL round bottom flask containing a magnetic stirring bar, the ODPA and MADA are added to dry, freshly distilled NMP. Not all of the ODPA and MADA dissolve in the 5 mL of NMP added. APB dissolved in 1.0 mL of NMP is added dropwise to the stirred solution at 0°C. After finishing the addition of APB/NMP solution into the flask, the syringe is rinsed with fresh dry NMP. The solution containing 10% (mol) MADA polymer becomes clear, light tan, and viscous. However, polymerizations with higher mole percentages of MADA give clear, brownish tinted viscous solutions. Stirring of the mixtures at room temperature are continued for 2 h before the polymer solutions are stored in the cool room at temperature of about 5°C. The reaction yielded a 15.0 wt% concentration of polymer.

Poly(amic acid) powder is obtained by precipitating the polymer solution into a crystallization dish filled with stirring anhydrous ether at room temperature. The polymer is then filtered and vacuum dried at room temperature for at least two days until it reaches a constant weight.

2.6 Zirconium Pendent Poly(amic acid) Co-polymers

Zr(adsp)(dsp) Pendent of co-Poly(oxydiphthalic anhydride/mellitic dianhydride/1,3-aminophenoxybenzene), PAA[ODPA/MADA/APB/Zr]

The complex Zr(adsp)(dsp) pendent poly(amic acid) is prepared by the addition of mixed ligand complex Zr(adsp)(dsp) to the poly(amic acid) in the presence of N,N'-dicyclohexycarbodiimide (DCC). Yellow Zr(adsp)(dsp) powder is dissolved in the poly(amic acid)/NMP solution. To the resulting solution, a stoichiometric amount of DCC/NMP solution is added to the polymer dropwise from a 3 mL syringe with needle, and extra 10% amount of DCC is needed to ensure the complete reaction of complex. Tendency to form gel is greatest when addition of DCC is almost complete, and is comparable for each of the MADA concentrations. The mixture is then allowed to be stirred at room temperature for 24 h, resulting in a very viscous orange solution. After finishing the addition of DCC into the poly(amic acid) solution, the solution containing 10% (mol) Zr pendent poly(amic acid) becomes clear orange and viscous. However, appending higher mole percentages of Zr give clear, darker orange red, viscous solutions. To confirm the reaction is completed, the resulting solution is spotted onto a silica gel TLC plate adjacent to a spot of Zr(adsp)(dsp) and eluted with methylene chloride-ethyl acetate solution (7:3). No spot due to free complex was observed in the resultant chromatogram when sufficient DCC was added.

After the reaction is complete, cyclohexylurea formed as a by-product from DCC is removed by cooling the solution to 0°C and allowing the urea to crystallize. The solution is then filtered to remove the crystals.

The polymer solution is precipitated by slowly adding the pendent polymer solution into a crystallization dish with stirring anhydrous ether at room temperature. The polymer is then vacuum dried at room temperature for at least two days until it reaches constant weight.

2.7. Films

15 wt% solutions of co-PAA(APB/ODPA/MADA) in NMP are used to cast films on glass slides. Imidization of the poly(amic acid)s is then allowed to occur via heating in a forced-air oven. The polymer is heated to 100°C and held at this temperature for one hour to drive off residual water and solvent. The temperature is then increased to 200°C and 300°C each for an hour to effect conversion of the amide acids to the imides. The thin films are then allowed to cool to room temperature. Removal from the glass plates is accomplished by soaking the films at room temperature in distilled water.

3. RESULTS

3.1 Preparation of Starting Materials and Mellitic Dianhydride (MADA).

TLC data are consistent with the synthesis of N,N'-disalicylidene-1,2-phenylenediamine, H₂dsp as shown in Figure 3.1.

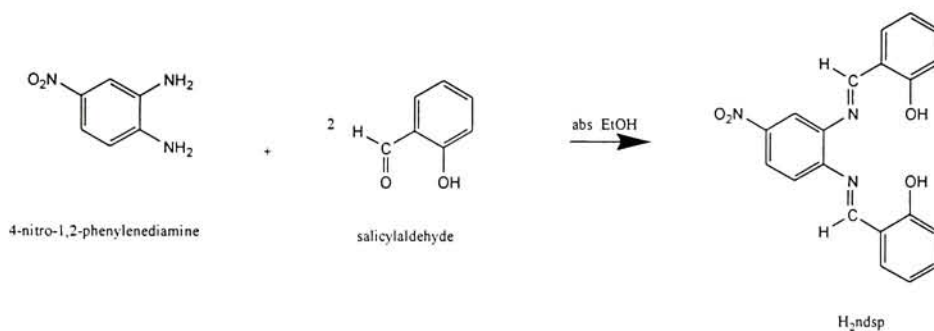


Figure 3.1. Synthesis of H₂ndsp

The data are consistent with the synthesis of N,N'-disalicylidene-1,2-phenylenediamine, H₂dsp is shown in Figure 3.2

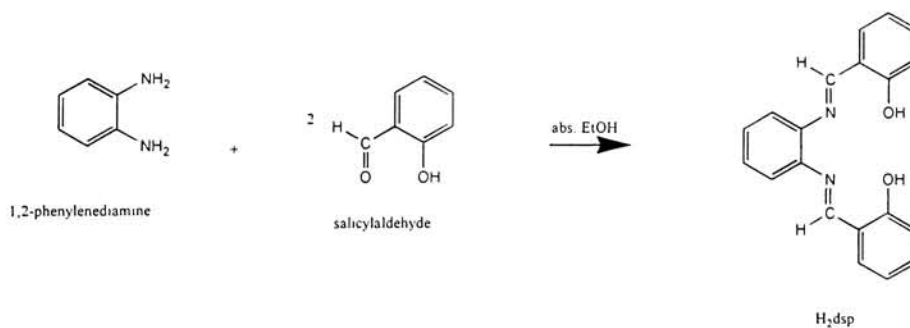


Figure 3.2. Synthesis of H₂dsp

The data are consistent with the structure of $\text{Zr}(\text{ndsp})(\text{dsp})$ as shown in Figure 3.3.

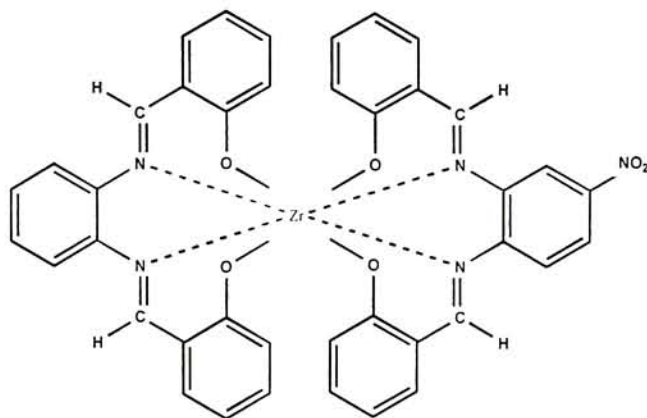


Figure 3.3. The structure of $\text{Zr}(\text{ndsp})(\text{dsp})$

The data are consistent with the structure of $\text{Zr}(\text{adsp})(\text{dsp})$ as shown in Figure 3.4.

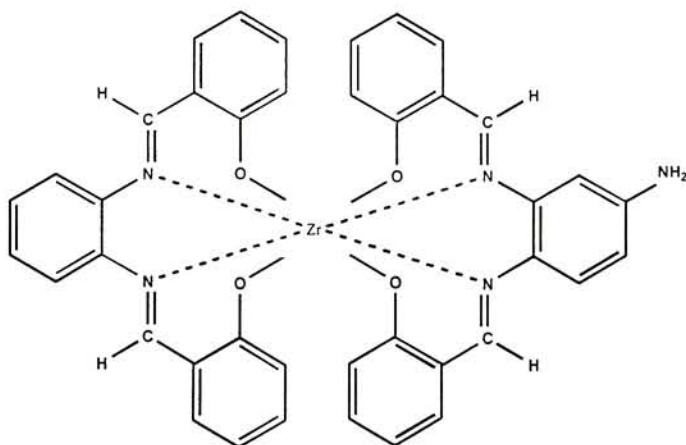


Figure 3.4. The structure of $\text{Zr}(\text{adsp})(\text{dsp})$

Figure 3.5, the TGA curve of mellitic dianhydride, shows one weight loss step before the decomposition occurs. The first step agreed well with the calculated value of one mole water lost per mole of MADA, 5.8% weight loss, which indicated the formation of trianhydride.

The TGA data are consistent with the preparation reaction of MADA and the further reaction of MADA to mellitic trianhydride as shown in Figure 3.6.

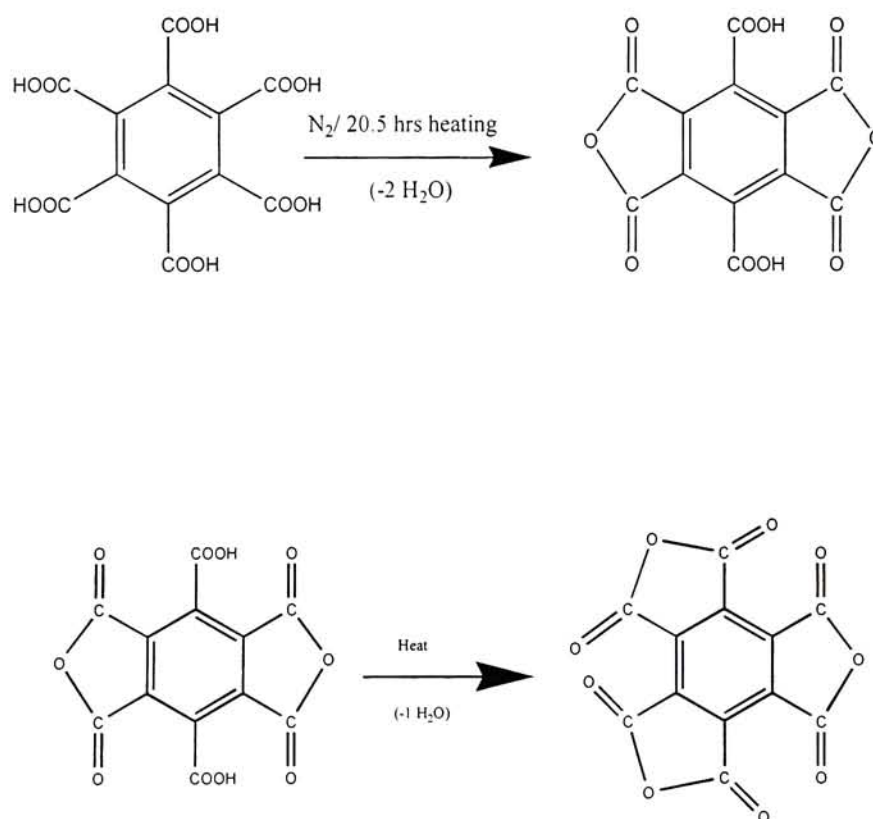


Figure 3.6. The Synthesis Reactions for MADA and 5.8% wt loss to Mellitic Acid Trianhydride

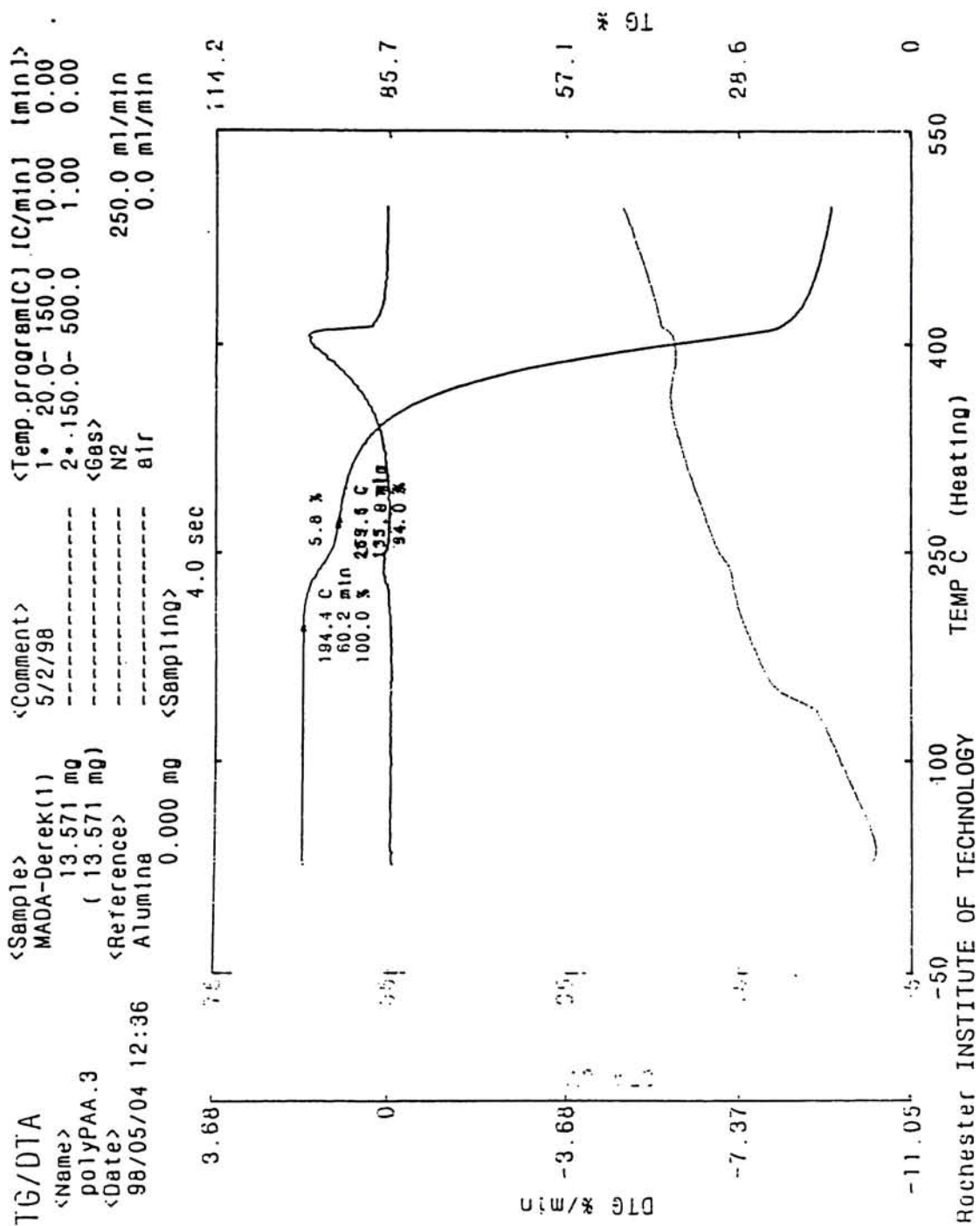


Figure 3.5. shows the TGA curve of mellitic dianhydride

3.2 Polymer Synthesis

3.2.1. ODP/ABP/MADA Poly(amic acid), co-PAA[ODP/ABP/MADA]

Color and viscosity changes are consistent with the synthesis of polyamic acid as shown in Figure 3.7.

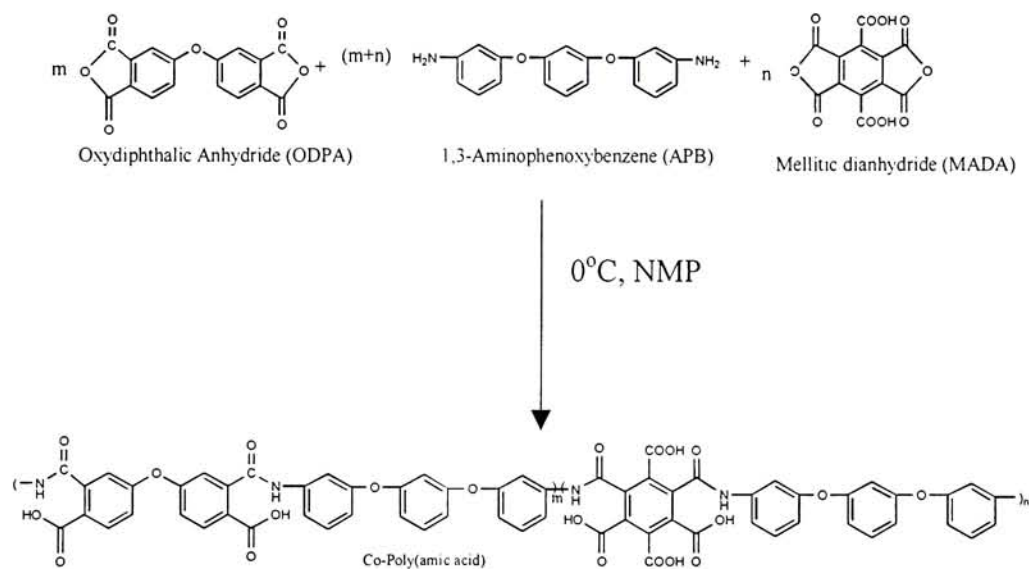


Figure 3.7. Synthesis of co-PAA[ODP/ABP/MADA]

3.2.2 Zr(adsp)(dsp) Pendent PAA[ODP/ABP/MADA], PAA(ODP/ABP/MADA/Zr)

The zirconium complex pendent poly(amic acid) was prepared by the attachment of zirconium complex Zr(adsp)(dsp) to the ODP/ABP/MADA co-polymer. The presence of the amino group in the mixed ligand complex allowed further reaction with the anhydride-like intermediate in MADA of carboxylic acid formed from the dehydration of the adjacent carboxylic acid with DCC at room temperature. TLC and

color changes are consisted with the reaction of 10 mol%, 20 mol%, 30 mol%, and 50% MADA content poly(amic acid), PAA(ODPA/APB/MADA) to form 10 mol%, 20 mol%, 30 mol%, and 50% Zr(adsp)(dsp) pendent polymers, PAA(ODPA/APB/MADA/Zr) as shown in Figure 3.8.

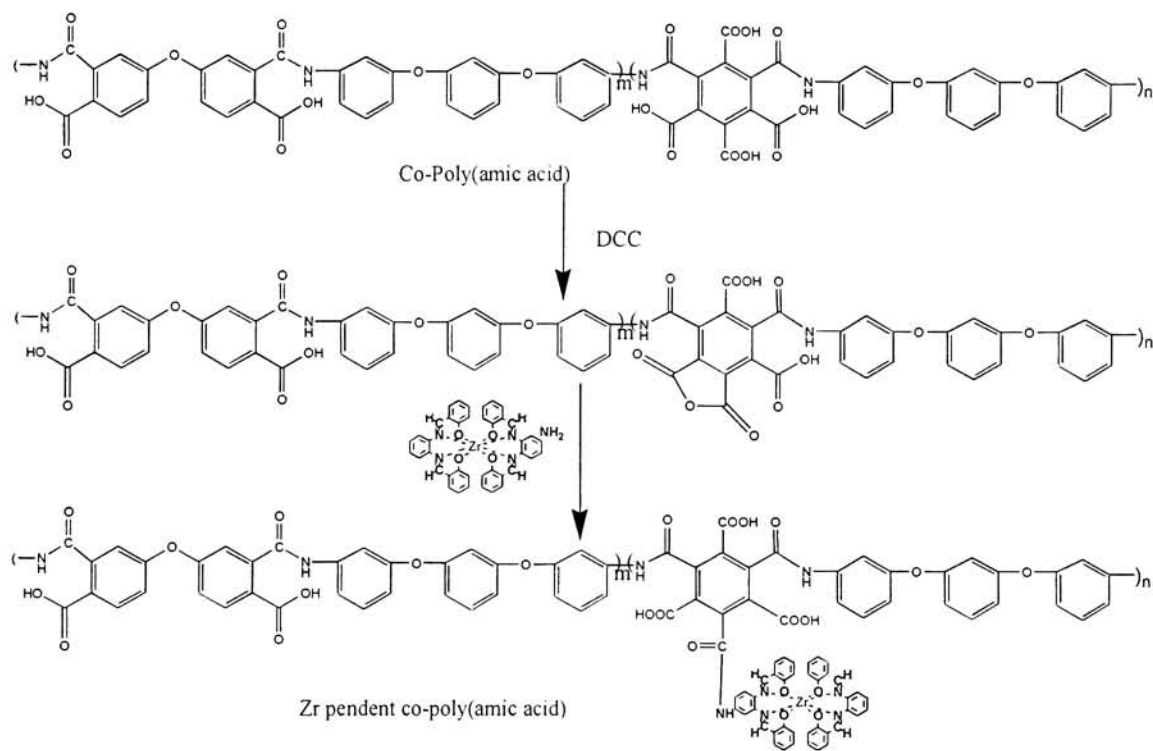


Figure 3.8. The Synthesis of Zr pendent poly(amic acid)

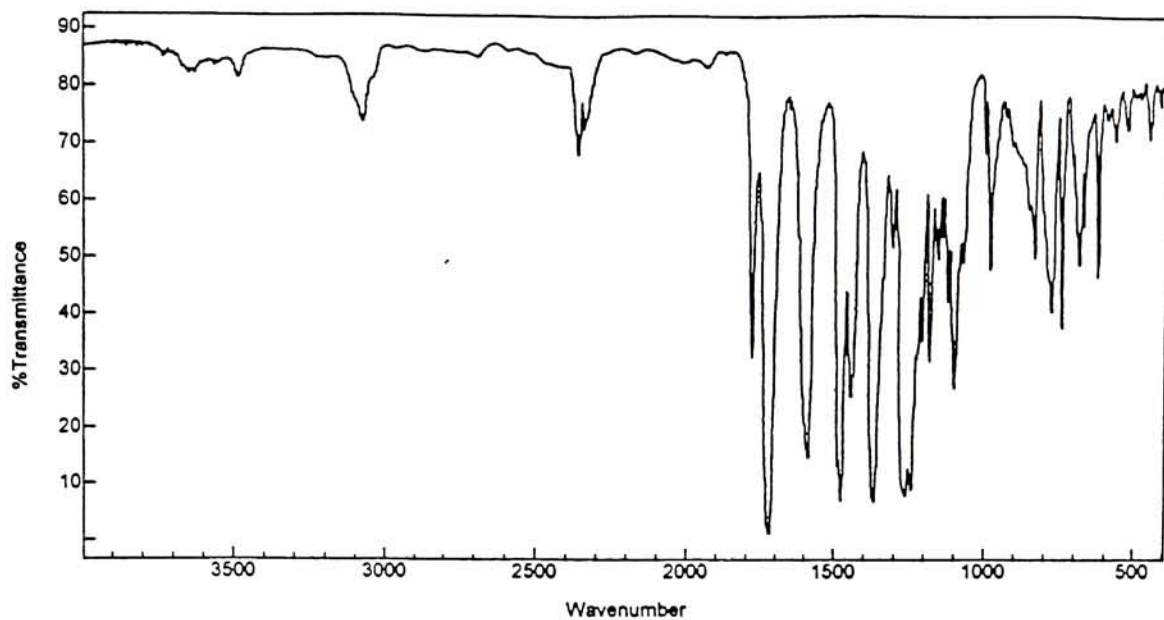
During the addition of DCC the solution of poly(amic acid) and Zr(adsp)(dsp), formation of an orange gel was sometimes observed. The tendency to form gel for the 10 mol%, 20 mol%, 30 mol%, and 50 mol% Zr pendent polymers was unavoidable if the purity of the monomers was sufficiently high. However, to convert the gel back to the solution again, the pendent polymer solution is heated at 40°C for 5 minutes.

3.3. Thermal Imidization of Poly(amic acid)s followed by FT-IR

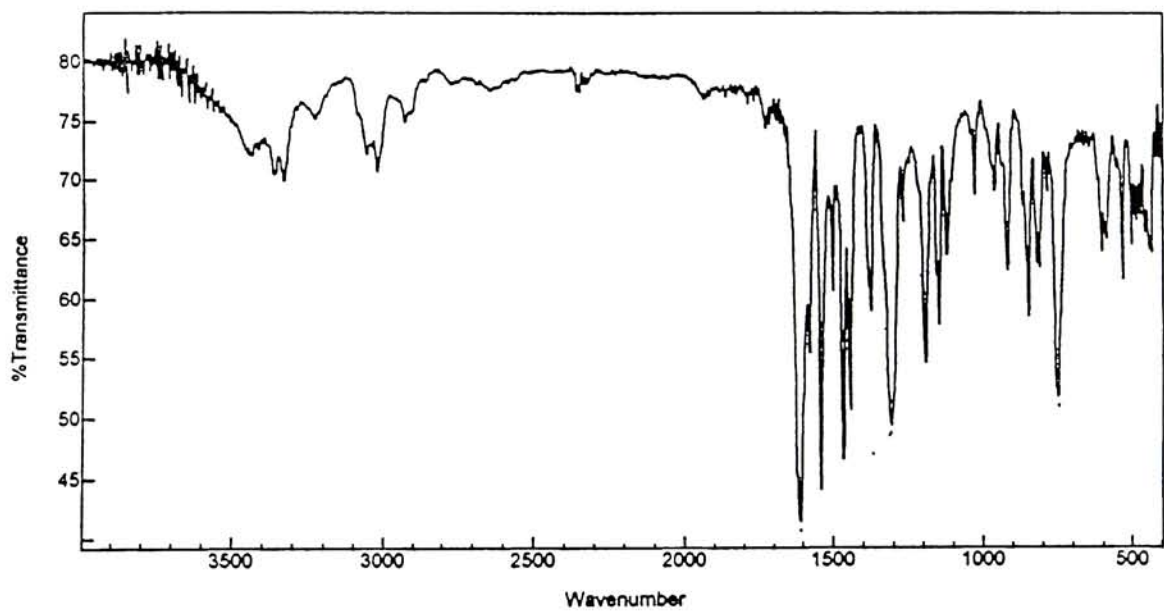
Since imidized products are not soluble in organic solvents, FT-IR was chosen to monitor the changes in structure caused by thermal treatment of co-PAA.

The FT-IR spectra of PI(ODPA/APB) and Zr(adsp)(dsp) are shown in Figure 3.9. The major characteristic peaks of the former are 1780, 1700, 1550 and 1213 cm^{-1} due to C=O (imide), C=O, aromatic ring and C-O-C stretching frequency, respectively. The major characteristic peaks for Zr complex are 3400, 1610 and 1310 cm^{-1} . When comparing the two spectra, the main absorption peaks of the polyimide is masking the Zr complex characteristic peaks, ex: 1610 cm^{-1} due to (C=N)-Zr and 1310 cm^{-1} due to (Ph-O-)Zr.

Figure 3.10 shows the FT-IR spectra for co-poly(amic acid)s prepared with the method described above. The major characteristic absorption bands in the polyamic acids are 3600, 3300, 1710, 1655, 1502, 1211 cm^{-1} , which due to NH stretch, OH stretch, carboxylic acid C=O stretch, amide C=O stretch, aromatic ring, C-O-C stretching frequency, respectively. Figure 3.11 shows the FT-IR for the pendent poly(amic acid)s. The absorption bands of the pendent poly(amic acid)s show the same characteristic peaks to the FT-IR spectra of the nonpendent poly(amic acid)s.

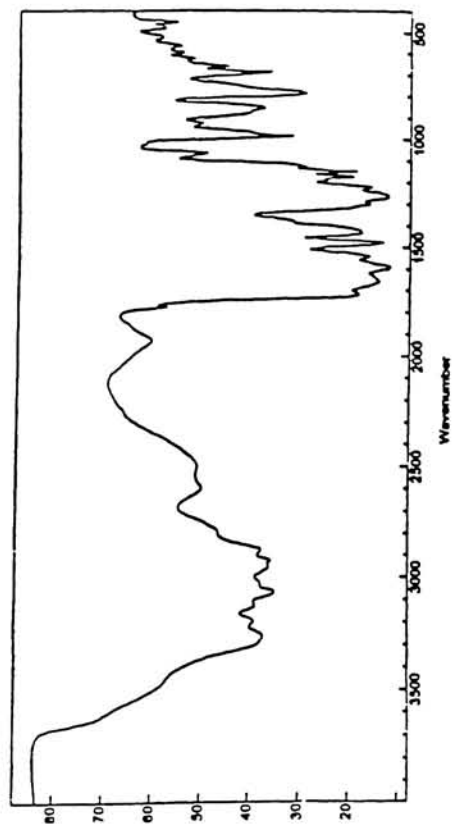


PI(ODPA/APB)

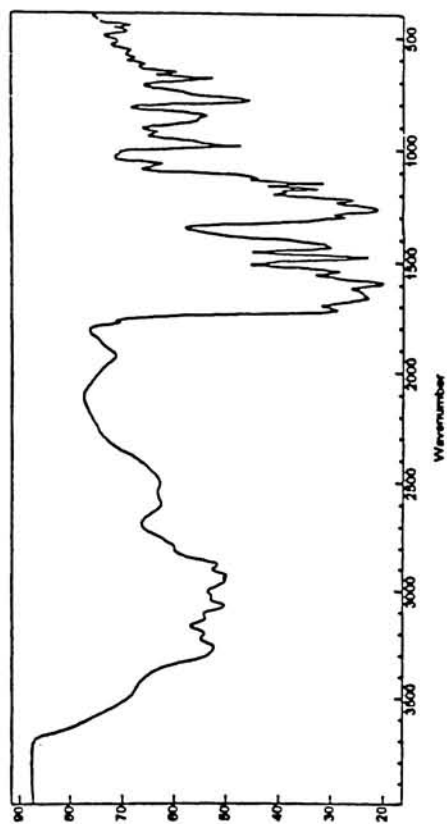


Zr(adsp)(dsp)

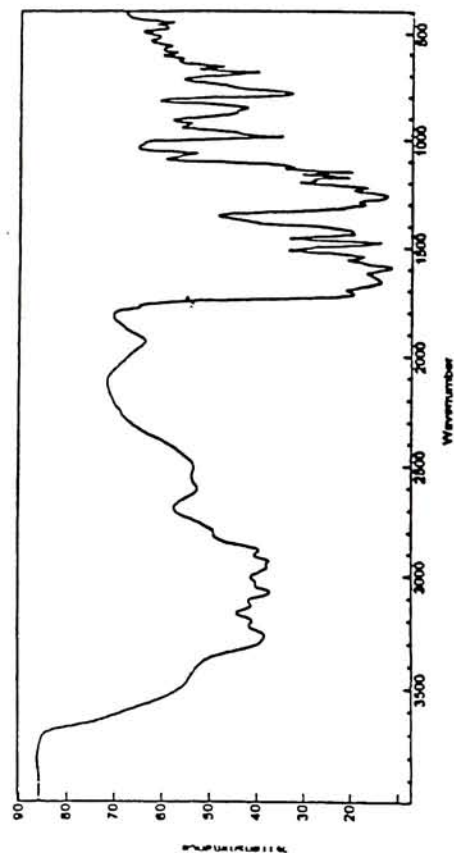
Figure 3.9. FT-IR spectra of PI(ODPA/APB) and Zr(adsp)(dsp)



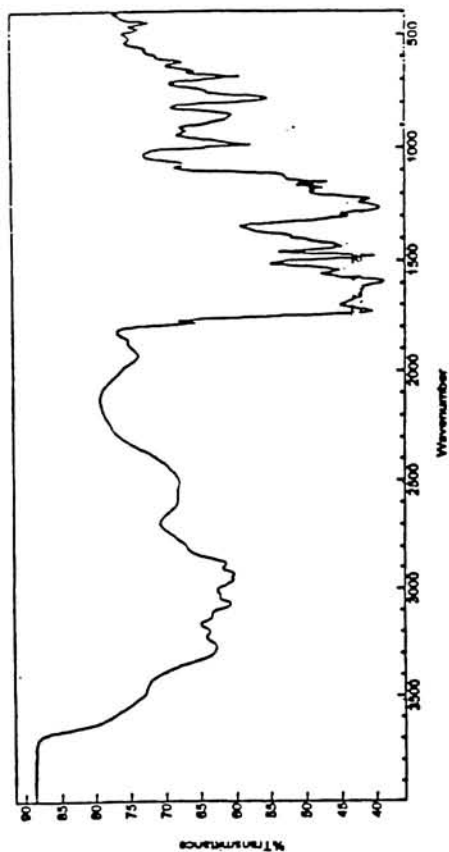
PAA(ODPA/APB/10 mol% MADA)



PAA(ODPA/APB/20 mol% MADA)

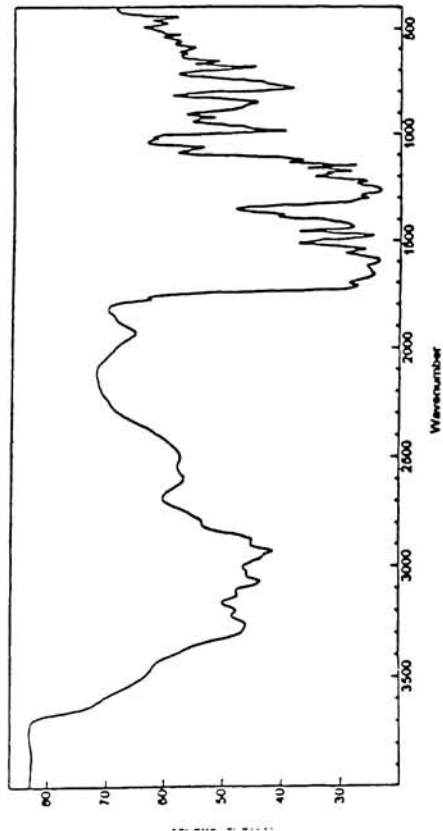


PAA(ODPA/APB/30 mol% MADA)

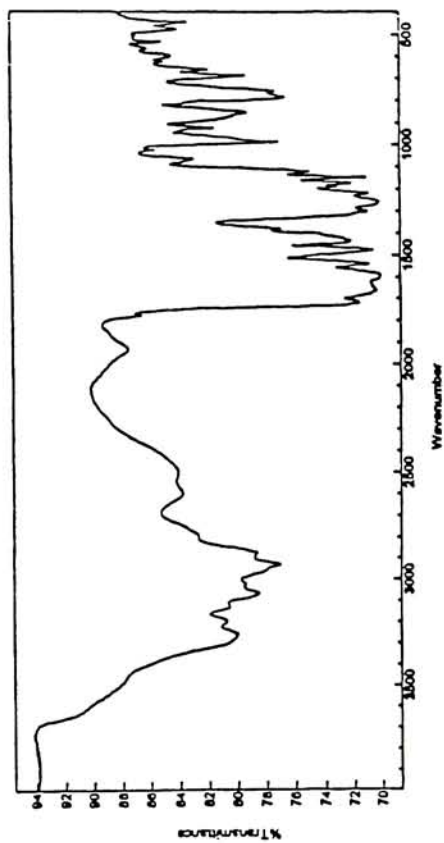


PAA(ODPA/APB/50 mol% MADA)

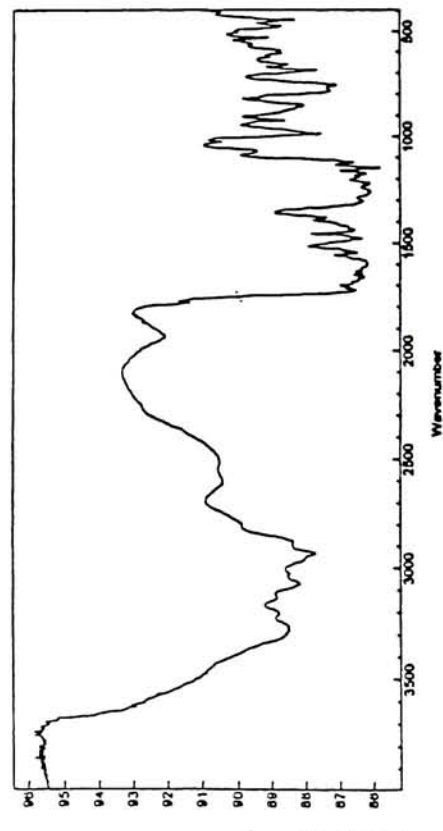
Figure 3.10. FT-IR Spectra of Polyamic Acids Films.



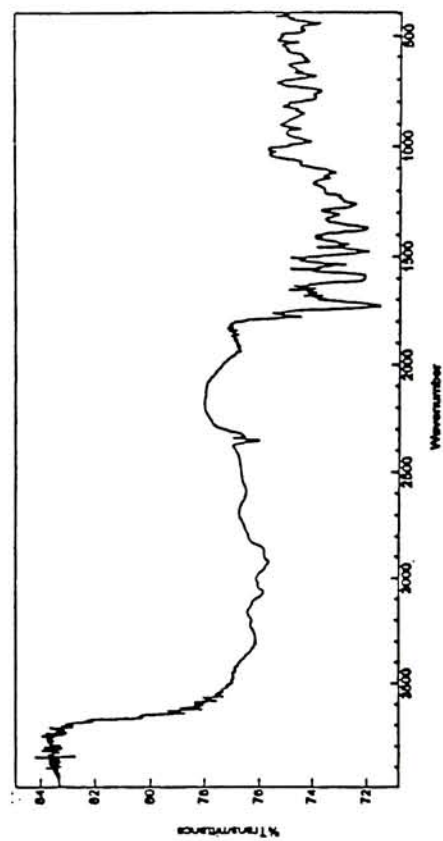
PAA(ODPA/APB/10 mol% MADA/10 mol% Zr)



PAA(ODPA/APB/20 mol% MADA/20 mol% Zr)



PAA(ODPA/APB/30 mol% MADA/30 mol% Zr)



PAA(ODPA/APB/50 mol% MADA/50 mol% Zr)

Figure 3.11. FT-IR Spectra of Pendent Polyamic Acids Films.

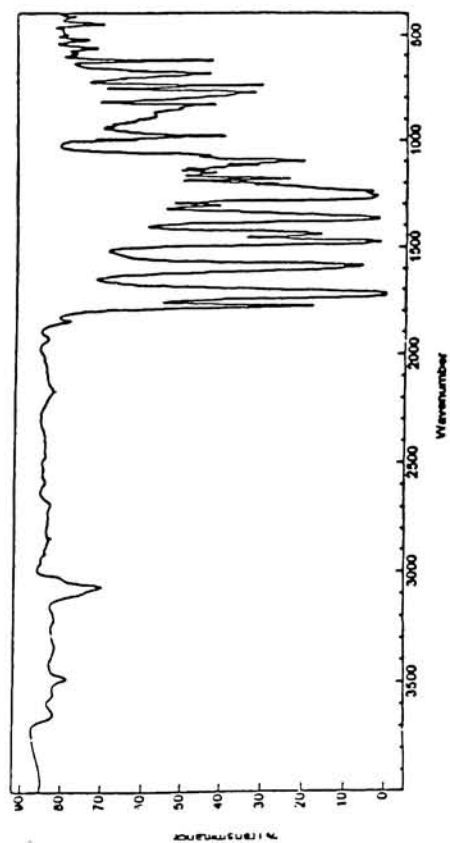
Figure 3.12 shows the FT-IR spectra for co-polyimides. The major characteristic absorption bands in their spectra are 3636, 3492, 1862, 1778, 1379, 727 cm^{-1} , which due to NH stretch, OH stretch, anhydride stretch, imide C=O stretch, C-N stretch and imide ring bending, respectively. As seen in the figure, a gradual increase in intensity of five membered aromatic imide absorption bands at 1778 cm^{-1} (C=O symmetrical stretching), 1720 cm^{-1} (C=O asymmetrical stretching), and 727 cm^{-1} (C=O) bending and decrease in intensity of amic acid absorption bands at 3636 cm^{-1} (N-H stretching) and at 1662 cm^{-1} (amide C=O stretching) were observed. An increase in the peak at 1860 cm^{-1} is due to anhydride ring formation, and increase with greater MADA concentration.

Figure 3.13 shows the FT-IR spectra for zirconium polyimides. The absorption bands of the zirconium polyimides show the same characteristic peaks to the FT-IR spectra of the polyimides. However, there is no anhydride stretch absorption at 1860 cm^{-1} observed in the FT-IR spectrum of PI(ODAP/APB/MADA/Zr) as there are for PI(ODPA/APB/MADA).

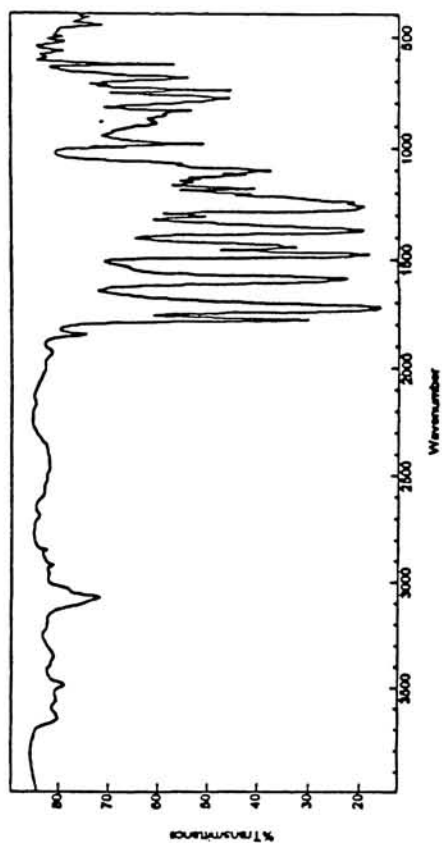
Figure 3.14 shows the FT-IR spectra of PAA(ODPA/APB/10 mol % MADA) and PAA(ODPA/APB/50 mol % MADA). Comparing the two spectra, the intensity of the peaks at 1700- 1800 cm^{-1} due to carboxylic acid (COOH) are greater for the PAA(ODPA/APB/50 mol % MADA) due to the higher MADA concentration. The peak at 1655 cm^{-1} is due to NMP's amide (C=O) group.

Figure 3.15 shows the FT-IR spectra of the PAA(ODPA/APB/10 mol% MADA/10 mol % Zr) and PAA(ODPA/APB/50 mol% MADA/50 mol % Zr). Having more MADA, the intensity at 1750 cm^{-1} (carboxylic acid C=O peak) is greater for the

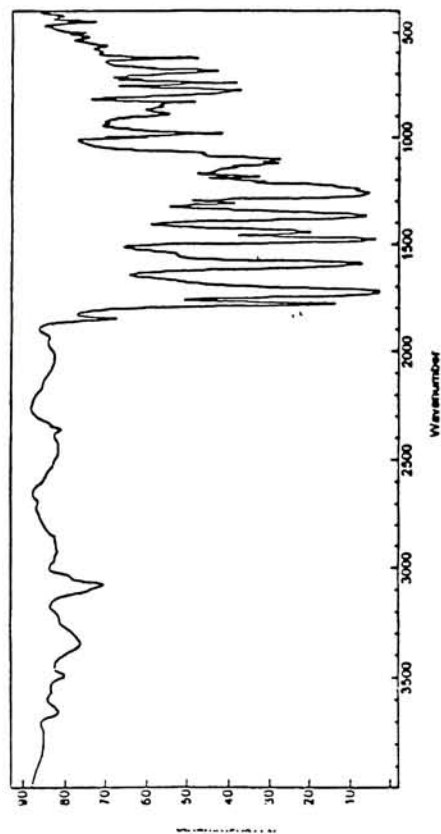
PAA with 50 mol % MADA than the corresponding C=O peak in the PAA with 10 mol % MADA. Again, the amide peak is caused by the NMP having the amide group.



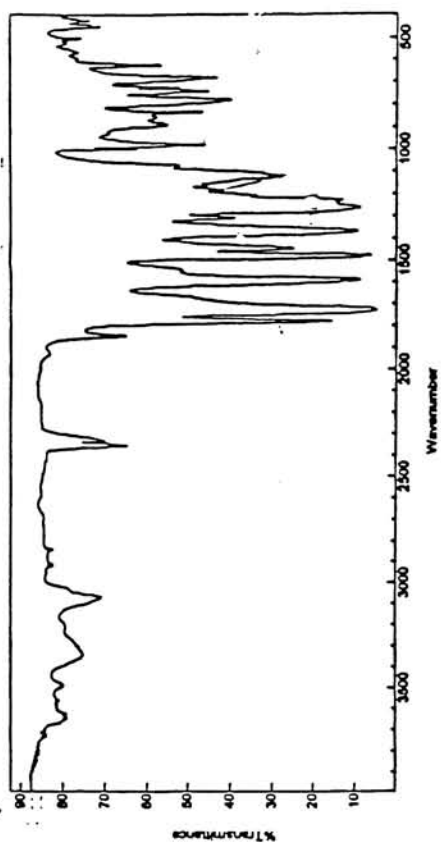
PI(ODPA/APB/10 mol% MADA)



PI(ODPA/APB/20 mol% MADA)

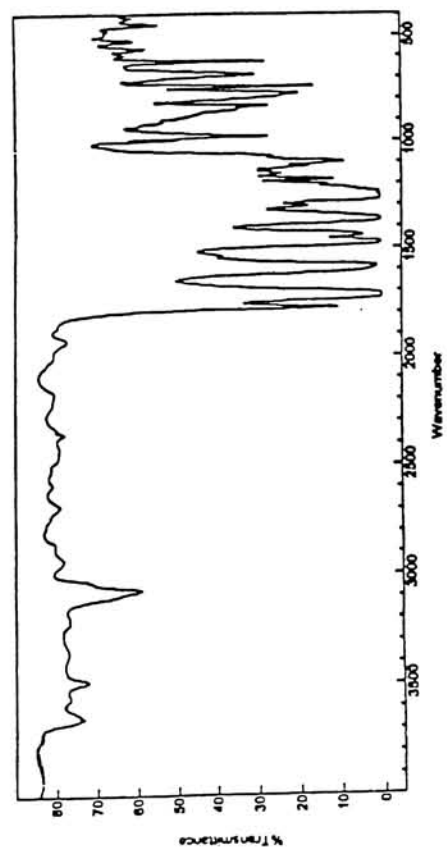


PI(ODPA/APB/30 mol% MADA)

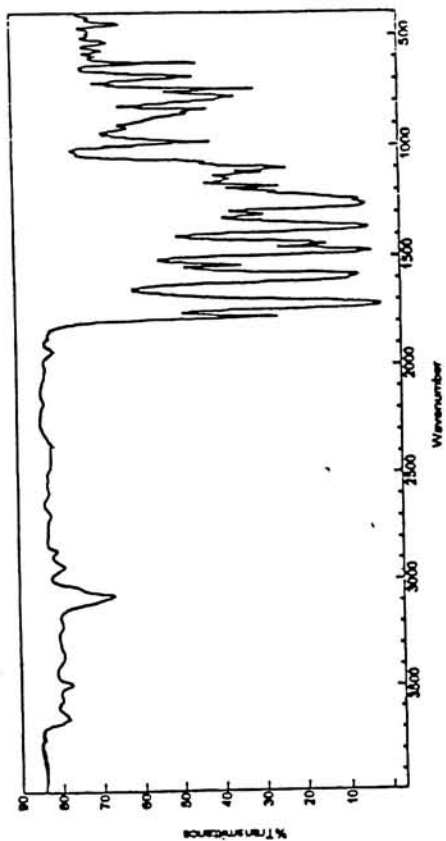


PI(ODPA/APB/50 mol% MADA)

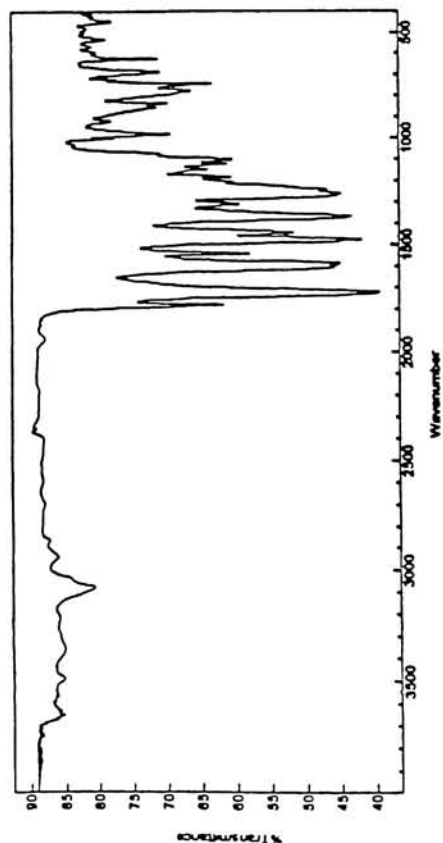
Figure 3.12. FT-IR Spectra of Polyimides Films.



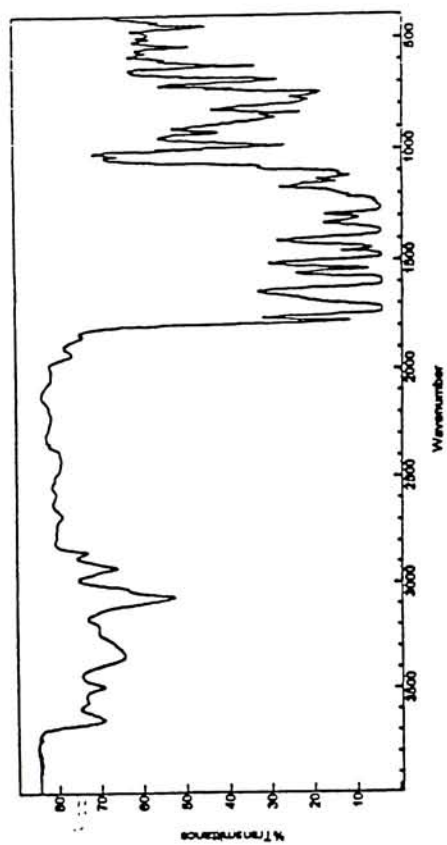
PI(ODPA/APB/10 mol% MADA/10 mol% Zr)



PI(ODPA/APB/20 mol% MADA/20 mol% Zr)

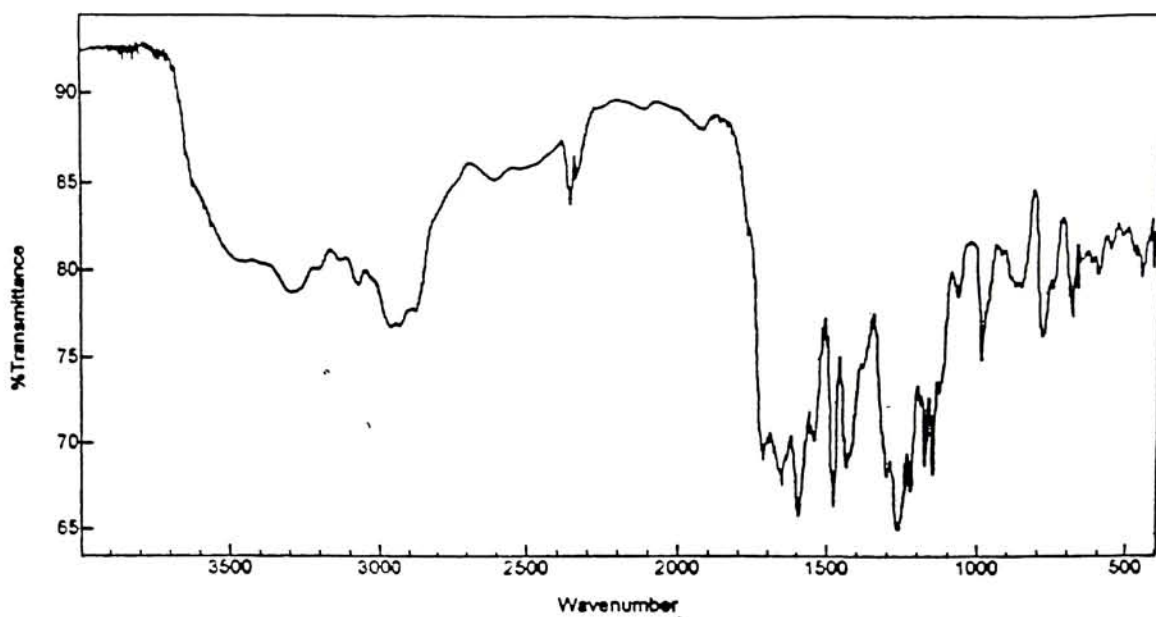


PI(ODPA/APB/30 mol% MADA/30 mol% Zr)

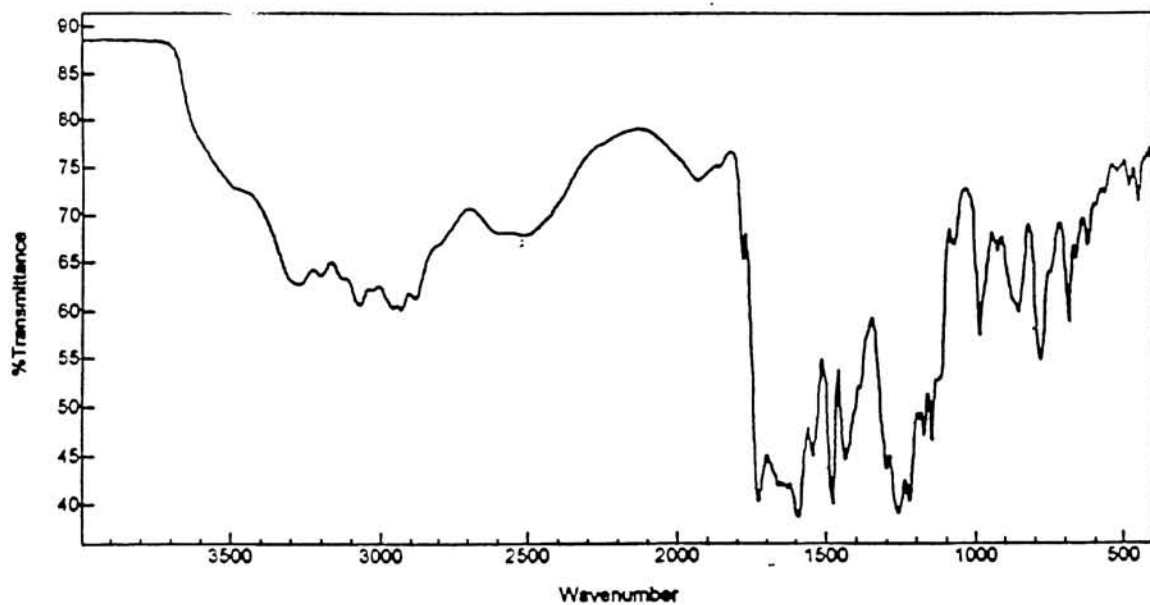


PI(ODPA/APB/50 mol% MADA/50 mol% Zr)

Figure 3.13. FT-IR Spectra of Pendent Polyimides Films.

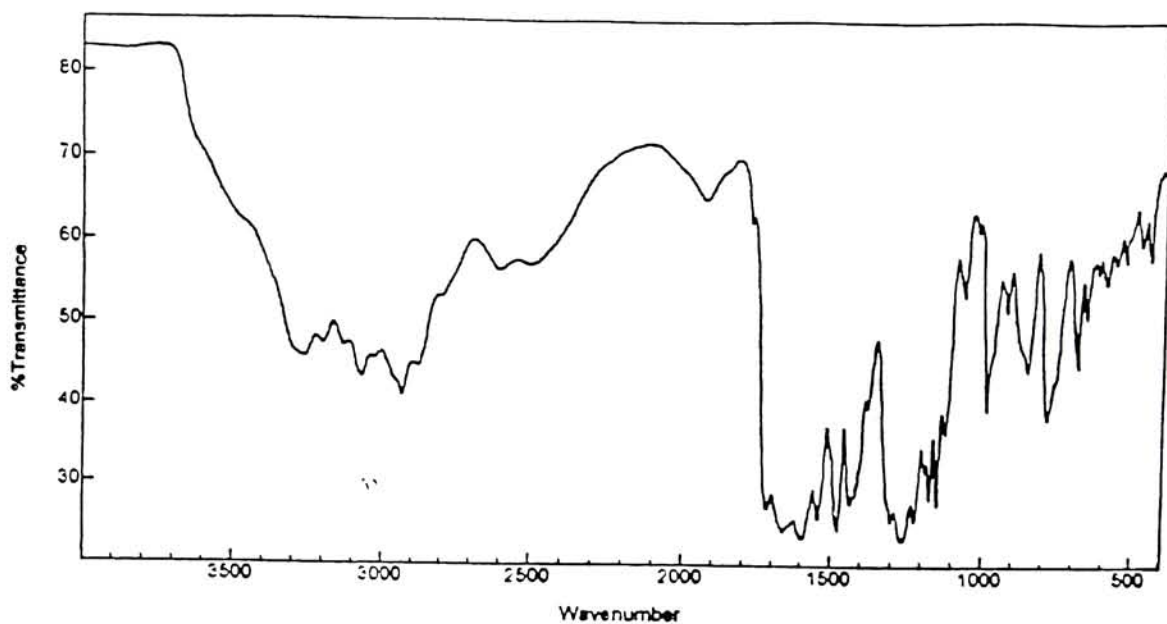


PAA(ODPA/APB/10 mol% MADA)

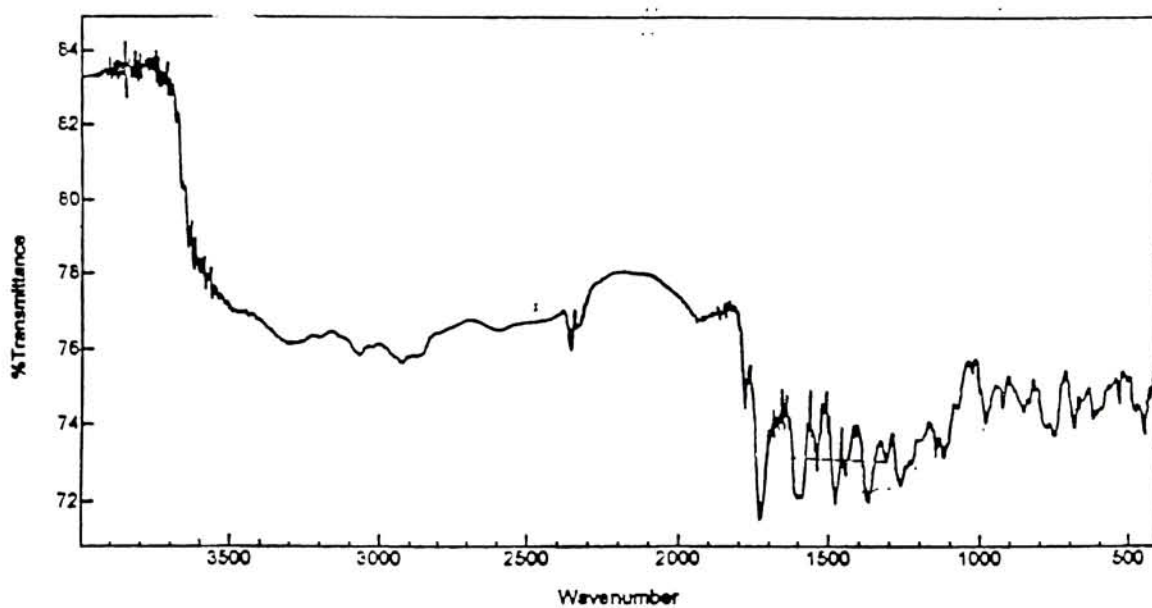


PAA(ODPA/APB/50 mol% MADA)

Figure 3.14. FT-IR spectra of PAA(ODPA/APB/10 mol% MADA) and PAA(ODPA/APB/50 mol% MADA)



PAA(ODPA/APB/10 mol% MADA/10 mol% Zr)



PAA(ODPA/APB/50 mol% MADA/50 mol% Zr)

Figure 3.15. FT-IR spectra of PAA(ODPA/APB/10 mol% MADA/10 mol% Zr) and PAA(ODPA/APB/50 mol% MADA/50 mol% Zr)

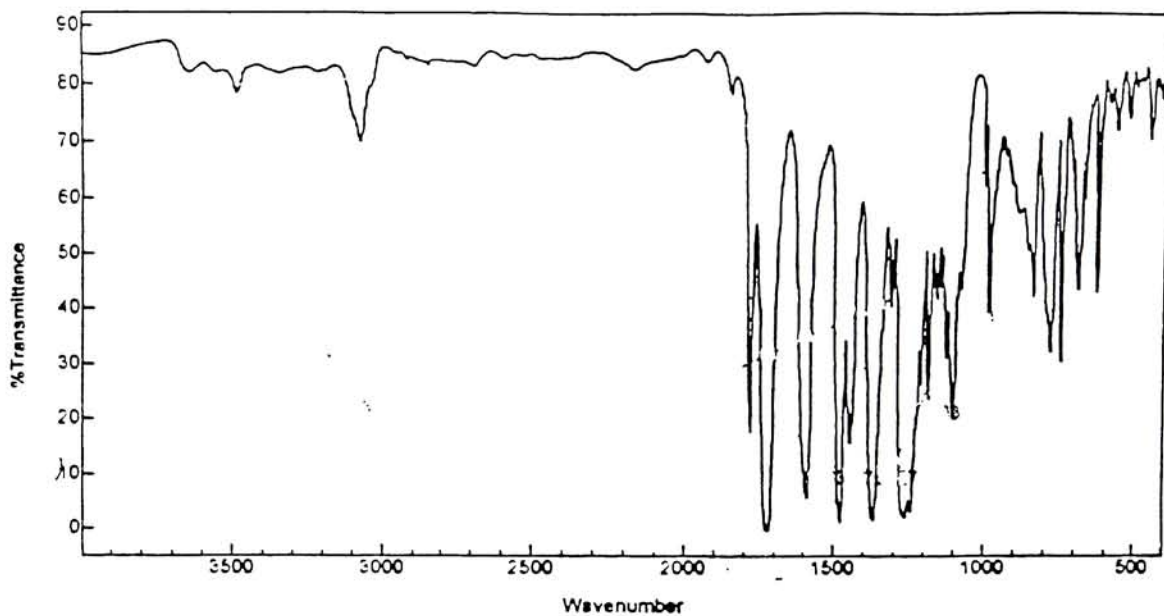
Figure 3.16 shows the FT-IR spectra of the PI(ODPA/APB/10 mol% MADA) and PI(ODPA/APB/50 mol% MADA). A noticeable difference between these two spectra is that the anhydride peak at 1800 cm^{-1} is stronger in the PI with 50 mol % MADA.

Figure 3.17 shows the FT-IR spectra of the PI(ODPA/APB/10 mol% MADA/ 10 mol % Zr) and PI(ODPA/APB/50 mol% MADA/50 mol % Zr). The later shows peaks at 3200 and 1550cm^{-1} due to a higher residual concentration of N-H bonds.

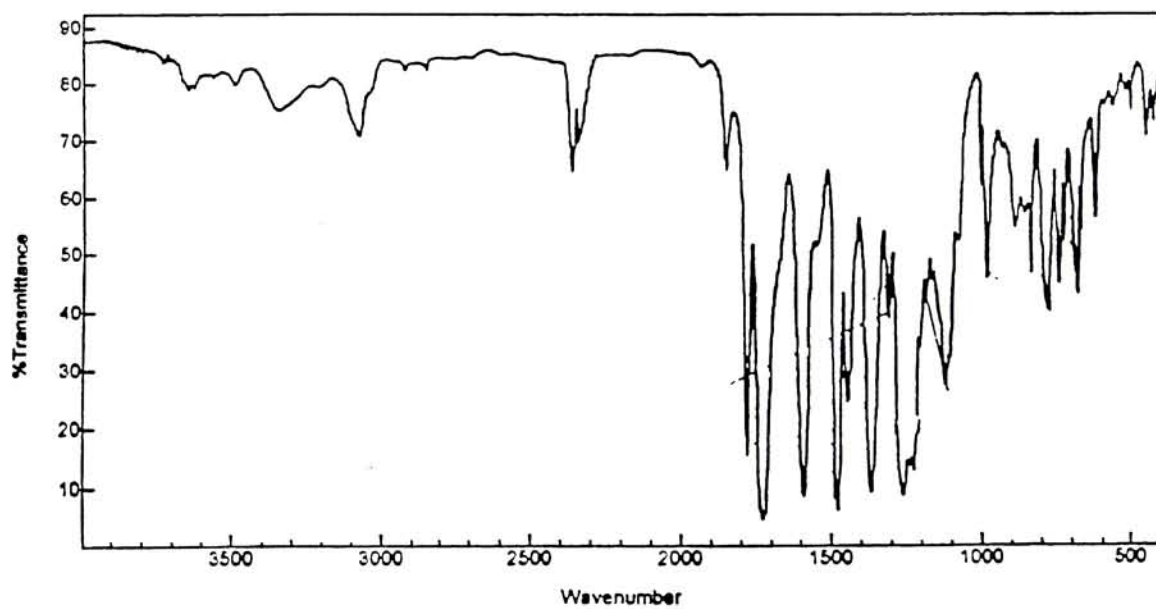
Figure 3.18 shows the FT-IR spectra of the PAA(ODPA/APB/10 mol% MADA) and PAA(ODPA/APB/10 mol% MADA/ 10 mol % Zr). There is no difference between the two spectra. Due to the NMP and the polymer, Zr peaks are masked.

Figure 3.19 shows the FT-IR spectra of the PI(ODPA/APB/10 mol % MADA) and PI(ODPA/APB/10 mol % MADA/10 mol % Zr). Attachment of Zr complex to the polymer causes the intensity of some peaks to change, e.g., there is a small anhydride ($\text{O}=\text{C}$) peak at 1860 cm^{-1} in the former, but there is no corresponding peak in the latter.

Figure 3.20 shows the FT-IR spectra of the PAA(ODPA/APB/10 mol % MADA) and the FT-IR spectrum of PI(ODPA/APB/10 mol % MADA). PAA and PI show characteristic absorption bands that are similar to the FT-IR spectra of the nonpendent poly(amic acid). There is an increase in intensity in PI due to the five member aromatic imide absorption band at 1780 cm^{-1} , and the $\text{C}=\text{O}$ symmetrical stretching at 1720 cm^{-1} . Also, there is a decrease in intensity in absorption bands at 3636 and 1662 cm^{-1} which are due to NH stretch and amide $\text{C}=\text{O}$ stretch, respectively. Less NMP would explain this, too.

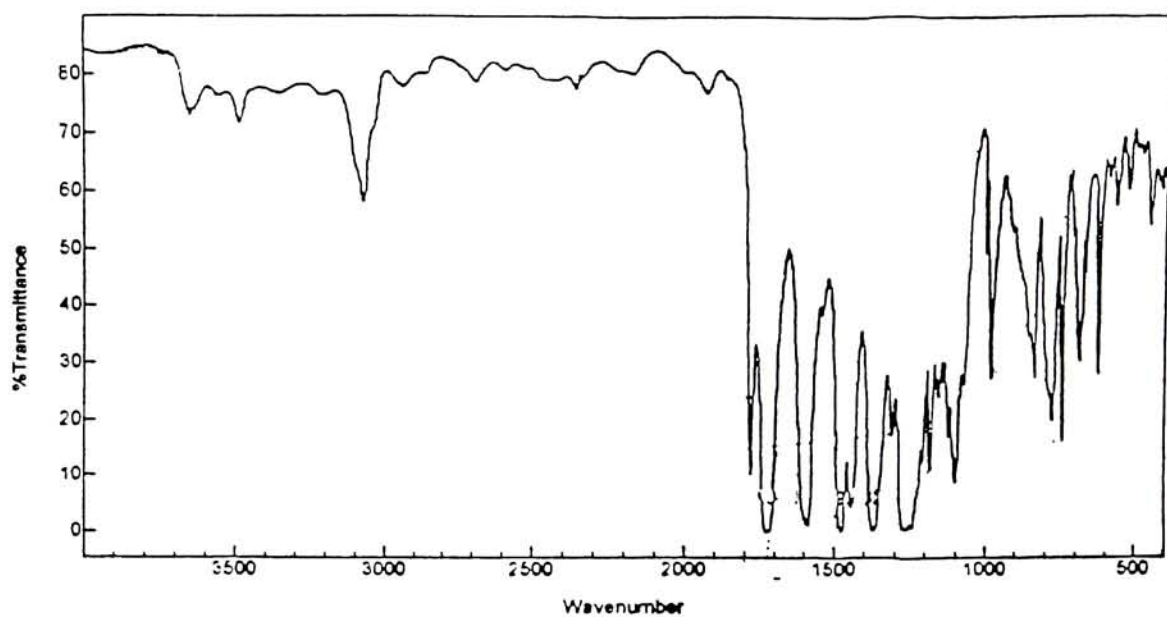


PI(ODPA/APB/10 mol% MADA)

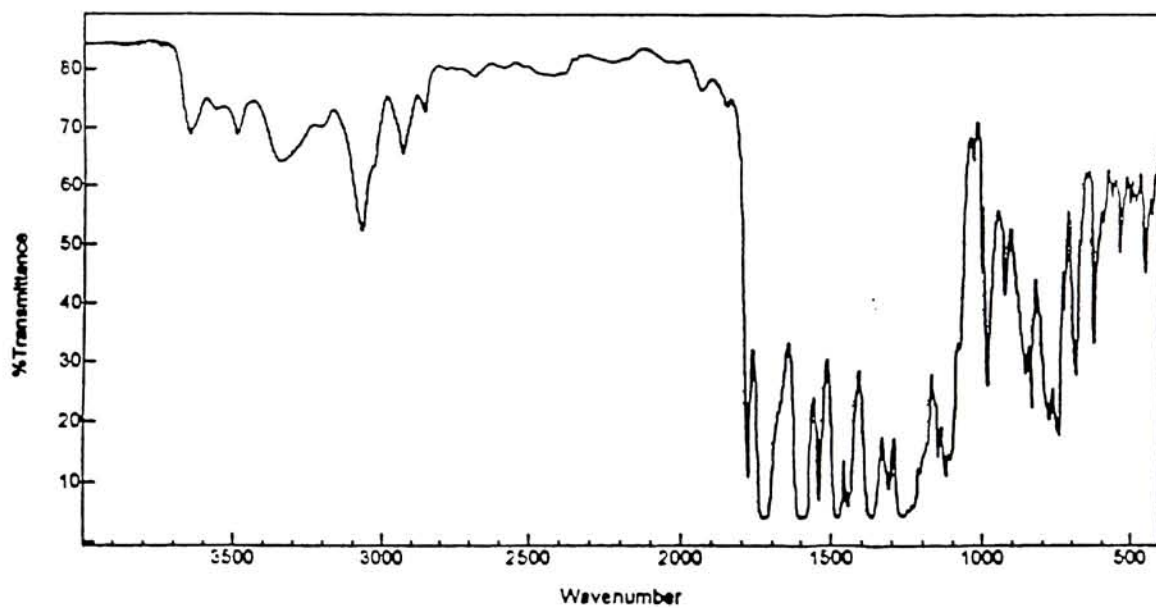


PI(ODPA/APB/50 mol% MADA)

Figure 3.16. FT-IR spectra of PI(ODPA/APB/10 mol% MADA) and PI(ODPA/APB/50 mol% MADA)

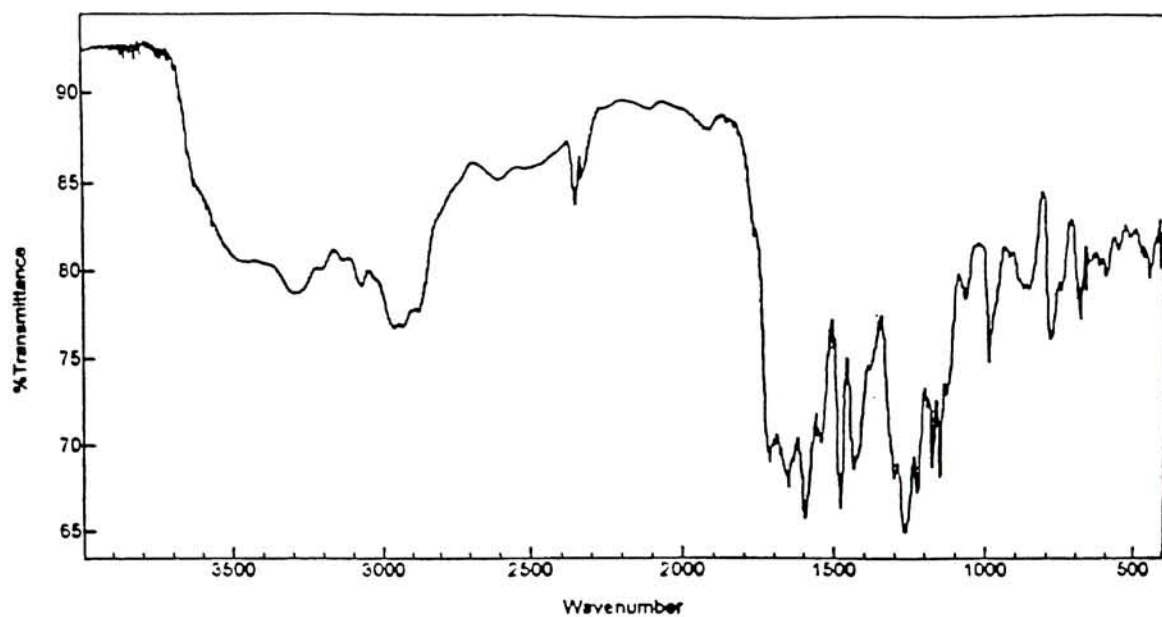


PI(ODPA/APB/10 mol% MADA/10 mol% Zr)

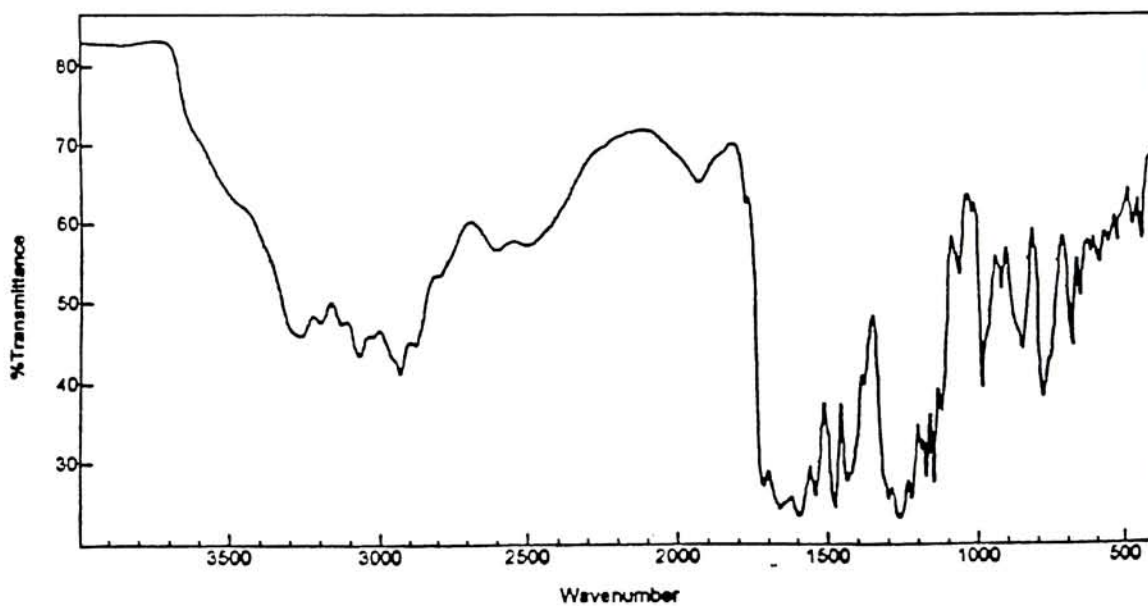


PI(ODPA/APB/50 mol% MADA/50 mol% Zr)

Figure 3.17. FT-IR spectra PI(ODPA/APB/10 mol% MADA/10 mol% Zr) and PI(ODPA/APB/50 mol% MADA/50 mol% Zr)

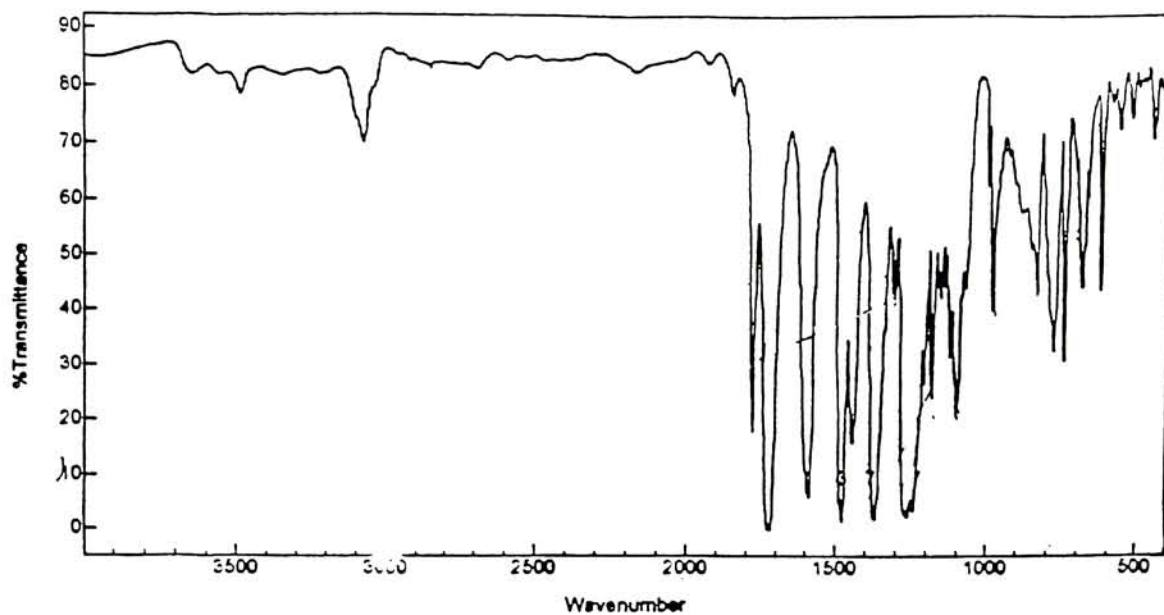


PAA(ODPA/APB/10 mol% MADA)

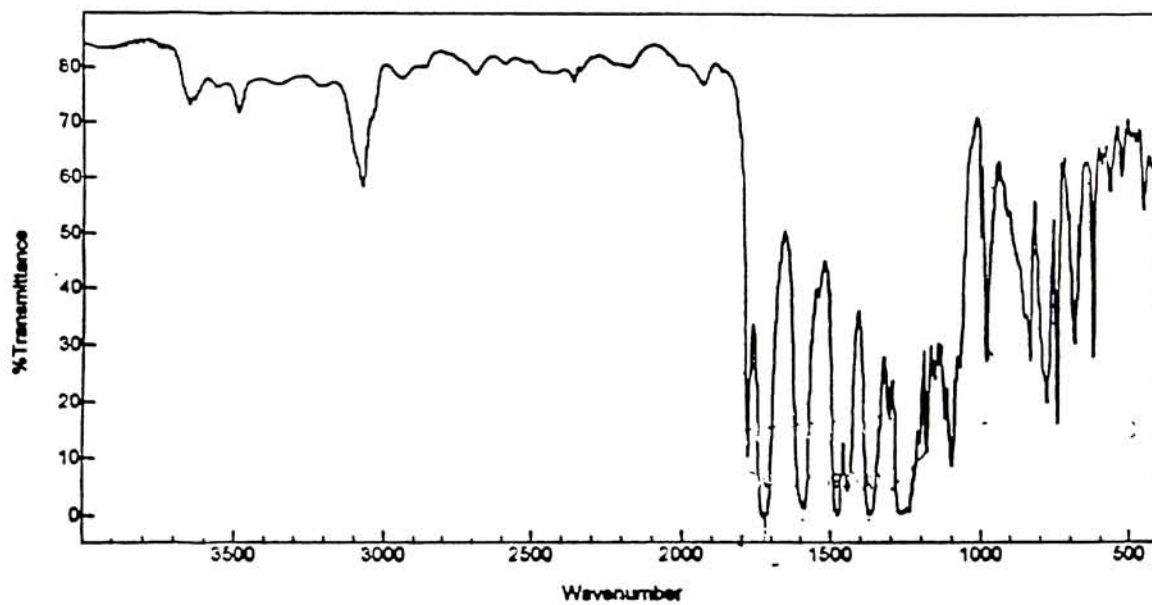


PAA(ODPA/APB/10 mol% MADA/10 mol% Zr)

Figure 3.18. FT-IR spectra PAA(ODPA/APB/10 mol% MADA) and PAA(ODPA/APB/10 mol% MADA/10 mol% Zr)

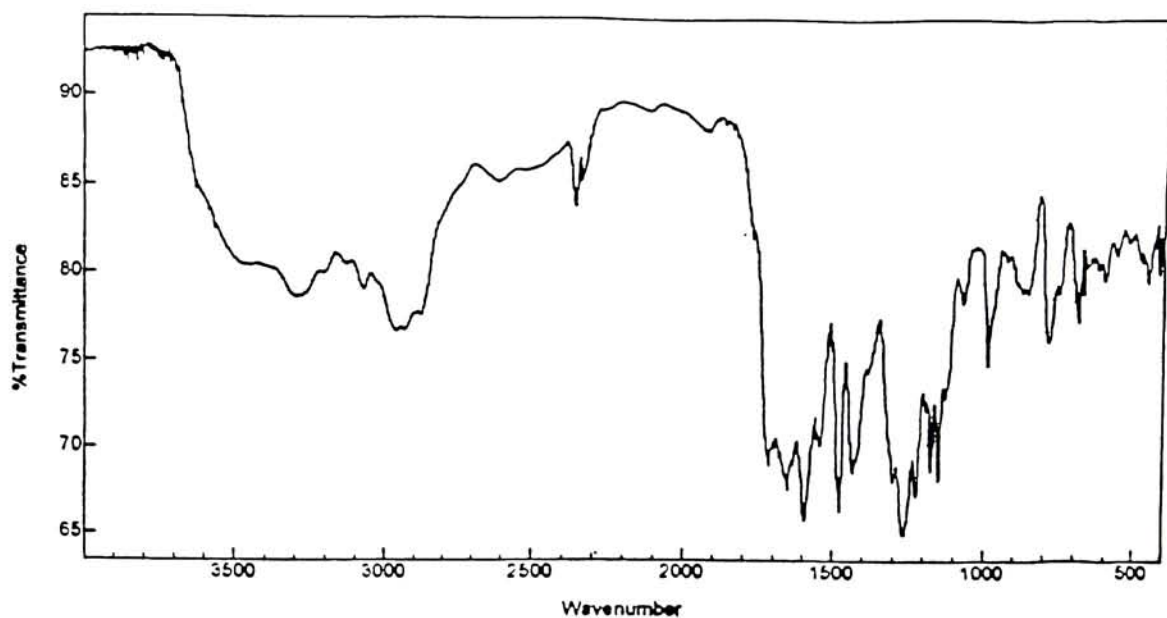


PI(ODPA/APB/10 mol% MADA)

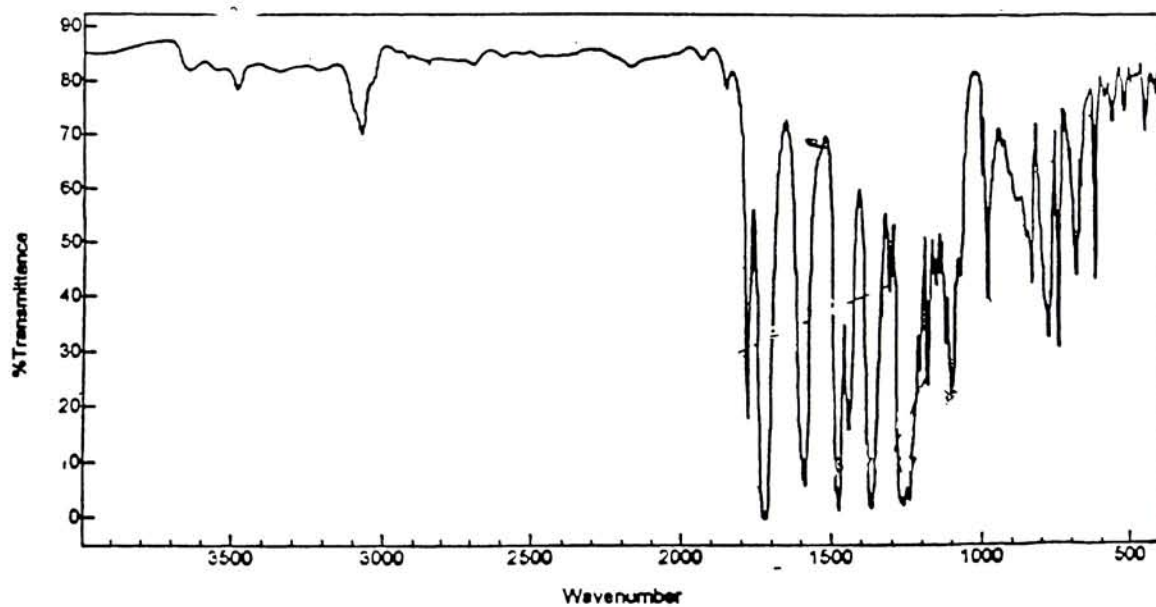


PI(ODPA/APB/10 mol% MADA/10 mol% Zr)

Figure 3.19. FT-IR spectra PI(ODPA/APB/10 mol% MADA) and PI(ODPA/APB/10 mol% MADA/10 mol% Zr)

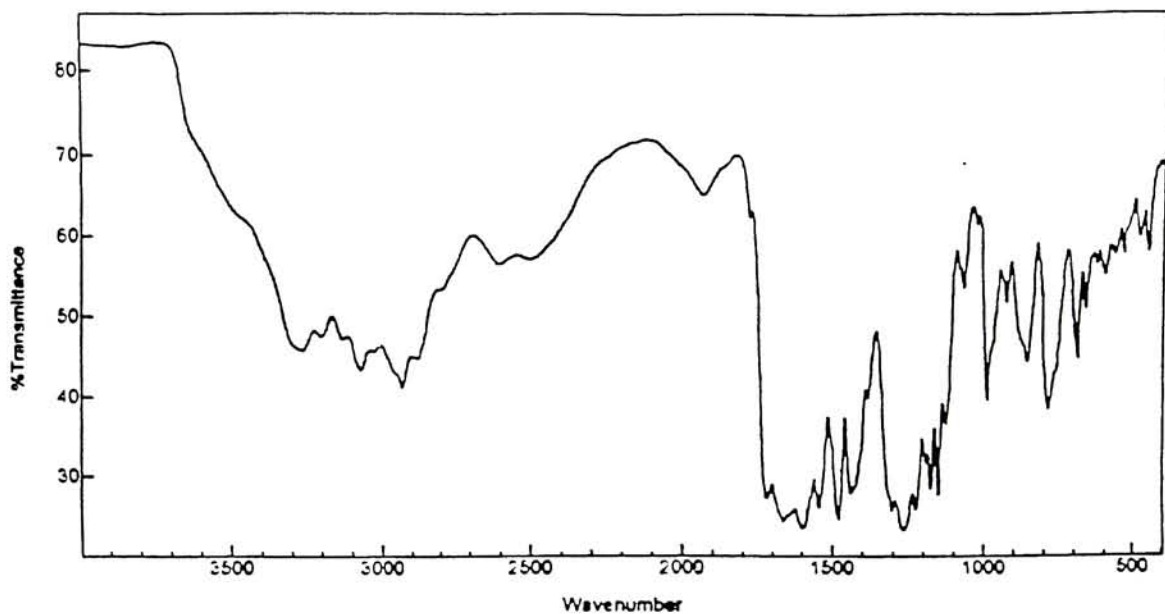


PAA(ODPA/APB/10 mol% MADA)

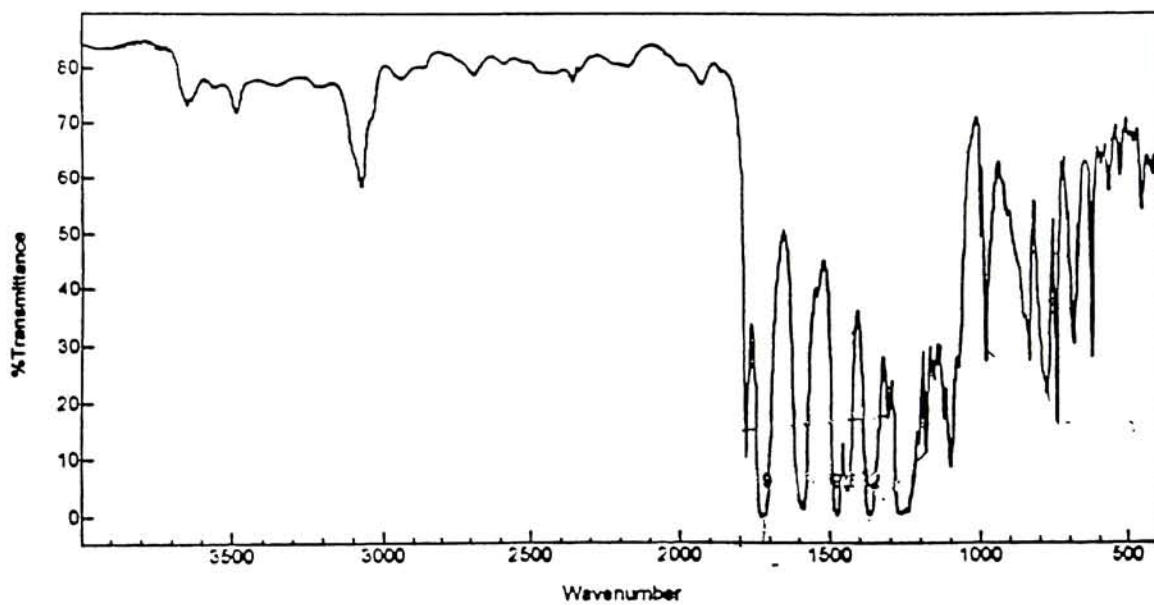


PI(ODPA/APB/10 mol% MADA)

Figure 3.20. FT-IR spectra PAA(ODPA/APB/10 mol% MADA) and PI(ODPA/APB/10 mol% MADA)



PAA(ODPA/APB/10 mol% MADA/10 mol% Zr)



PI(ODPA/APB/10 mol% MADA/10 mol% Zr)

Figure 3.21. FT-IR spectra PAA(ODPA/APB/10 mol% MADA/10 mol% Zr) and PI(ODPA/APB/10 mol% MADA/10 mol% Zr)

Figure 3.21 shows the FT-IR spectra of the PAA(ODPA/APB/10 mol % MADA/10 mol % Zr) and the FT-IR spectrum of PI(ODPA/APB/10 mol % MADA/10 mol % Zr). Comparing the two spectra, the absorption bands of the pendent poly(amic acid) show the same characteristic peaks as the nonpendent poly(amic acid) and nonpendent polyimide.

These IR data are consistent with the imidization reaction shown in Figure 3.22.

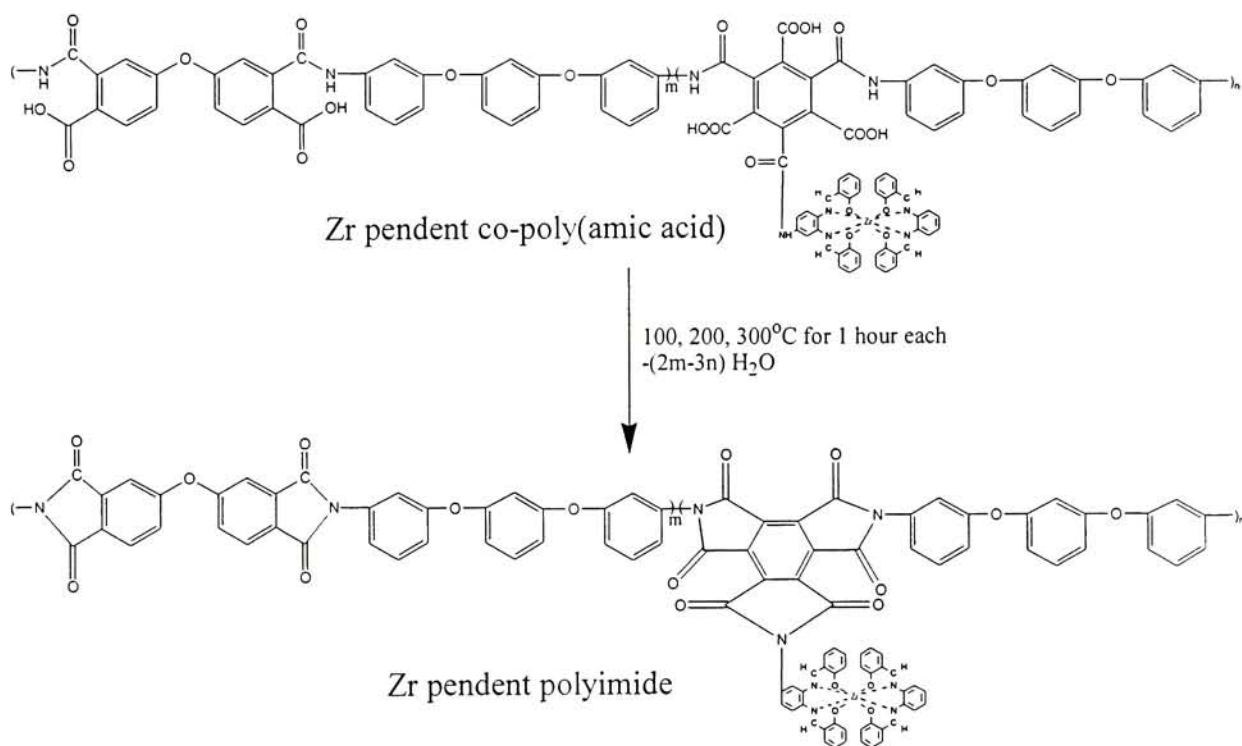


Figure 3.22. Synthesis of Zr Pendent Polyimide.

3.4 Proton Nuclear Magnetic Resonance (^1H NMR) Study

NMR can be used to facilitate the analysis of the structure of the polyamic acids. Assignment of resonance positions was usually accomplished with known substituent effects, reference spectra, and/or the 2-D NMR.

The structure of $\text{Zr}(\text{adsp})(\text{dsp})$ is shown in Figure 3.4.

Figure 3.23 is the ^1H -NMR spectrum of $\text{Zr}(\text{adsp})(\text{dsp})$. ^1H -NMR signals, in ppm downfield from TMS with the corresponding integrations in parentheses, including a singlet at 8.70 (2), two singlets at 8.46(1) and 8.33(1), multiplets which range from 7.5-7.4(4), 7.35-7.23(5), 7.03-6.86(4), 6.71-6.68(2), 6.47-6.38(4), a doublet at 5.88-5.84(2), a triplet at 5.76-5.69(2) and singlet at 5.43(1). The singlet farthest downfield is assigned to imine protons of dsp(2-) ligand and the two adjacent singlets assigned to the two imine protons of the adsp-(2-) ligand. The amino group causes the two protons in the adsp(2-) ligand to be unsymmetric and show two singlet peaks in its ^1H -NMR spectra. These downfield peaks can be assigned as the characteristic peaks of $\text{Zr}(\text{adsp})(\text{dsp})$. The multiplets, doublet and triplet are assigned to the aromatic protons of the coordinated ligands.²⁹

Current Data Parameters
 NAME Zr_adsp_dsp-7-2
 EXPNO 3
 PROCNO 1

F2 - Acquisition Parameters
 Date_ 990722
 Time 11 11
 INSTRUM spect
 PROBHD 5 mm QNP 1H
 PULPROG zg30
 TO 32768
 SOLVENT DMSO
 NS 16
 DS 2
 SWH 6172.839 Hz
 FIDRES 0.188380 Hz
 AQ 2.6542580 sec
 RG 322.5
 DW 81.000 usec
 DE 6.00 usec
 TE 300.0 K
 D1 1.0000000 sec
 P1 9.00 usec
 DE 6.00 usec
 SF01 300.1318534 MHz
 NUC1 1H
 PL1 -5.00 dB

F2 - Processing parameters
 SI 16384
 SF 300.1300000 MHz
 MDW EM
 SSB 0
 LB 0.30 Hz
 GB 0
 PC 1.00

1D NMR plot parameters
 CX 20.00 cm
 F1P 11.000 ppm
 F1 3301.43 Hz
 F2P -1.000 ppm
 F2 -300.13 Hz
 PPMCM 0.60000 ppm/cm
 HZCM 180.07800 Hz/cm

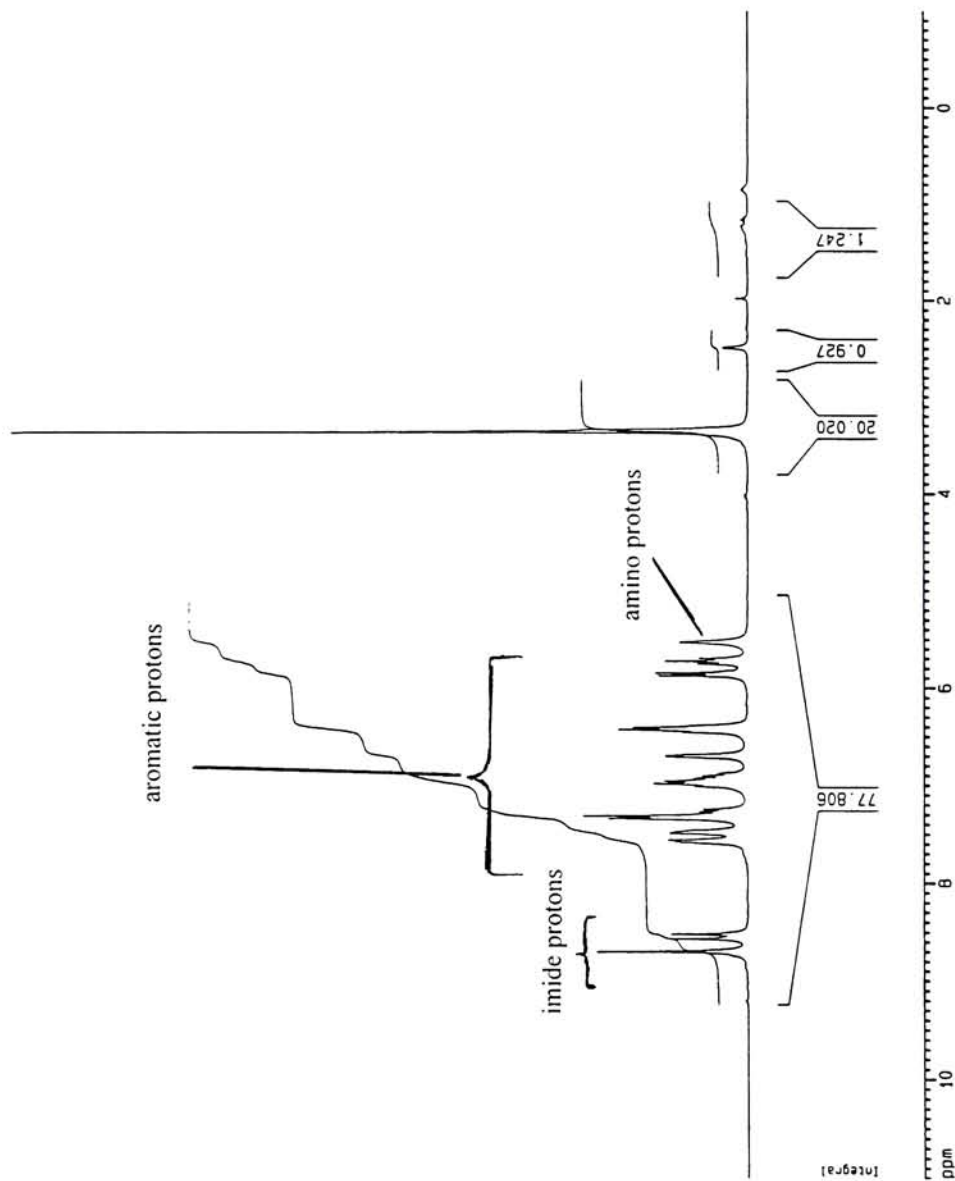


Figure 3.23. 300 MHz ¹H NMR Spectrum and Assignments of Zr(adsp)(dsp)

The ^1H NMR spectra of 10%, 20%, 30% and 50% poly(amic acid)s with its proton assignment are shown in Figures 3.24, 3.25, 3.26, and 3.27, respectively. The ^1H NMR spectra show DMSO and NMP peaks in the region 1.75 ppm to 3.95 ppm. The singlet peak due to the methyl protons of DMSO peaks at $\delta = 2.69$ ppm, and the methyl and methylene protons of NMP peaks at $\delta =$ t, 2.93; s, 2.70; t, 2.50; m, 2.0.

The spectrum of the polymer showed signals of amide protons, a, a' at 10.55 ppm. The doublet peak found at 8.00 ppm is attributed to the proton C_2 ortho to carboxylic acid group and meta to the amide group of the ODPA rings. The two singlet at 7.25 ppm is due to the proton C_1 ortho to both oxygen and carboxylic acid group or both oxygen and amide group. The overlapped two doublet at 7.00 ppm due to proton C_3 ortho to oxygen, meta to amide group, and para to carboxylic acid group. The two doublet peaks at 7.7 and 7.8 ppm are ascribable to the two benzene ring protons, b and i in the APB ring; the two doublet peak at 7.4 ppm due to proton d meta to oxygen and amide group; and the doublet peak at 6.9 ppm due to proton e ortho to oxygen and para to the amide group. In the second ring of the APB, the signal at 6.8 ppm is a singlet due to proton, f ortho to both oxygen; a doublet at 6.9 ppm is a doublet due to proton g ortho and para to the oxygen; and a singlet at 7.5 ppm due to proton h meta to both oxygens.

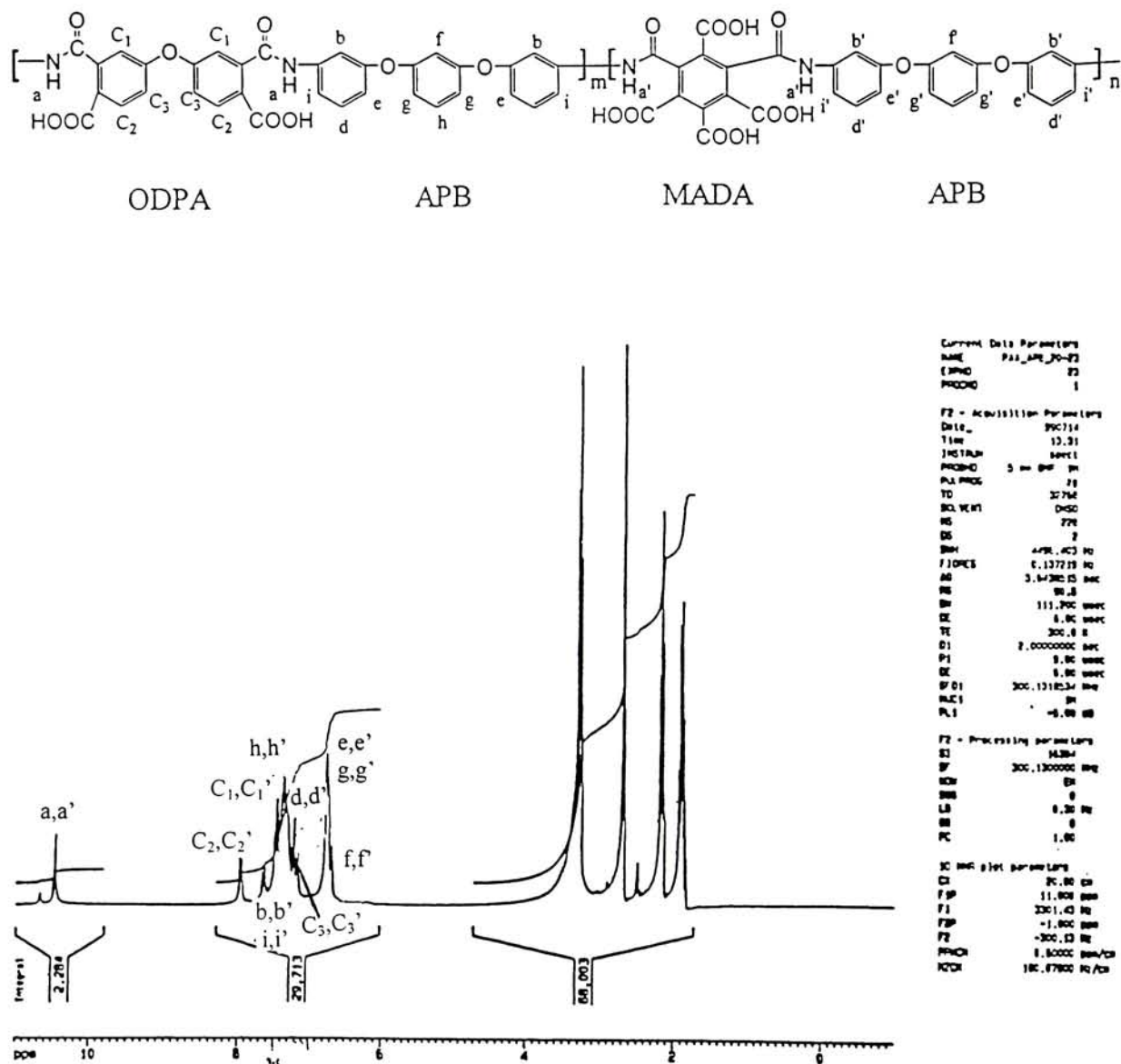


Figure 3.25. 300 MHz ^1H NMR Spectrum and Assignments of PAA(ODPA/APB/20 mol% MADA)

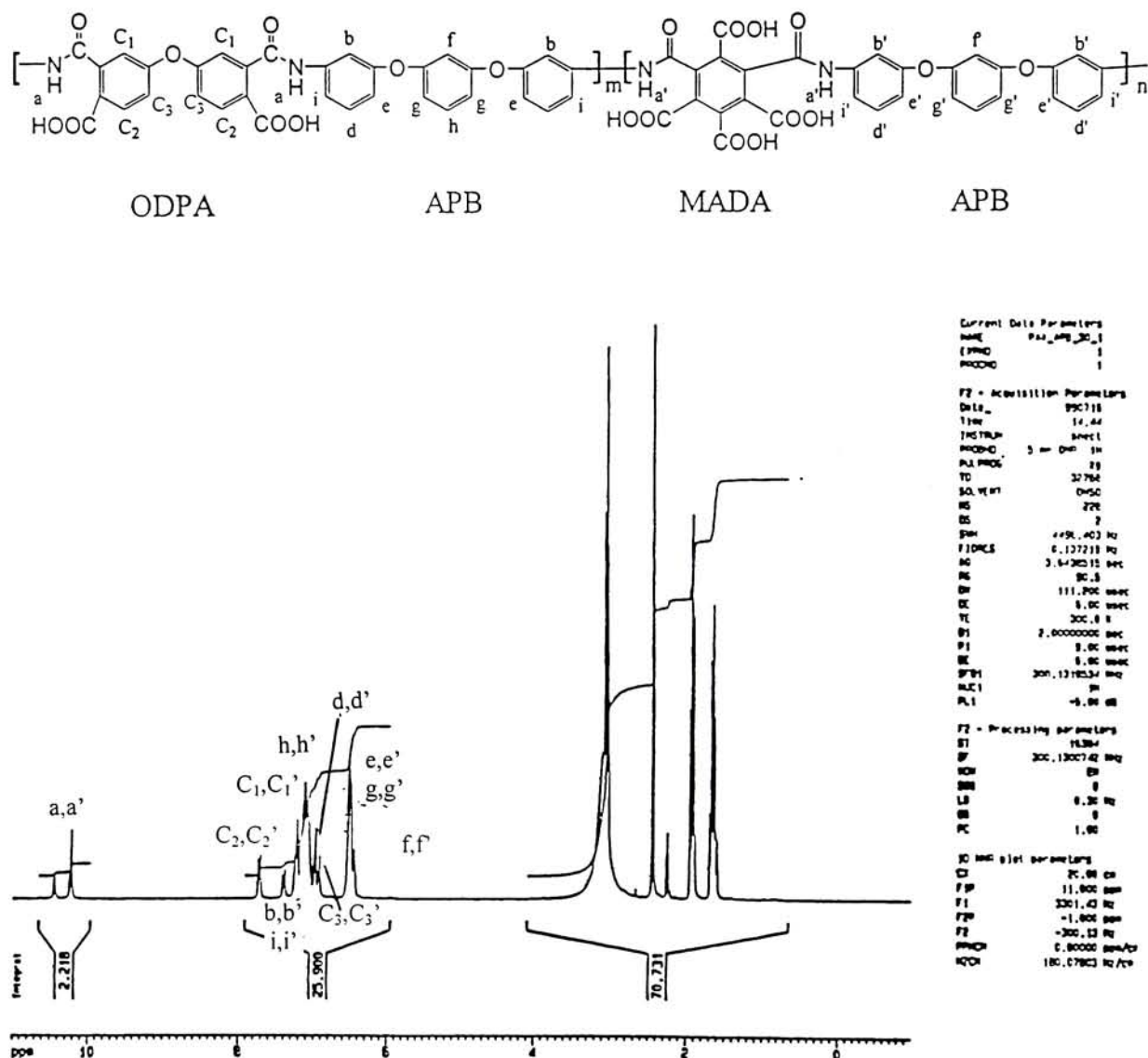


Figure 3.26. 300 MHz ^1H NMR Spectrum and Assignments of PAA(ODPA/APB/30 mol% MADA)

PAA(OPDA/APB/MADA/Zr)

The proton NMR spectrum of 10%, 20%, 30% and 50% Zr pendent polyamic acid are shown in Figures 3.28, 3.29, 3.30, and 3.31, respectively. When compared to the nonpendent polyamic acid, there are additional peaks in the pendent polymer. The three peaks from 8.4-8.7 ppm are the characteristic peaks of Zr(adsp)(dsp). The peak at 8.7 ppm is due to the two imine protons (C=N-H) in the dsp ligand, and the two singlet peaks at approximately 8.5 ppm are due to the imine protons of the adsp ligand.²⁸ The ring protons Y meta to oxygen ligand and ortho to imine group show chemical shift at 6.43 ppm, while multiplet peaks at 5.76 ppm signal are due to protons X and X' meta or para to oxygen ligand, and doublet at 5.59 ppm is due to ring proton W ortho to oxygen ligand and meta to imine group. These additional peaks, apparent in the pendent polymer, become more intense as mole percentage of pendent complex is increased.

3.5 Gel Permeation Chromatography (GPC)

Table 3.1 summarizes the GPC analysis results for selected PAA[ODPA/APB/MADA] polymers. All the samples show high average molecular weights for step growth polymers. The increase in polydispersity ratios for the polyamic acids indicates that the polymers have broader distributions of molecular weight with very high and low molecular weight species present in the solution. Based on M_z/M_w , the polydispersity index yields a value of 1.5.

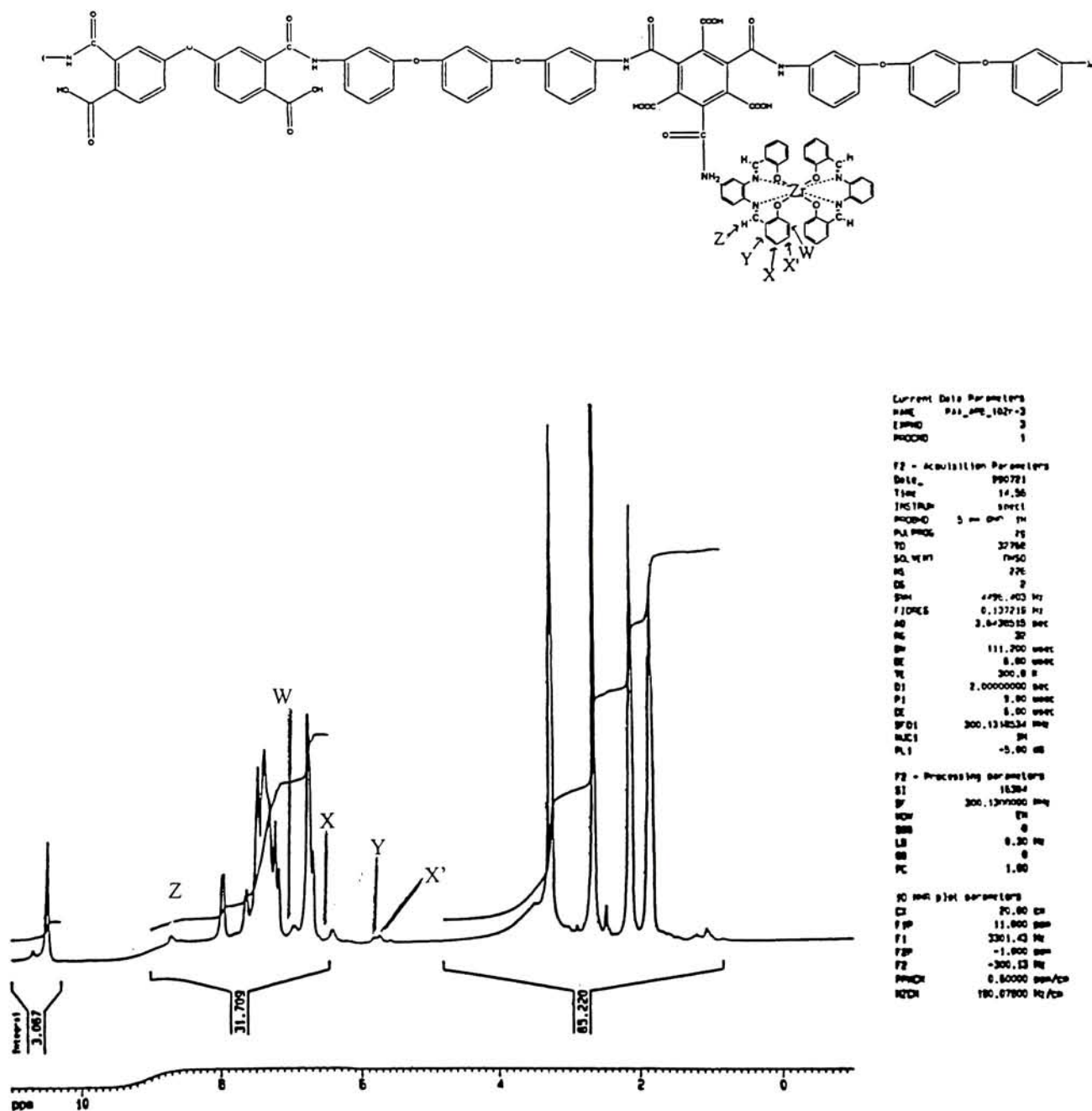


Figure 3.28. 300 MHz ^1H NMR Spectrum and Assignments of PAA(ODPA/APB/10 mol% MADA/10 mol% Zr)

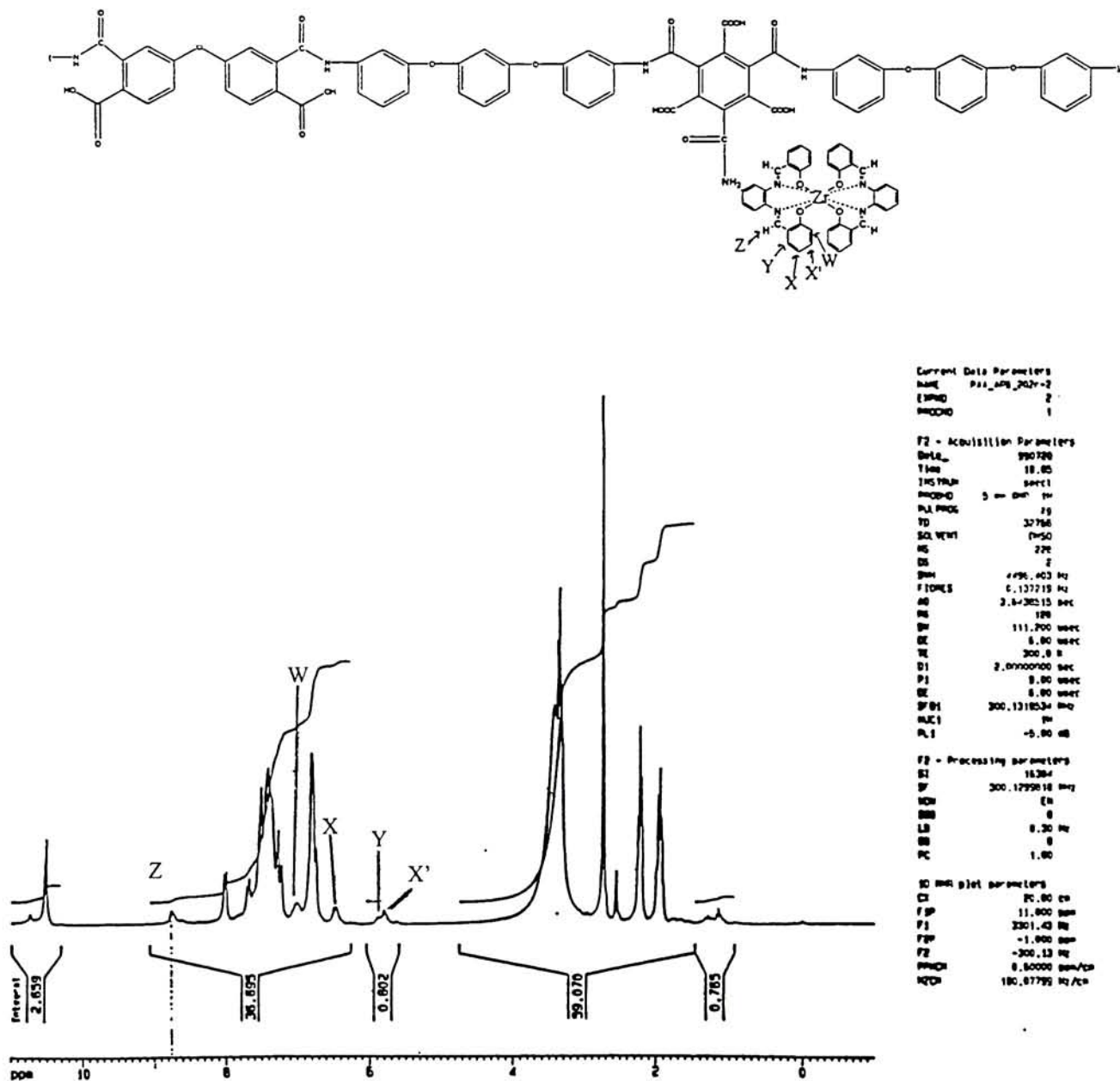


Figure 3.29. 300 MHz ¹H NMR Spectrum and Assignments of PAA(ODPA/APB/20 mol% MADA/20 mol Zr)

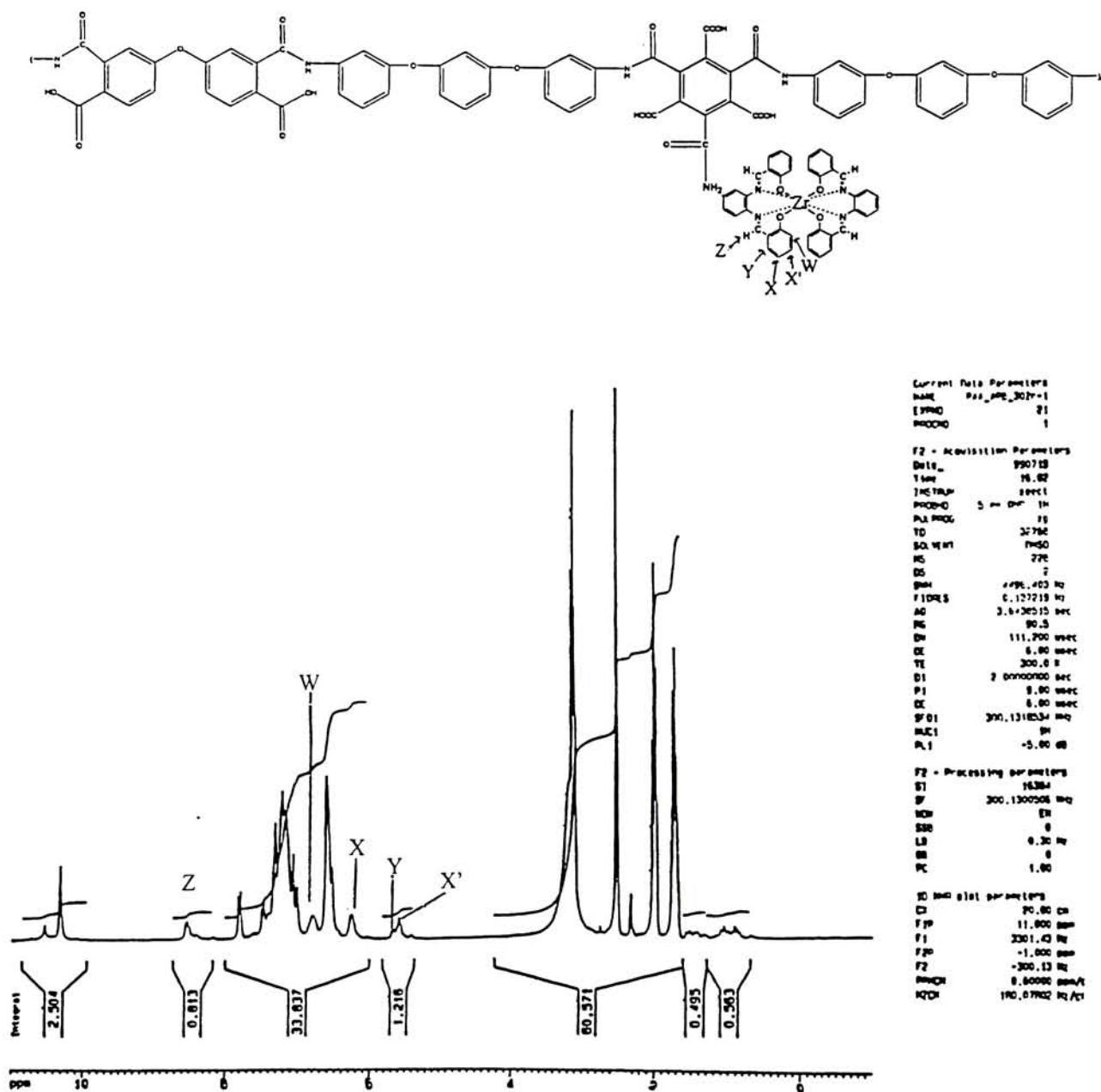
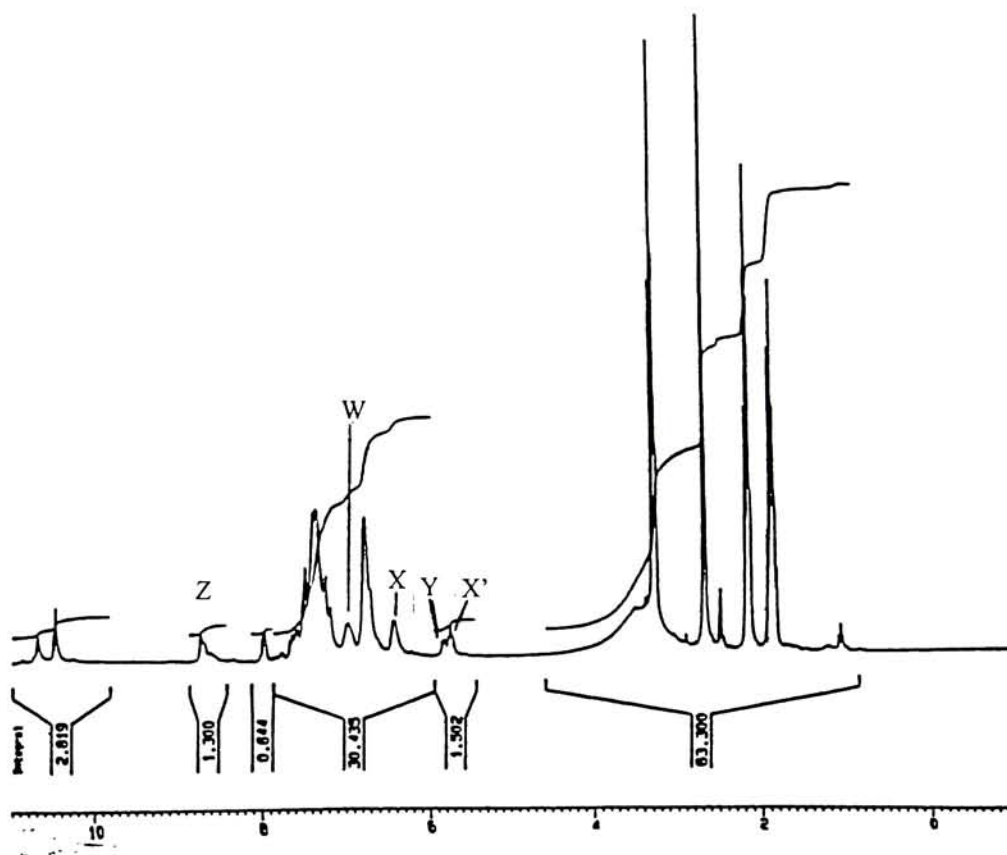


Figure 3.30. 300 MHz ^1H NMR Spectrum and Assignments of PAA(ODPA/APB/30 mol% MADA/30 mol% Zr)



54

The differential molecular weight distribution of PAA(ODPA/APB/10 mol% MADA), PAA(ODPA/APB/20 mol% MADA) and PAA(ODPA/APB/30 mol% MADA) in Figure 3.32 show that the differential molecular weights are essentially the same.

Table 3.1

GPC Analysis Results of PAA(ODPA/APB/MADA)^a

Sample	Mn (g/mol)	Mw (g/mol)	Mz (g/mol)	Mw/Mn	Intrinsic Viscosity (dL/g)
MADA10	3770	111800	165600	29.7	0.589
	3720	110600	163500	29.7	0.596
MADA20	5010	122700	178600	24.5	0.600
	4990	121000	175500	24.2	0.600
MADA30	5220	118100	174200	22.6	0.543
	5200	113800	167900	21.9	0.546

a: Analysis performed at NASA Langley, in NMP at 60°C.

3.6 Thermal Gravimetric Analysis (TGA)

PAA[ODPA/APB/MADA]

Thermogravimetric analysis is conducted to determine the effect of structural variations on thermal stability. The extrapolated onset temperature for thermal decomposition was determined by the intersection point of baseline and the derivative trace for the maximum weight loss. Figure 3.33 shows TGA curves of temperature vs. weight percent for the PAA with different ratios of MADA/ODPA in oxygen at a programmed heating rate of 10 °C /min. There is a noticeable weight lost before the materials' decomposition in the TGA curves. When comparing the TGA curves of the polyamic acid, an increase of the MADA/ODPA ratio in the polymer chain has a greater

File: MADA10-1

id: 1st run APB/ODPA/MADA 10% PAA

Run Date: Wed Mar 17 1999 11:28:17

Mn: 3,770 IV: 0.589

Mw: 111,800

Differential Molecular Weight Distribution

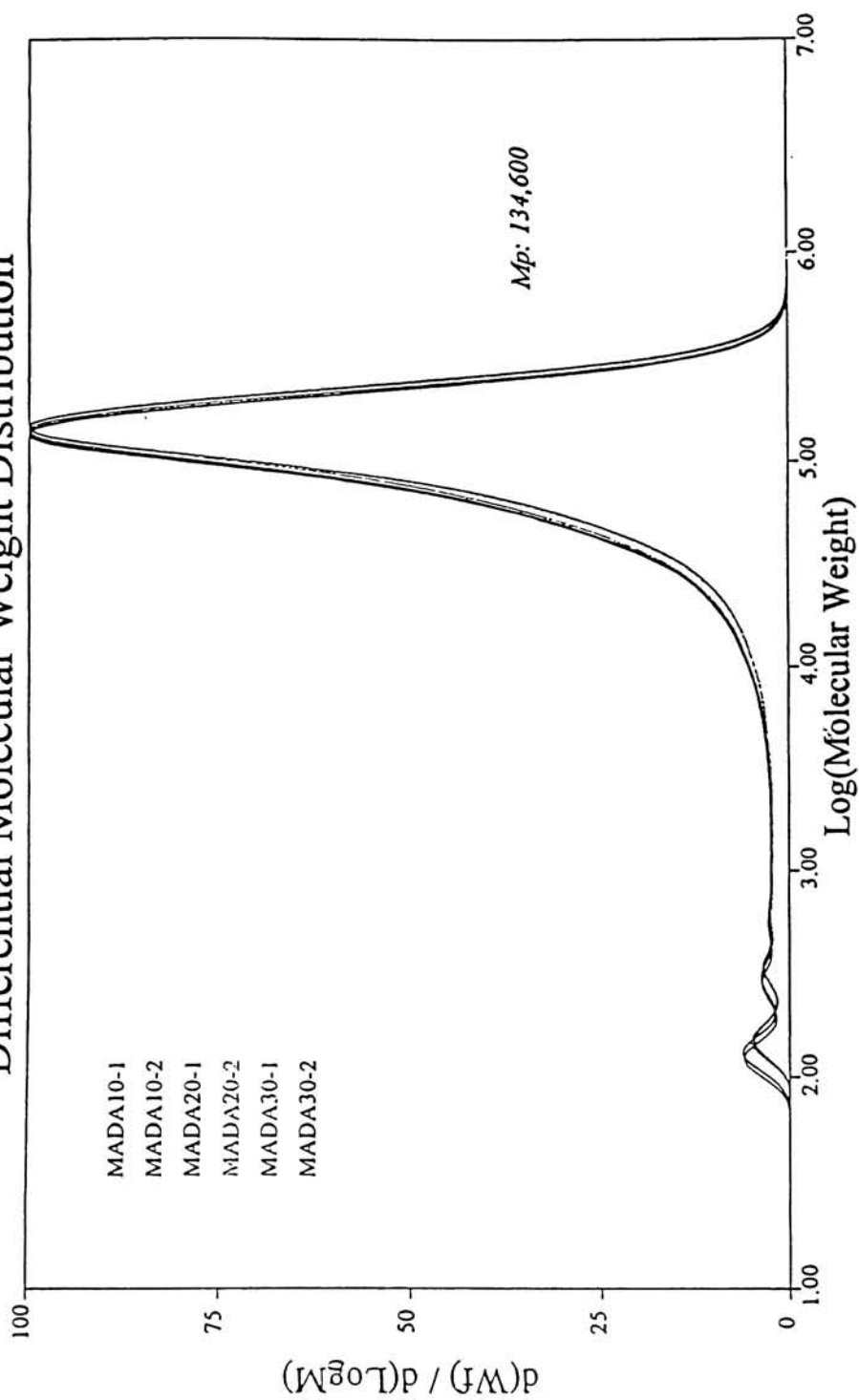


Figure 3.32. GPC Result for Polyamic Acids.

weight lost. Initial weight loss and decomposition temperatures are determined for PAA[ODPA/APB/MADA] and are listed in Table 3.2. No noticeable weight loss is observed below 100°C for 10%PAA. However, the temperatures required for 20%PAA, 30%PAA and 50%PAA to undergo their first weight lost are at or below 100°C. The temperatures for the polyamic acids to undergo their second weight lost are observed below 550°C. The PAA[ODPA/APB/50% mol MADA] is the least stable, and the PAA[ODPA/APB/10% mol MADA] is the most stable of the three.

Table 3.2. Thermal Properties of PAA(ODPA/APB/MADA)

Sample	Monomer Ratio (mmole)			Temperature (°C)	
	MADA	ODPA	APB	T _i ^a	T _d ^b
10% PAA	0.1	0.9	1.0	109.64	555.43
20% PAA	0.2	0.8	1.0	100.69	536.04
30% PAA	0.3	0.7	1.0	91.75	528.24
50% PAA	0.5	0.5	1.0	72.37	525.61

a: Initial weight loss temperature determined by TGA in air at a heating rate of 10°C/min.

b: Decomposition temperature determined by TGA in air at a heating rate of 10°C/min.

PAA[ODPA/APB/MADAZr]

Figure 3.34 shows the TGA curve of temperature vs. weight percent for pendent PAA with the same mole ratio of MADA with respect to Zr(adsp)(dsp). From the graph, the content of zirconium complex is roughly proportional to the weight of the residue remaining after thermal heating above 700°C in air.

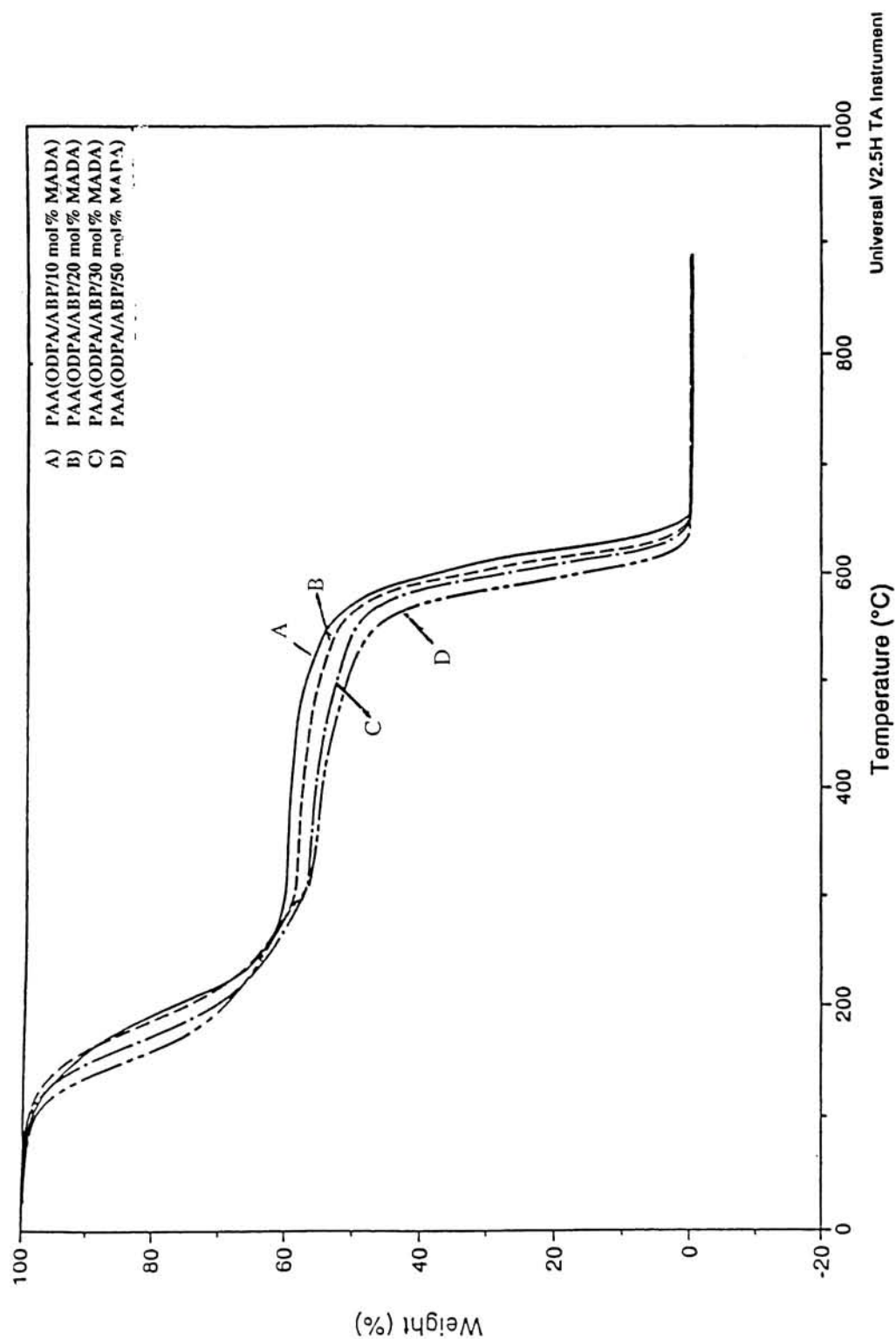


Figure 3.33. TGA Curves of Poly(amic acid)s at a Heating Rate of 10°C/min in air.

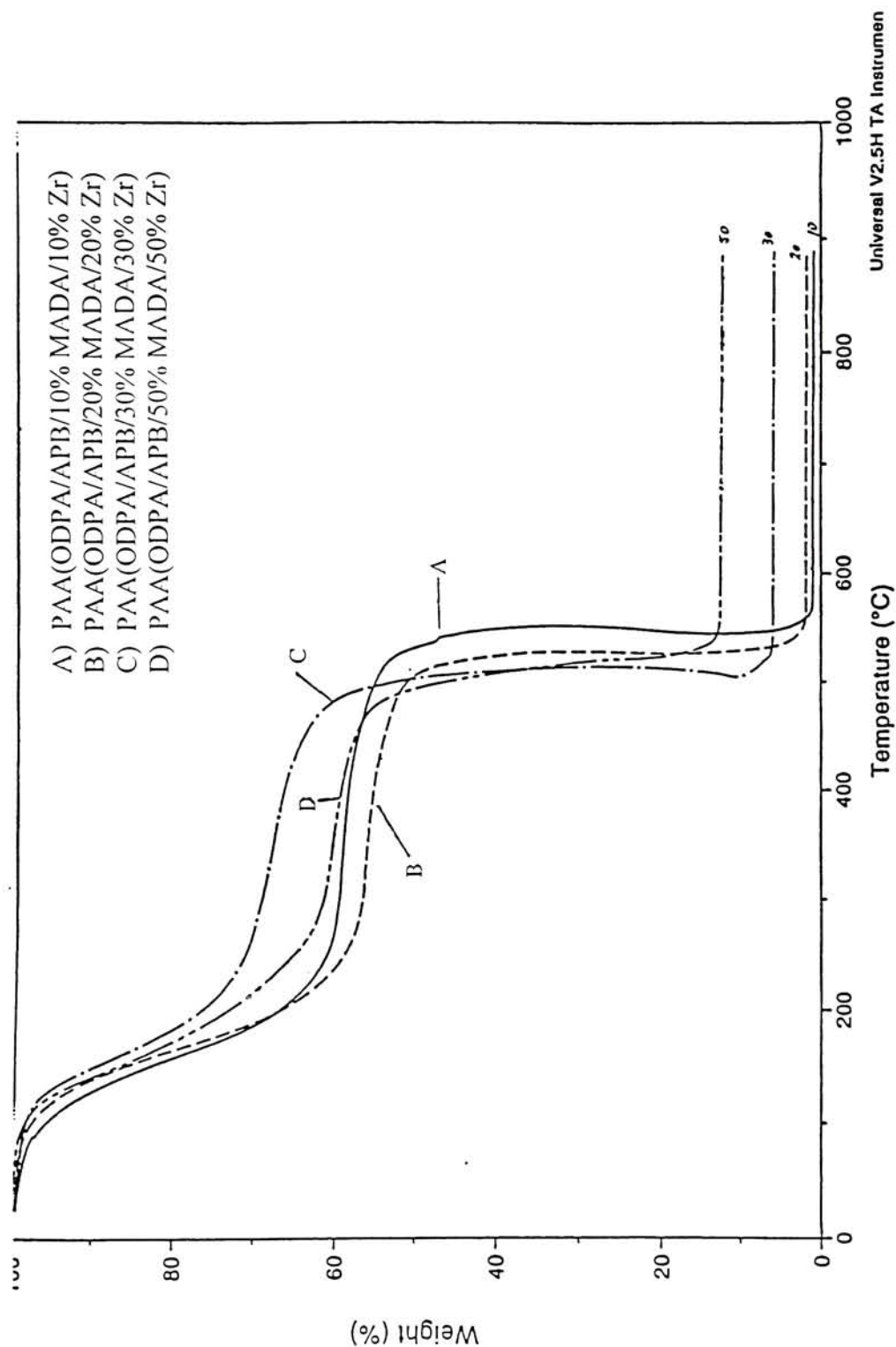


Figure 3.34. TGA Curves of Zr Pendant PAAs at a Heating Rate of 10°C/min in air.

Table 3.3 summarizes the initial weight loss and decomposition temperatures for the Zr pendent polymers. The temperatures required to induce the first weight lost for all four Zr pendent polyamic acids are below 100°C. The temperatures required to induce the second weight loss for all the polyamic acids are in the range of 455°C to 518°C with decomposition becoming essentially complete upon heating to temperatures of 540°C to 580°C. From the analysis, the decomposition temperatures of the pendent polymers are lower than the nonpendent polymers. This indicates that the introduction of zirconium complex lowers the thermal stability of these materials.

Table 3.3. Thermal Properties of PAA(ODPA/APB/MADA/Zr)

Sample	Monomer Ratio (mmole)				Temperature (°C)		%Residual
	MADA	ODPA	APB	Zr	T _i ^a	T _d ^b	
10% PAA-Zr	0.1	0.9	1.0	0.1	84.29	518.15	0.993
20% PAA-Zr	0.2	0.8	1.0	0.2	85.78	491.32	1.835
30% PAA-Zr	0.3	0.7	1.0	0.3	77.37	464.48	5.938
50% PAA-Zr	0.5	0.5	1.0	0.5	81.31	455.53	12.52

a: Initial weight loss temperature determined by TGA in air at a heating rate of 10°C/min.

b: Decomposition temperature determined by TGA in air at a heating rate of 10°C/min.

3.7 Differential Scanning Calorimetry (DSC)

The imidization process is strongly affected by the heating rate. There is generally one endothermic peak in the first scan for both polyamic acids and pendent polyamic acids. There is also one endothermic peak in the scan for both the nonpendent and pendent polyimides. Typical DSC curves of heat flow versus temperature of

polyamic acids, pendent polyamic acids, polyimides and pendent polyimides are shown in Figures 3.35, 3.36, 3.37 and 3.38, respectively.

Glass transition temperatures T_g , as determined by DSC for all of the imidized films, are listed in Tables 3.4 to 3.7. The polyamic acid DSC thermograms show shifts characteristic of glass transition between 64.1 to 74.6°C (Table 3.4), while shifts characteristic of glass transition between 57.6 to 83.1°C for pendent polyamic acid are shown in Table 3.5. Again there are shifts characteristic of glass transition from 188.3 to 242.9°C for the nonpendent polyimides (Table 3.6), while shifts at 198.5 to 245°C are observed for the pendent polyimides films as shown in Table 3.7.

The PI(ODPA/APB/MADA) and the PI(ODPA/APB/MADA/Zr) showed no T_m . These polyimide films were annealed at 550°C for 10 minutes, allowed to cool slowly, and the DSC rerun, but again no T_m s were observed.

Table 3.4. DSC Result for PAA(ODPA/APB/MADA)

Sample	Monomer Ratio (mmole)			Temperature (°C)		
	MADA	ODPA	APB	T_{onset}	T_{end}	T_g
10% PAA	0.1	0.9	1.0	58.8	67.8	64.1
20% PAA	0.2	0.8	1.0	n.a.	n.a.	n.a.
30% PAA	0.3	0.7	1.0	60.2	69.9	65.4
50% PAA	0.5	0.5	1.0	68.4	80.7	74.6

Table 3.5. DSC Result for PAA(ODPA/APB/MADA/Zr)

Sample	Monomer Ratio (mmole)				Temperature (°C)		
	MADA	ODPA	APB	Zr	T _{onset}	T _{end}	T _g
10% PAA-Zr	0.1	0.9	1.0	0.1	55.0	65.5	57.6
20% PAA-Zr	0.2	0.8	1.0	0.2	68.0	73.0	69.6
30% PAA-Zr	0.3	0.7	1.0	0.3	n.a.	n.a.	n.a.
50% PAA-Zr	0.5	0.5	1.0	0.5	79.7	90.1	83.1

Table 3.6. DSC Result for PI(ODPA/APB/MADA)

Sample	Monomer Ratio (mmole)			Temperature (°C)		
	MADA	ODPA	APB	T _{onset}	T _{end}	T _g
10% PI	0.1	0.9	1.0	185.2	191.1	188.3
20% PI	0.2	0.8	1.0	193.7	203.8	199.2
30% PI	0.3	0.7	1.0	205.8	218.1	212.2
50% PI	0.5	0.5	1.0	233.8	250.8	242.9

Table 3.7. DSC Result for PI(ODPA/APB/MADA/Zr)

Sample	Monomer Ratio (mmole)				Temperature (°C)		
	MADA	ODPA	APB	Zr	T _{onset}	T _{end}	T _g
10% PI-Zr	0.1	0.9	1.0	0.1	191.2	201.0	198.5
20% PI-Zr	0.2	0.8	1.0	0.2	190.1	211.5	203.3
30% PI-Zr	0.3	0.7	1.0	0.3	234.4	243.3	237.9
50% PI-Zr	0.5	0.5	1.0	0.5	238.8	264.5	245.3

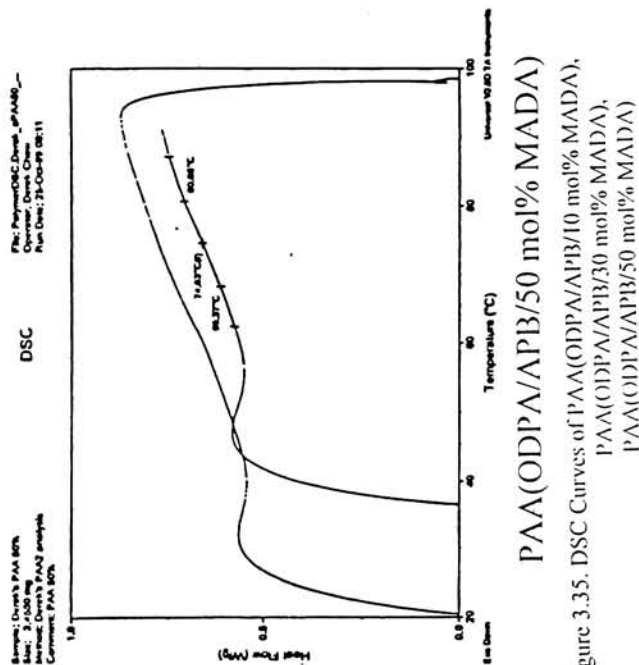
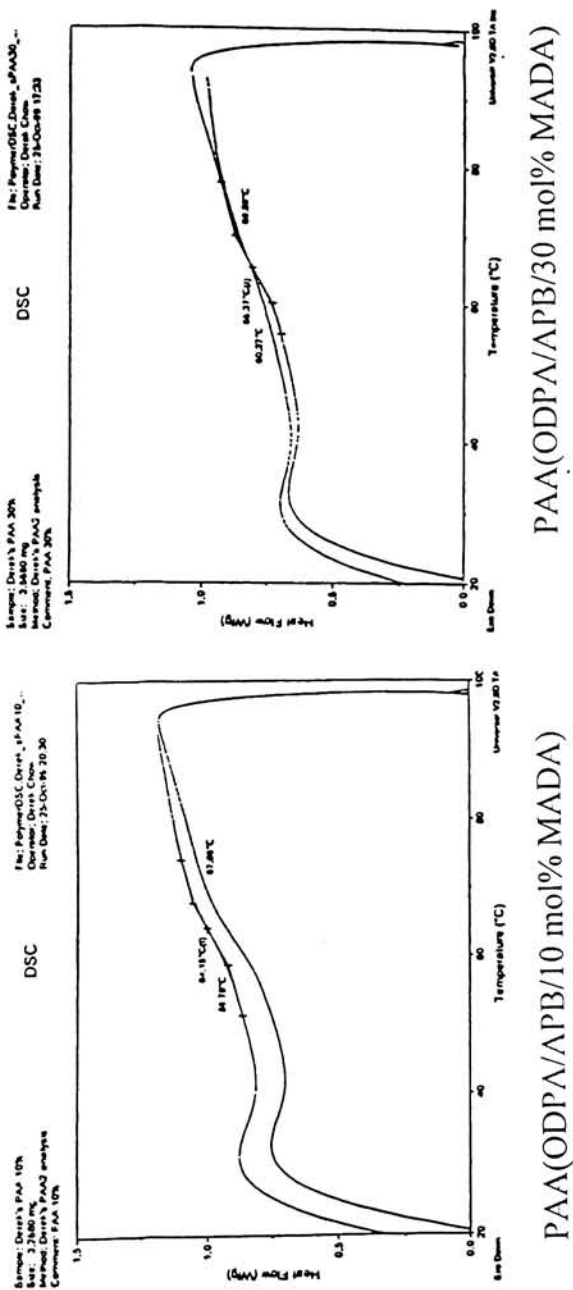
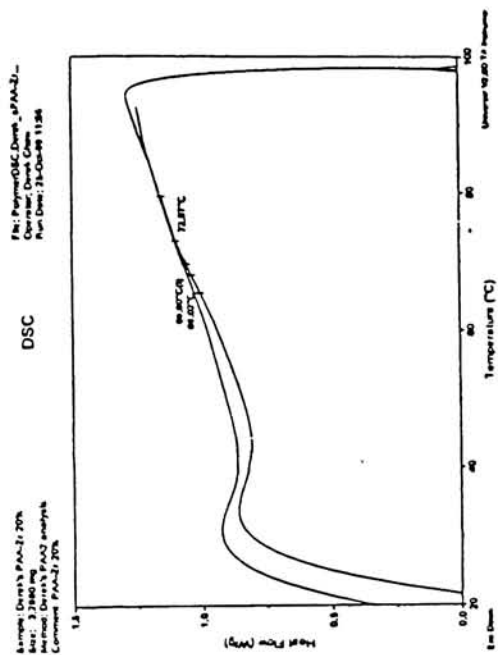
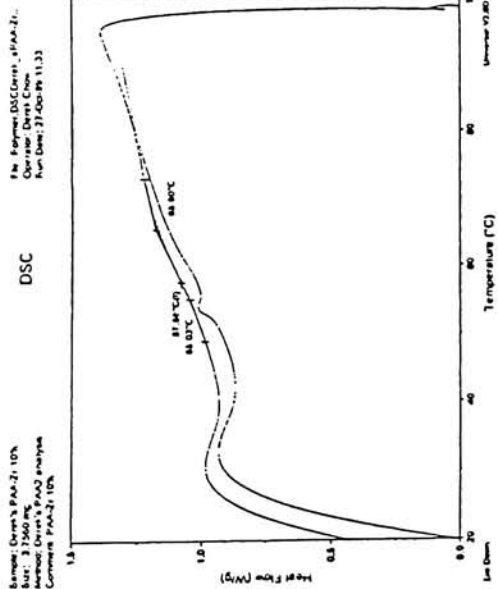
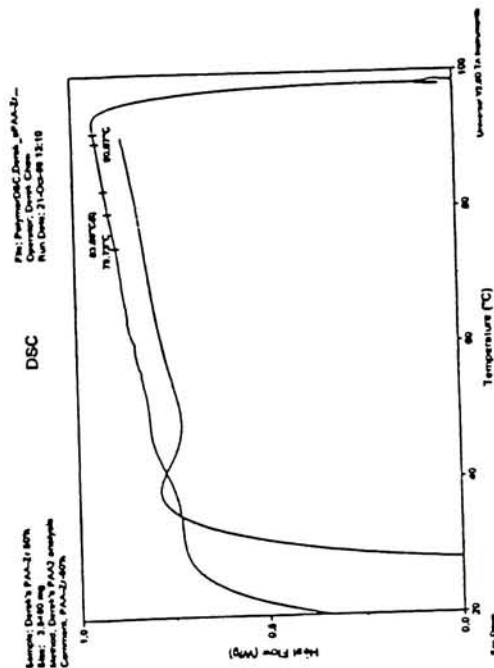


Figure 3.35. DSC Curves of PAA(ODPA/APB/10 mol% MADA),
 PAA(ODPA/APB/30 mol% MADA),
 PAA(ODPA/APB/50 mol% MADA)



PAA(ODPA/APB/10 mol% MADA/10 mol% Zr) PAA(ODPA/APB/20 mol% MADA/20 mol% Zr)



PAA(ODPA/APB/50 mol% MADA/50 mol% Zr)

Figure 3.36. DSC Curves of PAA(ODPA/APB/10 mol% MADA/10 mol% Zr),
PAA(ODPA/APB/20 mol% MADA/20 mol% Zr),
PAA(ODPA/APB/50 mol% MADA/50 mol% Zr)

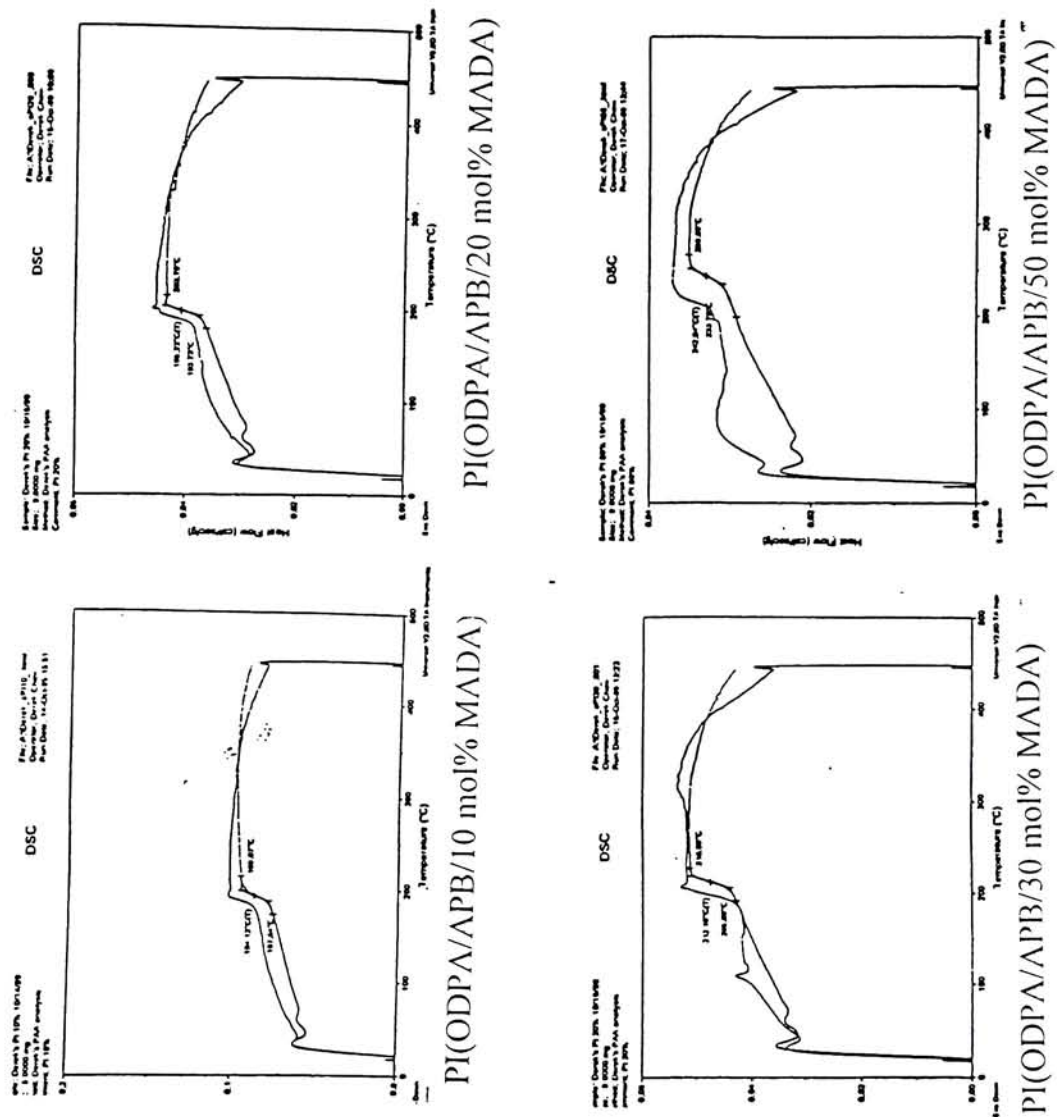


Figure 3.37. DSC Curves of PI(ODPA/APB/10 mol% MADA),

PI(ODPA/APB/20 mol% MADA),

PI(ODPA/APB/30 mol% MADA),

PI(ODPA/APB/50 mol% MADA)

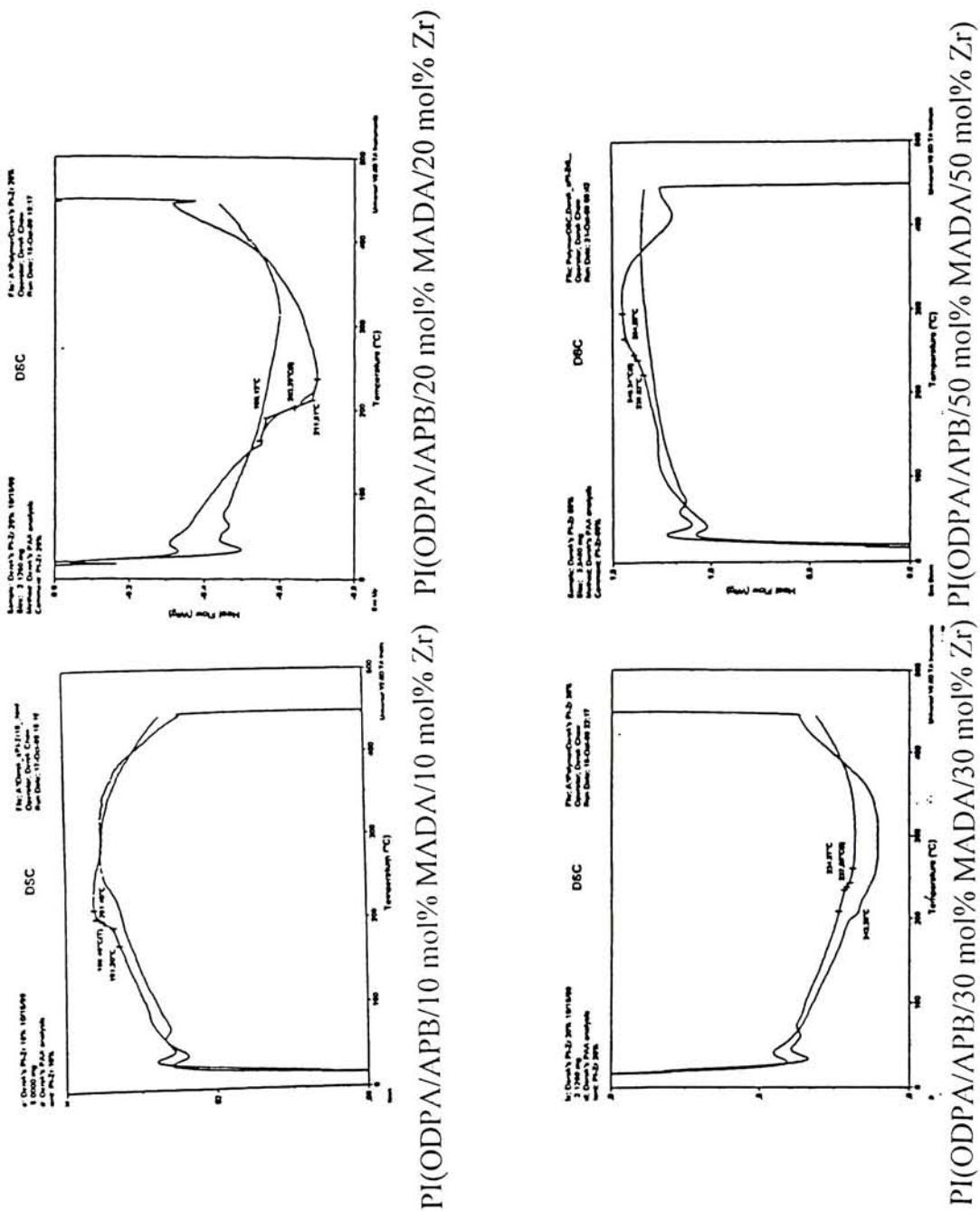


Figure 3.38. DSC Curves of PI(ODPA/APB/10 mol% MADA/10 mol% Zr), PI(ODPA/APB/20 mol% MADA/20 mol% Zr), PI(ODPA/APB/30 mol% MADA/30 mol% Zr), PI(ODPA/APB/50 mol% MADA/50 mol% Zr)

3.8 SEM

The original Zr pendent polyimide films are transparent with a yellow-tinted color. Upon exposing each film to atomic oxygen in a plasma asher, chalky white residue appeared on the surface.

The surface appearance of nonpendent polyimide and Zr pendent polyimide films before and after oxygen plasma asher for three hours were recorded by scanning electron microscopy (SEM). The SEM micrographs show nonpendent polyimide surfaces before and after atomic oxygen etching in Figures 3.39 to Figure 3.46, and the pendent polyimide surfaces before and after atomic oxygen etching in Figures 3.47 to 3.54.

All the nonpendent polyimide films' surface appears uniform before etching. After three hours of atomic oxygen exposure, it is evident that the surface of nonpendent polyimide samples have undergone large scale surface roughening. After identical etching, SEM shows that the Zr containing PI surface is likewise roughened as shown in Figure 3.47 to Figure 3.53. However, the latter displays a white residue visible to the eye. The photograph with 50 mol% Zr complex appears whiter than the rest of the pendent polyimide films undergoing the same treatment. With higher mole percentage of Zr complex in the polyimide, more of the white protective layer was formed on the surface.



Figure 3.39 PI(ODPA/APB 10% MADA) film before etching.
30KV, 500 spot size, 10,000K mag, 55° tilt.

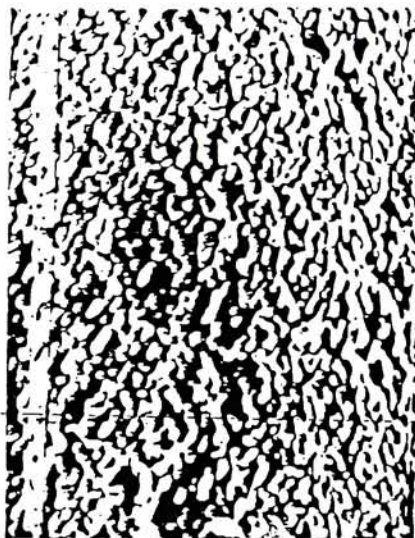


Figure 3.40 PI(ODPA/APB 10% MADA) film after etching.
30KV, 500 spot size, 10,000K mag, 55° tilt.



Figure 3.41 PI(ODPA/APB 20% MADA) film before etching.
30KV, 500 spot size, 10,000K mag., 55° tilt.

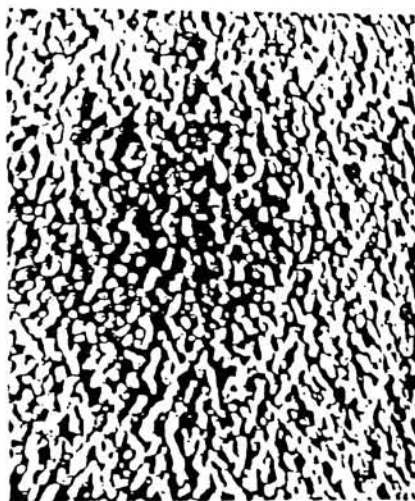


Figure 3.42 PI(ODPA/APB 20% MADA) film after etching.
30KV, 500 spot size, 10,000K mag., 55° tilt.

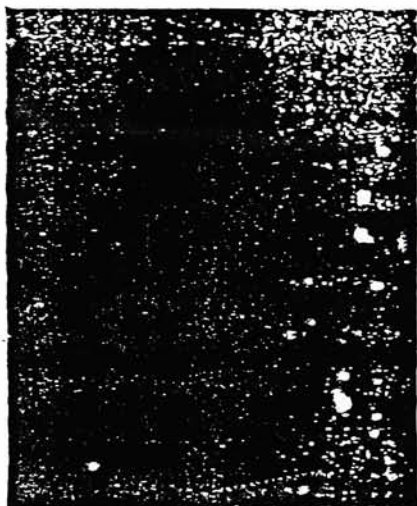


Figure 3.43. PI(ODPA/APB/30% MADA) film before etching.
30KV, 500 spot size, 10,000K mag., 55° tilt.



Figure 3.44. PI(ODPA/APB/30% MADA) film after etching.
30KV, 500 spot size, 10,000K mag., 55° tilt.



Figure 3.45. PI(ODPA/APB/50% MADA) film before etching.
30KV, 500 spot size, 10,000K mag., 55° tilt.

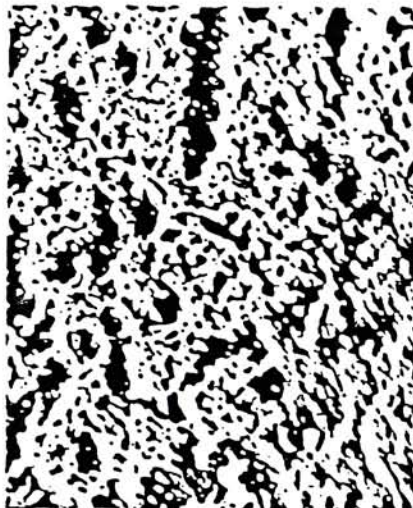


Figure 3.46. PI(ODPA/APB/50% MADA) film after etching.
30KV, 500 spot size, 10,000K mag., 55° tilt.

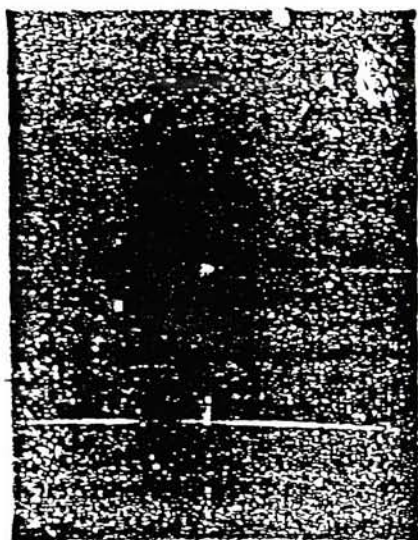


Figure 3.47. PI(ODPA/APB/10% MADA/10% Zr) film before etching.
30KV, 500 spot size, 10,000K mag., 55° tilt.

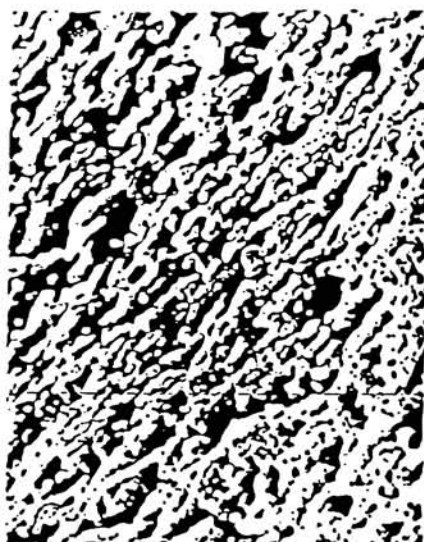


Figure 3.48. PI(ODPA/APB/10% MADA/10% Zr) film after etching.
30KV, 500 spot size, 10,000K mag., 55° tilt.



Figure 3.49. PI(ODPA/APB/20% MADA/20% Zr) film before etching.
30KV, 500 spot size, 10,000K mag., 55° tilt.

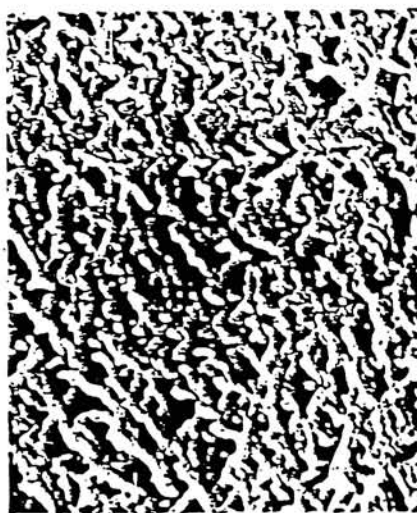


Figure 3.50. PI(ODPA/APB/20% MADA/20% Zr) film after etching.
30KV, 500 spot size, 10,000K mag., 55° tilt.

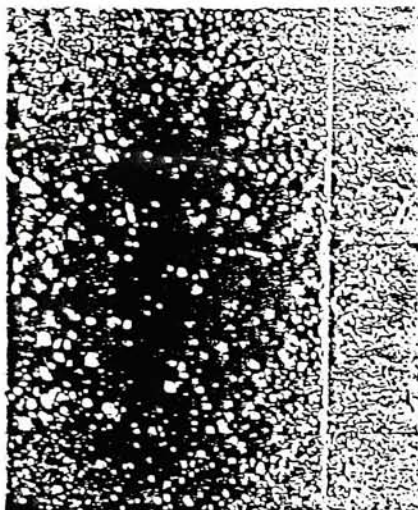


Figure 3.51. PI(ODPA/APB/30% MADA/30% Zr) film before etching.
30KV, 500 spot size, 10,000K mag., 55° tilt.

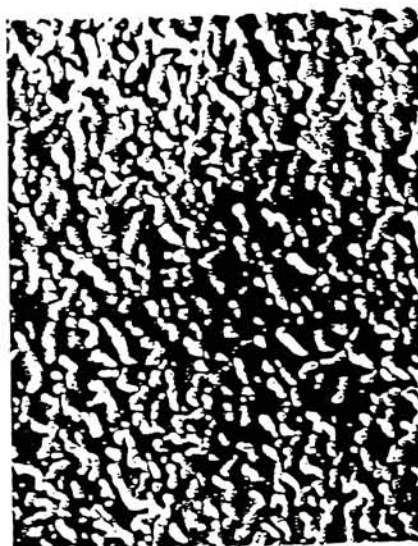


Figure 3.52. PI(ODPA/APB/30% MADA/30% Zr) film after etching.
30KV, 500 spot size, 10,000K mag., 55° tilt.



Figure 3.53. PI(ODPA/APB/50% MADA/50% Zr) film before etching.
30KV, 500 spot size, 10,000K mag., 55° tilt.



Figure 3.54. PI(ODPA/APB/50% MADA/50% Zr) film after etching.
30KV, 500 spot size, 10,000K mag., 55° tilt.

3.9 Solvent Resistance Test

Single layer 10% mol/mol Zr pendent polyimide films were immersed in six common solvents, and the results are listed in Table 3.8. None of the solvents had any visible effect on the films, which remained flexible, and did not break even when they were creased.

Table 3.8. Chemical Resistance in Organic Solvents. Films soaked for one hour at room temperature and blotted dry.

SOLVENT	EFFECT
ACETONE	NONE
CHLOROFORM	NONE
DIMETHYSULFOXIDE (DMSO)	NONE
TOLUENE	NONE
1-METHYL-PYRROLIDINONE (NMP)	NONE

3.10 Preparation of Zr(adsp)(dsp) Pendent Polyimide Films

Films containing pendent zirconium complex were dark brown and flexible, with no visible phase separation observed during the drying and curing steps. Films containing more than 30 mole % zirconium pendent cracked after making eight layers, while for films containing equal 20 mole % or less zirconium pendent, ten layers could be made as summarized in Table 3.9.

Table 3.9. Preparation of Zr(adsp)(dsp) Pendent Polyimide Films

PI Film	PAA Precursor	Zr(adsp)(dsp) mol%	# of Uncracked layers
10% PI-Zr	10% PAA-Zr	10%	10
20% PI-Zr	20% PAA-Zr	20%	10
30% PI-Zr	30% PAA-Zr	30%	8
50% PI-Zr	50% PAA-Zr	50%	8

4. Discussion

4.1 Synthesis of Starting Materials and Mellitic Dianhydride (MADA)

Synthesis of Zr(adsp)(dsp)

The TLC and NMR of Zr(adsp)(dsp) are consistent with those previously reported,²⁹ and confirm its identity.

Heating mellitic acid can yield two dianhydride isomers (A & B), monoanhydride (C), and trianhydride (D). Their structures are shown in Figure 4.1. The two dianhydride isomers are the preferred monomers for the polymerization, while the existence of impurities monoanhydride or trianhydride is the result of insufficient heating or overheating, respectively. In the polymerization, these impurities would result in chain termination to low molecular weight polymer or cross link to produce branching and, possibly, gel.

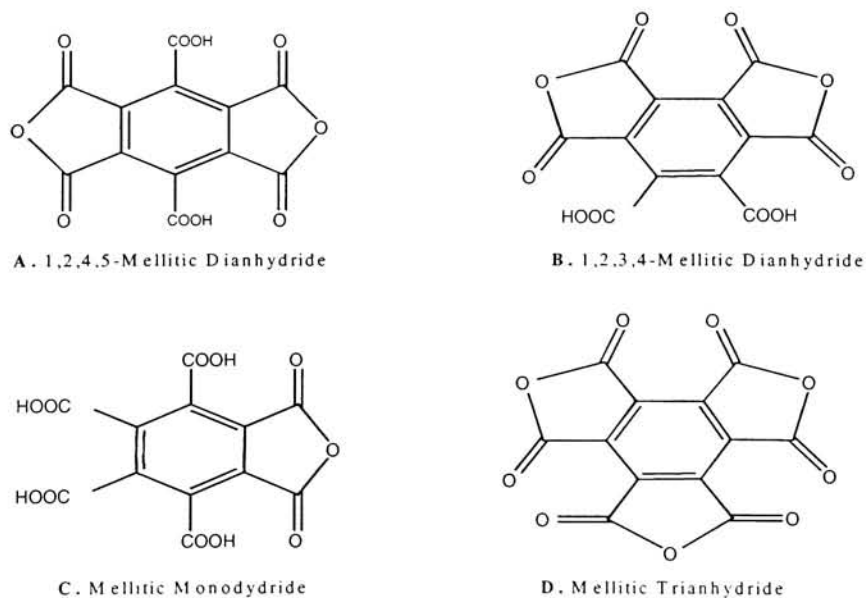


Figure 4.1 Chemical Structures of the Anhydrides Formed in the Heating of Mellitic Acid

4.2 Polymer Synthesis

The average of molecular weight of the polymer obtained depends on the purity of monomers and the NMP. The purer the starting materials and the more anhydrous the NMP, the higher the molecular weight.

For the purification of both the ODPA and APB, it is critical to control the sublimation temperature. If the sublimation temperature of ODPA exceeds 30°C above its melting temperature, decomposition of ODPA occurs and the formation of pink crystals occurs instead of white crystals of ODPA. If the sublimation temperature of APB exceeds 50°C above its melting temperature, decomposition of APB occurs and the formation of a sticky substance occurs instead of white crystals of APB.

For the drying of NMP, it is critical to remove water as much as possible. If the NMP is not anhydrous enough, water molecule will be introduced in the polymer solution, which will cause hydrolysis of anhydride rings, thus producing low molecular weight polymers.

Increasing the molecular weight of the copolymers depend on the mole ratio of the anhydrides (ODPA and MADA) and the diamine (APB). If one of the reactants is in slight excess, polymerization proceeds to a point where it becomes the end group of each polymer chain, and further polymerization is not possible resulting in low molecular weight. Therefore, it is critical to keep the anhydrides and the diamine as 1:1 ratio.

The reaction of a diamine and a dianhydride to poly(amic acid) is an equilibrium reaction. Thus, an increase in the temperature of polymerization nearly always lowers the molecular weight of the polymer produced due to the role of entropy, which favors

the starting materials. However, at the start of the reaction, the forward reaction is much faster than the reverse reaction due to high monomer concentrations to form higher molecular weight poly(amic acid).³⁰ High temperature would reverse the reaction due to the greater entropy of the reactants and thus decrease molecular weight of polymers. Efficient stirring is required to enable the reaction mixture successively mix well and to ensure the reaction favors the formation of higher molecular weight polymer.

4.3 Zr(adsp)(dsp) pendent PAA(ODPA/APB/MADA), PAA(ODPA/APB/MADA/Zr)

The addition of DCC to the poly(amic acid) is expected to dehydrate the adjacent carboxylic acid groups of the MADA repeat unit to form intermediates which emulate the reactivity of anhydrides. The amino group of the Zr(adsp)(dsp) will attack these intermediates to form an amide group bonded onto the polymer backbone.³¹ See Figure 3.8.

During the pendent polymer synthesis, the formation of gel can be explained by the conversion of the poly(amic acid) to the NMP insoluble poly(isoimide) where the adjacent carboxylic acid group and amic acid group react to form the isoimide ring.^{32,33} The reaction of the amino group of the complex with the isoimide functional group in the polymer chain gives the complex pendent poly(amic acid) which is soluble again when the pendent polymer solution is heated at 40°C for 5 minutes. Alternately, gel formation can be caused by diminished polymer chain mobility in solution. The incorporation of APB into MADA-containing polymer has allowed a 50% mol PAA film to be prepared on small scale without gel formation problems. See Figure 4.2.

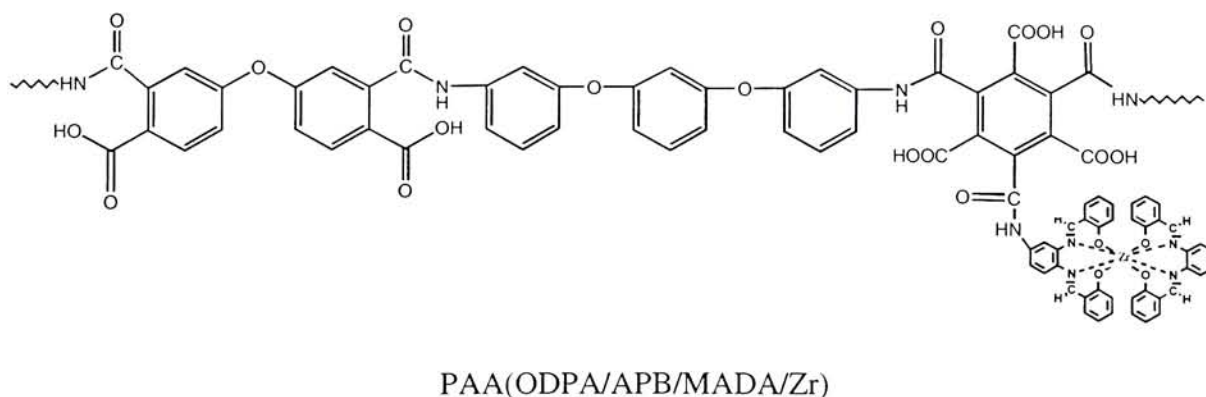


Figure 4.2. Formation of Polyamic Acid After Heat Treatment at 40°C for 5 minutes.

4.4 Preparation of Zr(adsp)(dsp) Pendent Polyimide Films

The proposed structure of Zr pendent polyimide is shown in Figure 4.3 . Cracks were apparent following imidization after 8 layers were cast for the 50 mole percent Zr complex polyimide films. This improved numbers of layers is attributed to the additional polymer backbone flexibility which results from the APB component of the polymer. The cracking may be due to the bulky pendent complex's suppression of the chain motion during the solvent evaporation and thermal imidization or their effect on the material's thermal expansion coefficient. Another possible explanation for the cracking of higher Zr(adsp)(dsp) content polyimide films involves the water generated from imidization reaction becoming trapped within film and causing degradation within the polyimide film.

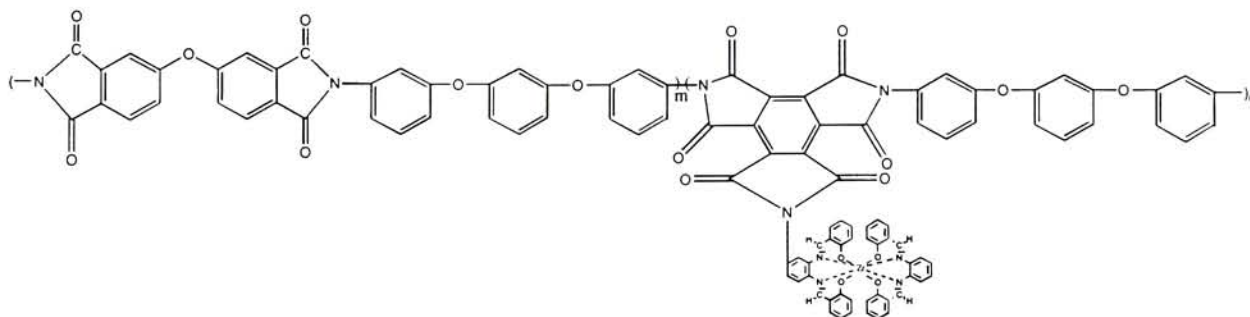


Figure 4.3. Proposed Structure of Zr Pendent Polyimide, PI(ODPA/APB/MADA/Zr).

4.5 Polymer Characterization

4.5.1 TLC, NMR, and FT-IR

To support that the Zr(adsp)(dsp) has become attached to the polymer backbone, the completion of the reaction was confirmed by silica gel TLC plate, eluting the reaction solution vs. free Zr(adsp)(dsp). The spot corresponding to free Zr complex was not apparent in the TLC of the DCC reaction solution.

The FT-IR spectra of zirconium complex, all nonpendent, pendent co-PAA and co-PI films are consistent with those proposed structure and reflects the concentration of MADA in imidized films by the intensity of the anhydride ring peak at 1860 cm^{-1} . The FT-IR peaks of NMP, PAA[APB/ODPA] and PI[APB/ODPA] overlap all the characteristic peaks of Zr(adsp)(dsp), so there is no indication to confirm the attachment of Zr complex to the polymer chain from the IR spectrum. Attempts to remove NMP from the co-PAA were not made due to the prospect of initiating imidization.

The bulkier substituent is likely to hinder imidization in the 50 mol% polymer. With a lower the degree of imidization, a stronger peak due to N-H stretch is observed.

The NMR spectra of Zr pendent polyamic acid included all the characteristic chemical shift of Zr(adsp)(dsp) and polyamic acid.

The ^1H -NMR spectrum of nonpendent co-PAA indicated that peaks near 10 ppm increase with MADA-APB mole percentage and is consistent with the proposed formulations of 10%, 20%, 30%, and 50% by mole.

The NMR spectra of the pendent co-polyamic acids show peaks with integrations consistent with the presence of Zr pendent groups in the expected 10%, 20%, 30%, and 50% by mole concentrations.

Since the nonpendent and pendent co-polyimides were too insoluble to obtain solution NMR spectra, no inferences could be drawn using the NMR at RIT regarding the effects of the imidization process on corresponding co-PAAs.

4.5.2 Gel Permeation Chromatography (GPC) and Viscosity

Polyamic acid and Zr pendent polyamic in NMP have broad distribution of molecular weights. This might be attributed to the presence of some variation in the mol percentage of MADA in the polymer chains, which would cause comparable variation in the mole percentage of Zr pendent groups, and thus broaden the molecular weight distributions. In addition, impurities in the Zr(adsp)(dsp) and incomplete removal of the DCC by-products are likely sources of low molecular weight species. GPC and viscosity indicate that there are long polymers chains in the PAA(ODPA/APB/10 mol% MADA), PAA(ODPA/APB/20 mol% MADA), and PAA(ODPA/APB/30 mol% MADA). The polydispersity index of 1.5 from M_z/M_w is reasonable for this kind of polymer.

There is no result for the 50 mol % PAA samples due to NASA reorganization.

4.5.3 Thermogravimetric Analysis (TGA)

The slight weight loss before 100°C in the TGA curves of polyamic acid and Zr pendent polyamic acids is due to the loss of NMP trapped in polymers, the presence of which is supported by their NMR spectra.

The first weight loss step in the TGA curve is due to more NMP loss and water, which is produced by imide ring formation from adjacent amide group with carboxylic acid group and anhydride cyclodehydration from two adjacent carboxylic acid groups. In addition, polymer with higher MADA concentration generates more water, so more weight loss at temperature above T_i . The higher MADA concentration also causes the onset of decomposition to occur at lower temperature (probably involving decarboxylation).

The decomposition temperatures of the pendent polymers are lower than the nonpendent polymers, but the difference is small and likely to be acceptable for the NASA application that drives this work. The approximately 400°C decomposition temperature of the complex itself is a likely explanation for this small drop in thermal stability. Alternately, this fact might indicate that the introduction of a bulky group such as zirconium complex hinders the formation of the five membered ring within the polymer backbone during the imidization process. In addition the zirconium complex groups might be less mobile in the polymer matrix, or more susceptible to hydrolysis reactions during imidization. However, the decrease in thermal stability with increasing zirconium complex may be offset by a corresponding beneficial lowering in T_g .

Also, TGA in air shows ZrO_2 residue that is roughly proportional to the mole percent of Zr pendent groups as shown in Table 3.2.

Differential Scanning Calorimetry (DSC)

The first endothermic peak in DSC curve is attributed mainly to the decomplexation of NMP hydrogen bonded to the amide and carboxylic groups of the co-PAA. The second endothermic peak is attributed mostly to the imidization, i.e., dehydrative cyclization of amide and carboxylic acid groups to form the imide rings. In addition, anhydride formation is accomplished at the MADA locations, as indicated by FT-IR.

Generally, T_g depends on the chemical structure. The incorporation a) benzene rings, b) oxygen bridges, and c) meta amine groups induced a lower T_g for the nonpendent and pendent polymers in this study vs. the corresponding non-APB-containing polymers.^{28, 34} The flexibility of the ether linkage from the dianhydride in the ODPa and the diamine in APB apparently sufficient to disrupt packing of segments of the polymer chains thereby enlarging the polymer volume. The meta amino substituted position on the APB derived polymers apparently interfere with the ability of the polymer chains to order thereby resulting in amorphous polymers.³

The polyimides' T_g 's were dependent on the presence of flexible meta phenoxy linkages in the backbone as witnessed by the fact that the T_g of the polyimide increased from 189 to 215°C, and from 194 to 240°C for the zirconium pendent polyimides when the meta phenoxy concentration (from ODPa) was decreased. See Tables 3.6 and 3.7.

From the literature, polyimides prepared from the same dianhydride but with different diamines exhibit a lower T_g as the number of ether linkages on the polymer increase.³ For example, when comparing the polyamic acids between PAA(ODPA/3,4-ODA/10 mol% MADA) prepared by KanWen Yang³⁴ and PAA(ODPA/APB/10mol% MADA) showed T_g s of 150 and 68°C, respectively. Comparing T_g for zirconium polyamic acid between 3,4'-ODA and APB showed T_g s of 139 and 58°C, respectively as shown in Table 4.1. The same trend is apparent when comparing the two polyimides between from PI(ODPA/3,4-ODA/10 mol% MADA) and PI(ODPA/APB/10mol% MADA). The two polymers exhibited T_g s of 236 and 195°C, respectively. PI(ODPA/3,4'-ODA/10%MADA/10%Zr) showed a higher T_g than PI(ODPA/APB/10%MADA/10%Zr) comparison of their T_g 's is due to the additional phenoxy group in APB. However, comparison of their T_g 's is complicated by their different average molecular weights as shown in Table 4.2.

Table 4.1. Comparing T_g of analogous polymers containing 3,4'-ODA and APB^{28, 34}

Sample	T_g (C)
PAA(ODPA/ODA/10%MADA)	n.a.
PAA(ODPA/3,4'-ODA/10%MADA)	150
PAA(ODPA/APB/10%MADA)	68
PAA(ODPA/ODA/10%MADA/10%Zr)	n.a.
PAA(ODPA/3,4'-ODA/10%MADA/10%Zr)	139
PAA(ODPA/APB/10%MADA/10%Zr)	58
PI(ODPA/ODA/10%MADA/10%Zr)	n.a
PI(ODPA/3,4'-ODA/10%MADA/10%Zr)	236
PI(ODPA/APB/10%MADA/10%Zr)	195

Table 4.2. Comparing the Average Molecular Weight of PAA(ODPA/3,4-ODA/10 mol% MADA/10mol % Zr) and PAA(ODPA/APB/10mol% MADA/10mol % Zr)

Sample	Ave. Mol. Weight
PAA(ODPA/3,4-ODA/10 mol% MADA/10mol % Zr)	18,450 ³⁴
PAA(ODPA/APB/10mol% MADA/10mol % Zr)	111,800

Table 4.1 shows PAA(ODPA/3,4'-ODA/10%MADA/10%Zr) and PAA(ODPA/APB/10%MADA/10%Zr) have a lower T_g than that of its parent polymers, PAA(ODPA/3,4'-ODA/10%MADA) and PAA(ODPA/APB/10%MADA). This could be due to the attachment of the Zr complex to the polymer chain, which leads to a volume increase in the polymer solution resulting in a lower T_g . Upon imidization, the T_g s for all the

Zr pendent polymers increased. These data suggest the possibility of varying the T_g of the polyimide over a wide temperature range by 1) varying the length of the polymer chain, 2) varying the structure of the polymer (3,4'-ODA vs. APB), 3) varying the amount of pendent group to the backbone of the polymer.

The absence of T_m suggests that melt process of the pendent PI polymers in this study would not be possible.

Atomic Oxygen Durability Characterization

After the plasma etching zirconium pendent PI samples, the white nonuniform layer of ZrO_2 on the surface described by SEM suggests that it thought to be atomic oxygen resistance.^{19,28} However; increasing the mole percentage of Zr complex in the polymer chain and increasing the thickness of the film more the white protective layer was formed on the surface to protect the underlying layers. This will indeed improve the atomic oxygen resistance of the films. The polyimides without the Zr complex, such as PI[ODPA/APB/10 mol% MADA] and PI [APB/ODPA], are less resistant to atomic oxygen.

Solvent Resistance

The fact that treatment with solvents caused no change is the flexibility of these films indicates that no dissolution of low molecular weight or unimidized polymer was occurring. The stiffness of the polymer backbone due to the presence of MADA probably

contributed to the excellent solvent resistance polyimide observed for all PI[ODPA/APB/MADA]. Thus, exposure to solvents or solvent vapors during the engineering of these materials should not cause any alteration of the materials' properties.

5. SUGGESTION FOR FUTURE WORK

Future work may concern the following points:

- (1) Synthesize higher molecular weight of PAA(ODPA/APB/10 mol% MADA), PAA(ODPA/APB/20 mol% MADA), PAA(ODPA/APB/30 mol% MADA), PAA(ODPA/APB/50 mol% MADA) and PAA(ODPA/APB/10 mol% MADA/10 mol% Zr), PAA(ODPA/APB/20 mol% MADA/20 mol% Zr), PAA(ODPA/APB/30 mol% MADA/30 mol% Zr), PAA(ODPA/APB/50 mol% MADA/50 mol% Zr) by varying MADA of higher purity.
- (2) Imidize pendent PAA films above their T_g s; i.e. avoid the 200°C step in the imidization process.
- (3) Spin coat the polyamic acid onto a wafer and test the adhesion of the film after baking.
- (4) Large scale synthesis of PAA(ODPA/APB/MADA/Zr) and determination of multilayer films for mechanical property studies. Determine the maximum single layer and multilayer film thicknesses before onset of imidization-induced cracking. Determine AO resistance of thick, high Zr mol% pendent PI films.
- (5) Test the adhesion of these polymers to copper.
- (6) Learn the mechanism for the DSC reaction and determine if it is a source of the reaction's specificity.
- (7) Adapt system to allow use of a solvent other than NMP.

6. REFERENCES

- 1) Hou, T.H.; Johnson, N.J.; St Clair, T.L. "IM7/LARCTM-IA Polyimide Composites", *High Perform. Polym.* **1995**, 105-124.
- 2) Harris, F.W.; Pamidimukkala, A.; Gupta, R.; Das, S.; Wu, T; Mock, G, "Synthesis and Characterization of Reactive End-Capped Polyimide Oligomers", *J. Macromol. Sci. Chem*, **1984**, 1117-1135.
- 3) Tamai, S.; Yamaguchi, A. "Melt Processible Polyimides and Their Chemical Structures" *Polymer* **1996**, 37(16), 3683-3692.
- 4) Lee, K.W; Walker, G.F.; Viehbeck, A. "Formation of Polyimide-Cu Complexes: Improvement of Direct Cu-on-Pi and Pi-on-Cu Adhesion" *J. Adhesion Sci. Technol.* **1995**, 1125-1141.
- 5) Schwartz, W.T. "A Novel to Aryl Diether Dianhydrides" *High Perform. Polym.* **1990**, 189-196.
- 6) Polymer Chemistry an Introduction; Carraher, Jr. C.E.; Marcel Dekker, Inc, 1996; Fourth Edition
- 7) Banks, G.A; Rutledge, S.K.; Auer, B.M.; Difilippo, F. "Atomic Oxygen Undercutting of Effects on SiO₂ Protected Polyimide Solar Array Blankets", *The Minerals, Metals & Materials Society*, **1990**, 15-48.
- 8) Rutledge, S.K; Copper, J.M.; Olle, R.M. "The Effect of Atomic Oxygen on Polysiloxane-Polyimide for Spacecraft Applications in Low Earth Orbit", Space Operations, Applications and Research Symposium, Albuguerque, NM, June 26-28, 1990
- 9) Banks, B.A.; Rutledge, S.K. "Low Earth Orbital Atomic Oxygen Simulation for Materials Durability Evaluation", Proceeding of the 4th International Symposium on Spacecraft in the Space Environment, Toulouse, France, September 6-9, 1988.
- 10) Golub, M.A. "ESCA Study of Kapton Exposed to Atomic Oxygen in Low Earth Orbit or Downstream from a Radio Frequency Oxygen Plasma", *Polym. Commun.*, **1988**, 29.
- 11) Golub, M.A.; Wydeven, T.; Corma, R.D. "ESCA Study of Kapton Exp;osed to Atomic Oxygen in LEO or Downstream from a Radio Frequency Oxygen Plasma", *Polym. Commun.*, **1988**, October, 29.
- 12) Arnold, G.S.; Peplinski, D.R. "Reaction of Atomic Oxygen with Polyimide Films" *AIAA Journal*, **1985**, October, 1621.

- 13) Rauschenback, H.S. "Solar Cell Array Design Handbook", Van Nostrand Reinhold Co., New York 1980.
- 14) Hansen, R.H.; Pascale, J.V.; DeBenedictis, T.; Rentzepis, R.M. "Effect of Atomic Oxygen on Polymers", *J. Poly. Sci.*, **1965**, A(3), 2205.
- 15) Stein, B.A. "LDEF Materials Overview", paper presented at the "LDEF-69 Months in Space" 2nd post-retrieval conference, June 1-5, 1992. NASA Conference Publication CP3194 Part 3, p. 741-789.
- 16) Banks, B.A.; Dever, J.A.; Gebeauer, L.; Hills, C.M. "Atomic Oxygen Interactions with FEP Teflon and Silicones on LDEF", paper presented at the First LDEF Post-Retrieval Symposium, Kissimmee, Florida, June 2-8, 1991.
- 17) Banks, B.A.; Rutledge, K.S.; de Groh, K.K.; Mirtich, M.J.; Gebauer, L.; Olle, R.; Hill, C.M. "The Implications of the LDEF Results on Space Station Freedom Power System Materials", paper for the 5th International Symposium on Materials in a Space Environment Cannes-Mandelieu, France, Sept. 16-20, 1991.
- 18) De Groh, K.K.; McCollum, T.A. "Low Earth Orbit Durability Evaluation of Protected Silicone for Advanced Refractive Photoaltic Concentrator Array", *J. Spacecr. Rockets*, **1995**, 32, 103.
- 19) Illingsworth, M.L.; Banks, B.A.; Smith, J.W.; Jayne, D.; Garlick, R.G.; Ruthledge, S.K.; de Groh, K.K. "Plasma and Beam Facility Atomic Oxygen Erosion of a Transition Metal Complex", *Plasma Chem. and Plasma Proc.*, **1996**, 16(1), 209.
- 20) Handbook of Chemistry and Physics, CRC, 74th edition, 1993-1994, Page 5-73.
- 21) John Emsley, "The Elements" 2nd edition, Oxford Univ. Press 1992.
- 22) Aldrich Catalog, 1994-1995.
- 23) Terschak, J.A.; Chen, Y.; Illingsworth, M.L. private communication.
- 24) Illingsworth, M.L.; Wagner, S.R.; He, L.; Betancourt, J.A.; Chen, Y.; Terschak, J.A.; Browning, T.A. "Polymeric Materials with Improved Atomic Oxygen Resistance. I. 1994-1995", 6th Annual NASA JOVE Retreat, Monterey, CA, July 5-8, 1995.
- 25) Wagner, S.R.; Illingsworth, M.L. "A New Mixed Ligand Bis(quadridentat)Zr(IV) Complex for Pendent Polymers", ACS Northeast Regional Meeting (NERM), Oct. 22-25, 1996.

- 26) Wagner, S.R.; Illingsworth, M.L. "Polyamic Acid and Polyimide Polymers with Contain Pendent Bis(quadridentate)Zr(IV) Complex", ACS Northeast Regional Meeting (NERM), October 22-25, 1996.
- 27) Archer, R.D.; Day, R.O.; Illingsworth, M.L. "Transition-Metal Eight-Coordination. 13. Synthesis, Characterization, and Crystal and Molecular Structure of the Schiff-Base Chelate Bis(N,N'-disalicylidene-1,2-phenylenediamino)zirconium(IV) Benzene Solvate", *Inorg. Chem.*, **1979**, 18, 2908.
- 28) Dai, H. "Synthesis and Characterization of Zirconium Complex Pendent Polyimides", MS thesis, Rochester Institute of Technology, August 1997.
- 29) He, L.; Wagner, S.R.; Illingsworth, M.L.; Jensen, A.J. "Homogeneous Polyimide Films with Increased Bis(N,N'-disalicylidene-1,2-phenylenediaminato)-zirconium(IV) Content" *Chem. Mater.* **1997**, 9, 3005-3011.
- 30) Svetlichnyi, V.M.; Kalnin'sh, K.K.; Kudryavtsov, V.V.; Koton, M.M. *Dokl. Acad. Nauk SSSR*, **1977**, 237(2), 612. English Transl., **1977**, 237(2), 693.
- 31) Smith, M.J. "Carbodiimides. VIII.¹ Observations on the Reactions of Carbodiimides with Acids and Some New Applications in Synthesis of Phosphoric Acid Esters" *Am. Chem. Soc.* **1958**, 80, 6204.
- 32) Cotler, R.J.; Sauers, C.K.; Whelan "The Synthesis of N-Substituted Isomaleimides" *J. Org. Chem.* **1961**, 26, 10.
- 33) Wallace, J.S.; Arnold, F.E.; Tan, L.S. "Insitu Rigid-Rod Aromatic Polyimides" *Poly. Preprints*, **1987**, 28(2), 316.
- 34) Yang, K.W. "Zirconium Pendent Poly(Amic Acid) And Polyimide Based on 3,4'-ODA and ODPA", MS thesis, Rochester Institute of Technology, May 2000.

7: CONCLUSION

The ODPA/APB/MADA polyamic acids with different MADA/ODPA ratios were synthesized. Their atomic oxygen resistant zirconium containing polyimide precursor, zirconium mixed ligand complex pendent poly(amic acid)s, were synthesized by bonding various amount zirconium complex to the polymer backbone as a pendent group.

The polyimides containing APB exhibited lower T_g s compared with those containing 3,4'-ODA. In addition, the materials that contain APB allowed 50 mol % zirconium complex to be attached onto the polymer backbone, gave uniform films, and an increased number of layers without film cracking. All of these materials have excellent thermal stability. Their decomposition temperatures were 450°C or above. In all cases, the thermally treated films were insoluble in all solvents tested.

Appendix: NMR Spectra Used to Facilitate Peak Assignments, and Pictures

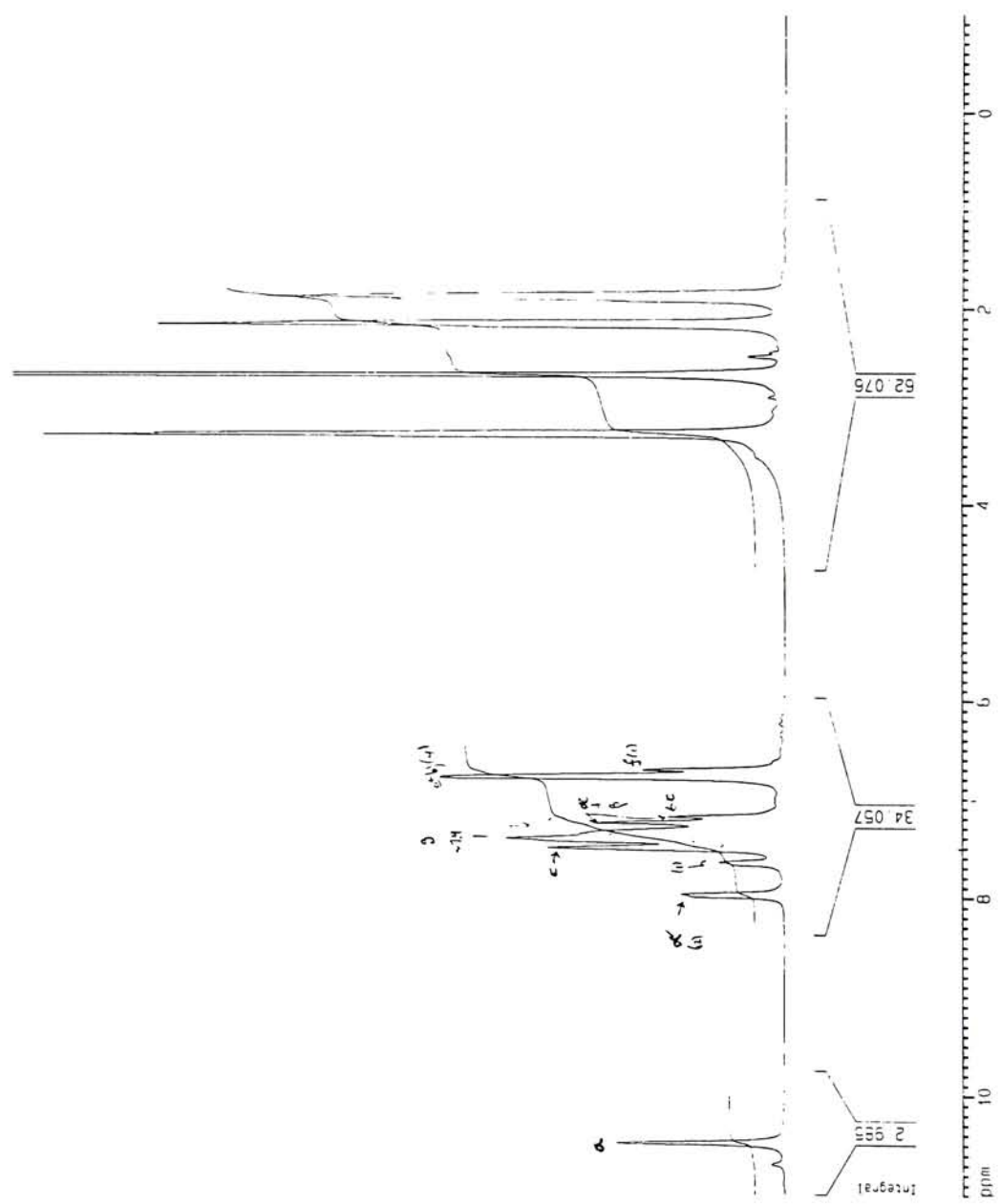
PAA (APB/ODPA/10% MADA)

Current Data Parameters
 NAME PAA_AP010-20
 EXPNO 31
 PROCNO 1

F2 - Acquisition Parameters
 Date_ 990731
 Time 19 19
 INSTRUM spect
 PROBHD 5 mm QNP 1H
 PULPROG zg
 TO 32768
 SOLVENT DMSO
 NS 278
 DS 2
 SWH 4416.403 Hz
 FIDRES 0.137219 Hz
 AQ 3.6438515 sec
 RG 35.9
 DM 111.200 usec
 DE 6.00 usec
 TE 300.0 K
 D1 2.00000000 sec
 P1 9.00 usec
 DC 6.00 usec
 SFO1 300.1318534 MHz
 NUC1 1H
 PL1 -5.00 dB

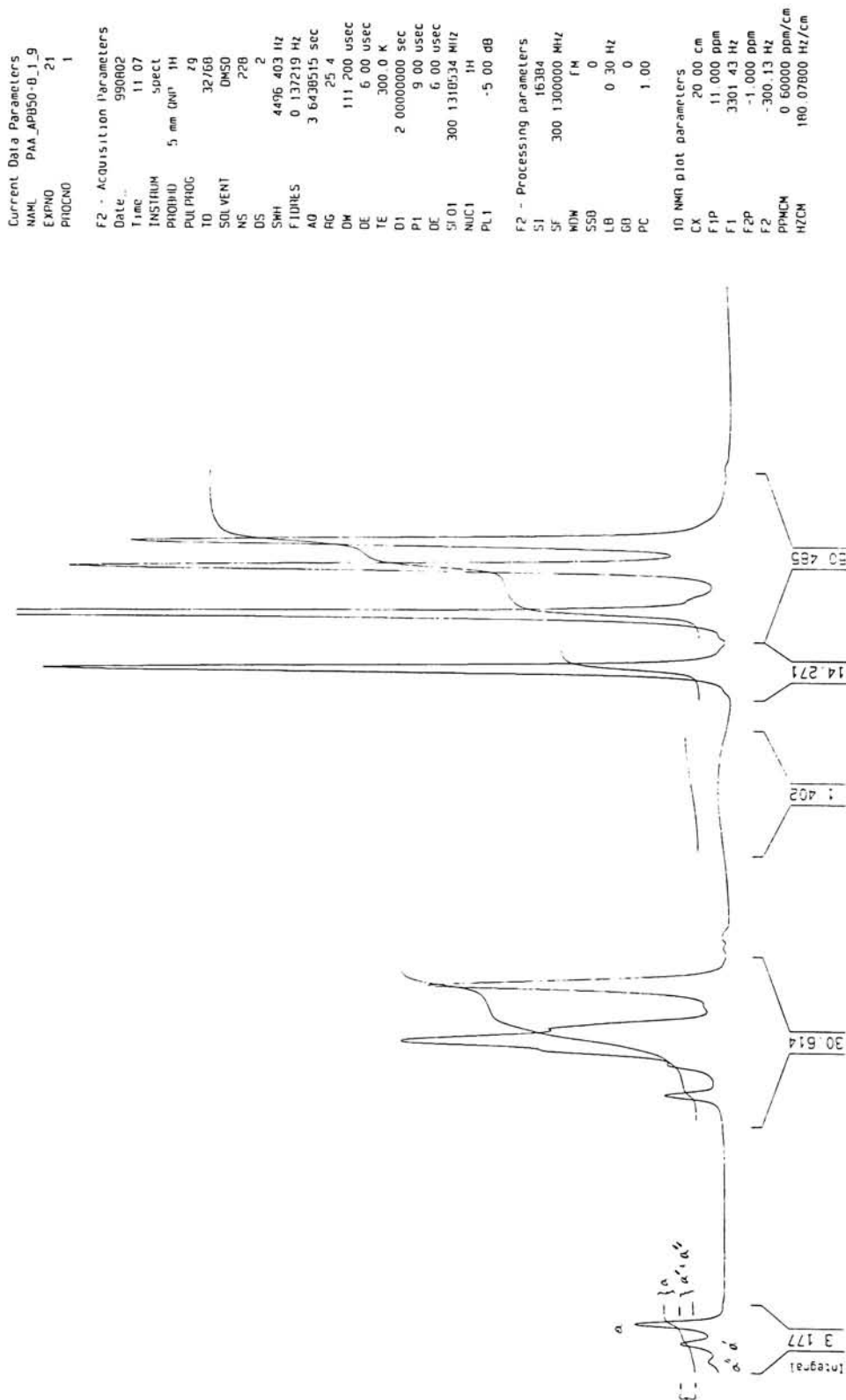
F2 - Processing parameters
 SI 15364
 SF 300.1300000 MHz
 WDW FM
 SSB 0
 LB 0.30 Hz
 GB 0
 PC 1.00

10 NMR plot parameters
 CX 20.00 cm
 FIP 11.000 ppm
 F1 3301.43 Hz
 F2P -1.000 ppm
 F2 -300.13 Hz
 PPHCM 0.60000 ppm/cm
 HZCM 100.07800 Hz/cm



PAA_APB_50
2D NMR 45

PAA(APB/DDPA/50% MADA)



2 Phthalic Anhydride + APB →
 "Amic Acid" (Model Compound)

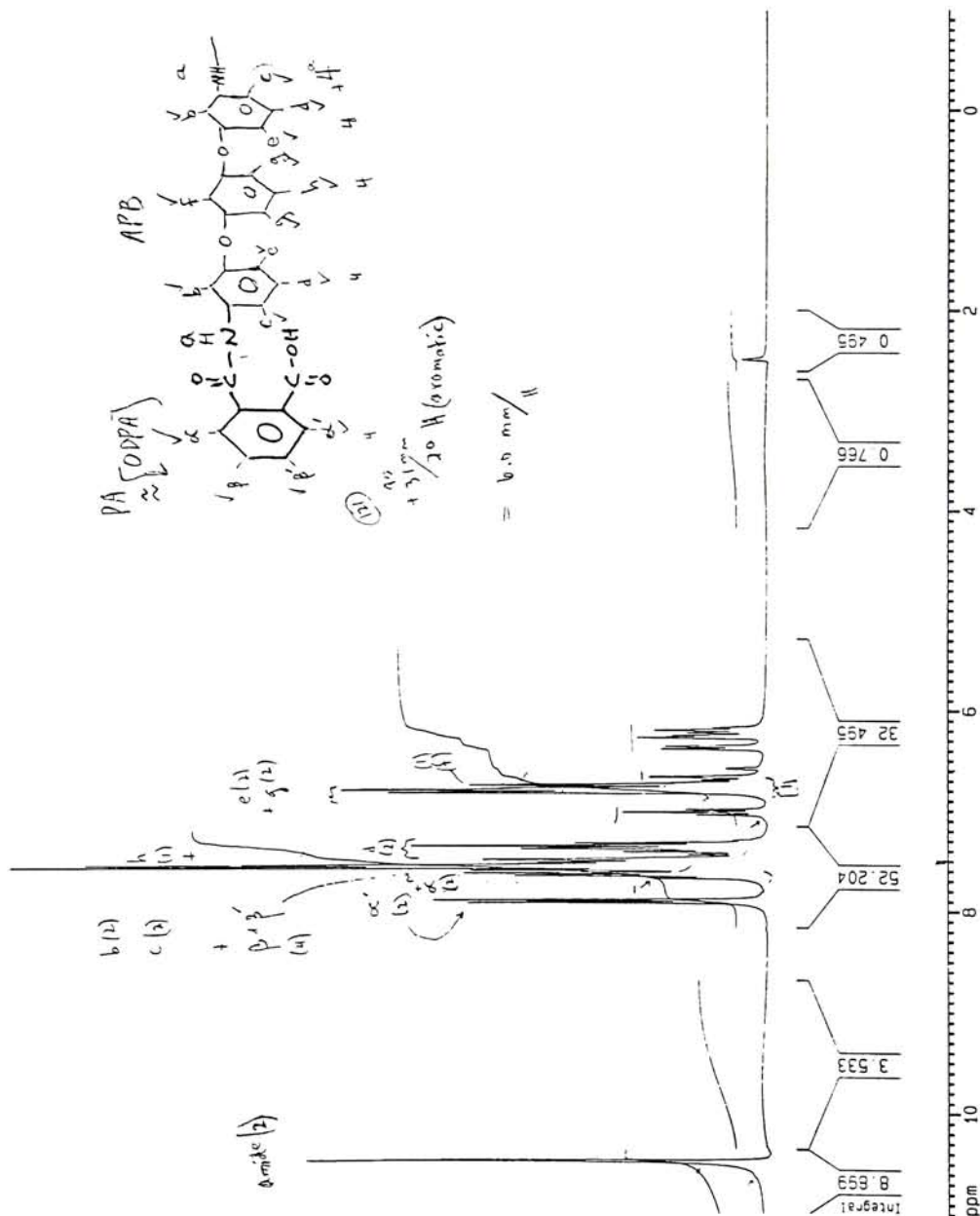
APB_PA

Current Data Parameters
 NAME APB_PA_7-27-99
 EXPNO 31
 PROCNO 1

F2 - Acquisition Parameters
 Date_ 990727
 Time 12 54
 INSTRUM spect
 PROBHD 5 mm QNP 1H
 PULPROG zg30
 TO 32768
 SOLVENT DMSO
 NS 16
 DS 2
 SHH 6172.839 Hz
 FIDRES 0.168360 Hz
 AQ 2.6542580 sec
 RG 71.8
 DM 81.000 usec
 DE 6.00 usec
 TE 300.0 K
 D1 1.0000000 sec
 P1 9.00 usec
 DE 6.00 usec
 SF01 300.1318534 MHz
 NUC1 1H
 PL1 -5.00 dB

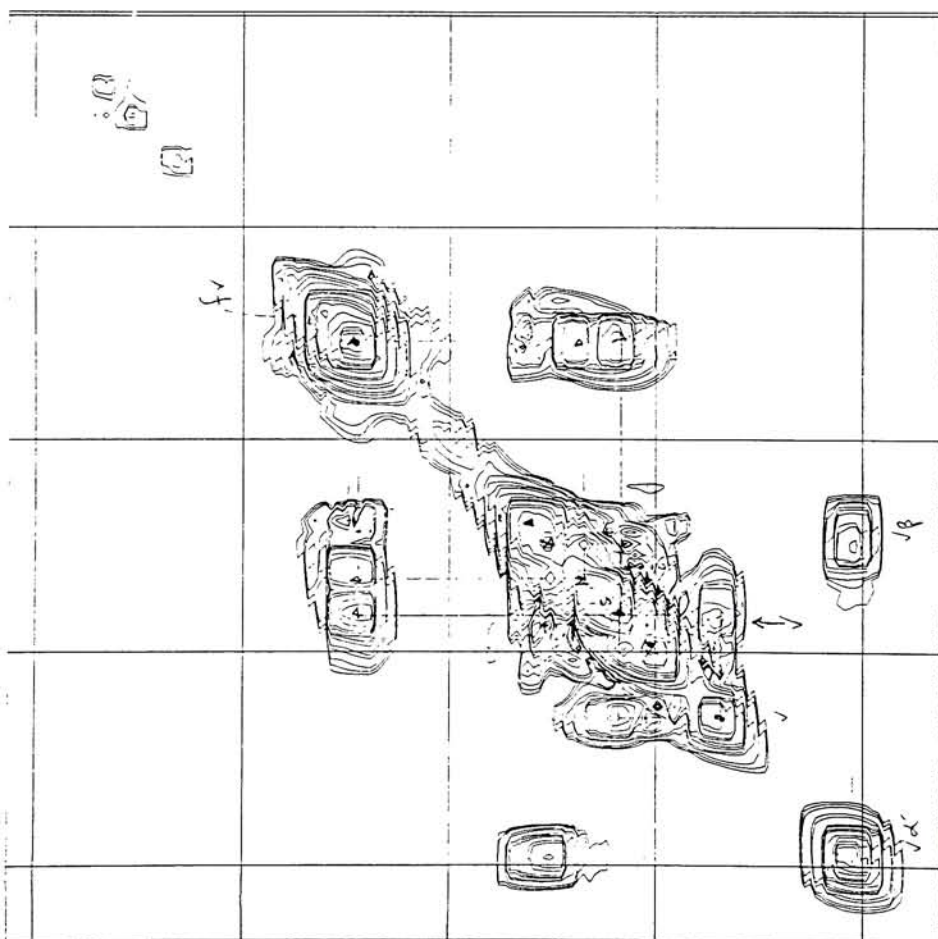
F2 - Processing parameters
 SI 16384
 SF 300.1300000 MHz
 NDM EM
 SSB 0
 LB 0.30 Hz
 GB 0
 PC 1.00

10 NMR plot parameters
 CX 20.00 cm
 FIP 11.000 ppm
 F1 3301.43 Hz
 F2P -1.000 ppm
 F2 -300.13 Hz
 PPMCH 0.60000 ppm/cm
 HZCH 100.07800 Hz/cm



PAA - APB/0

2D



Current Data Parameters
PAA APB/0-20

NAME	1
EXPNO	32
INSTRUM	1
PROBHD	5 mm QNP 1H/13
PULPROG	zgpg30
TD	65536
SOLVENT	DMSO
NS	119
DS	4
SWH	4194.631 Hz
FIDRES	0.000119 Hz
AQ	0.1271101 sec
RG	64
DM	119.200 usec
DE	6.00 usec
TE	300.2 K
OT	0.000000 sec
SI	2.0402010 sec
DF	5.00 usec
DE	6.00 usec
TE	300.15 K
NUC1	1H
NUC2	13C
INQ	0.0002300 sec

12 Acquisition Parameters

11 Acquisition Parameters

12 Processing Parameters

11 Processing Parameters

20 NMR data parameters

CH2	15.00 cm
CH1	15.00 cm
F2A0	0.174 ppm
F2B0	2453.37 Hz
F2C0	5.991 ppm
F2D0	1797.36 Hz
F1A0	0.100 ppm
F1B0	2457.47 Hz
F1C0	5.936 ppm
F1D0	1781.50 Hz
F2A1	0.1408 ppm/cm
F2B1	43.0607 Hz/cm
F2C1	0.1408 ppm/cm
F2D1	43.0607 Hz/cm

PAA_APB_50-DC-1-93
228 scans, 2 sec delay

